DEVELOPMENT OF A COMPUTER PROGRAM FOR GENERAL USE IN THE DESIGN OF SOLAR POWERED WATER PUMPING SYSTEMS

by

Ernest Edward Denny

Dissertation submitted in fulfilment of the requirements for the degree

Magister Technologiae

in the discipline

Electrical Engineering

Faculty of

Engineering

at

Vaal University of Technology

Supervisor: Prof. M.J. Case

Co-Supervisor: Mr. M.J. Joubert

May 2007

DECLARATION

This work has not previously been accepted in substance for any degree and is not being concurrently submitted in candidature for any degree.

Signed: 

Date: 2007/05/30

STATEMENT 1

This dissertation is being submitted in fulfilment of the requirements for the degree Magister Technologiae: Electrical Engineering, at the Vaal University of Technology, Vanderbijlpark, South Africa.

Signed: 

Date: 2007/05/30

STATEMENT 2

This dissertation is the result of my own independent work/investigation, except where otherwise stated. Other sources are acknowledged by giving explicit references as per the appended bibliography. Opinions expressed and conclusions arrived at are those of the author and are not necessarily to be attributed to the VUT.

Signed: 

Date: 2007/05/30

STATEMENT 3

I hereby give consent for my dissertation text, if accepted, to be available for photocopying and for interlibrary loan, and for the title and summary to be made available to outside organisations.

Signed: 

Date: 2007/05/30

ACKNOWLEDGEMENTS

I hereby wish to express my gratitude to the following individuals who enabled this document to be successfully completed:

- Professor Mike Case, my supervisor, for his advice, assistance and support during the study period.
- Mr. Martin Joubert, my co-supervisor, for his advice, assistance and support during the study period.
- Mr. Terrence Harrison, a friend who provided advice and the occasional "sanity check" – It was much appreciated.

Last but not least, a sincere thank-you to the family and friends who provided encouragement and support during the study period.

The success of this work hinges on detailed and accurate solar irradiance and ancillary information. The provision of satellite, surface meteorology and solar energy data by the Atmospheric Sciences Data Centre of NASA's Langley Research Centre is gratefully acknowledged.

This work was funded in part by a Research Award from the Vaal University of Technology (VUT), the receipt of which is hereby appreciatively acknowledged.

DEDICATION

This work is dedicated to my son Jason, the birth of whom made the completion of this work a challenge of note.

ABSTRACT

Water is one of the basic necessities of life. In addition to being essential for the maintenance of life, this basic resource is a crucial requirement for combating poverty, hunger and disease in South African communities. In excess of twenty-nine percent of South African households do not have water in either their dwellings, or on site (source: 2005 RSA census data).

This study documents an engineering solution to the problem of water pumping, utilising renewable energy (solar power) and readily available pumping hardware, configured via a structured design process. Resultant from the research, a software application has been developed that facilitates the design of solar (photovoltaic) powered water pumping applications. The selected design configuration of a non-tracking, stand-alone, directly coupled system provides for the most robust and least complex design possible, making it imminently suitable for application in rural African conditions. Operation of the program is via a simple graphical user interface, with full and context sensitive help provided. It is tailored for use in Southern Africa and is provided with comprehensive databases of location dependant design information such as solar radiation, meteorology and magnetic declination data, together with expandable databases of pre-configured pump and solar panel hardware specification data. The program is manufacturer and component independent, with no affiliations in the choice of hardware.

Design integrity is achieved via multi-parameter analysis and loss compensation methodologies, together with a component matching strategy. Optimisation is achieved by a quantitative and efficiency 'best fit' analysis of the selected hardware components within the design context. Design output predictions are tabulated and graphed by month for a period of one year, allowing design visualisation.

The application has been named 'South African Stand-alone Solar (PV) Water Pumping Design Aid', abbreviated as 'SAS-SWP' in its run-time form. The SAS-SWP application is illustrated in the functional overview provided in Figure 1.

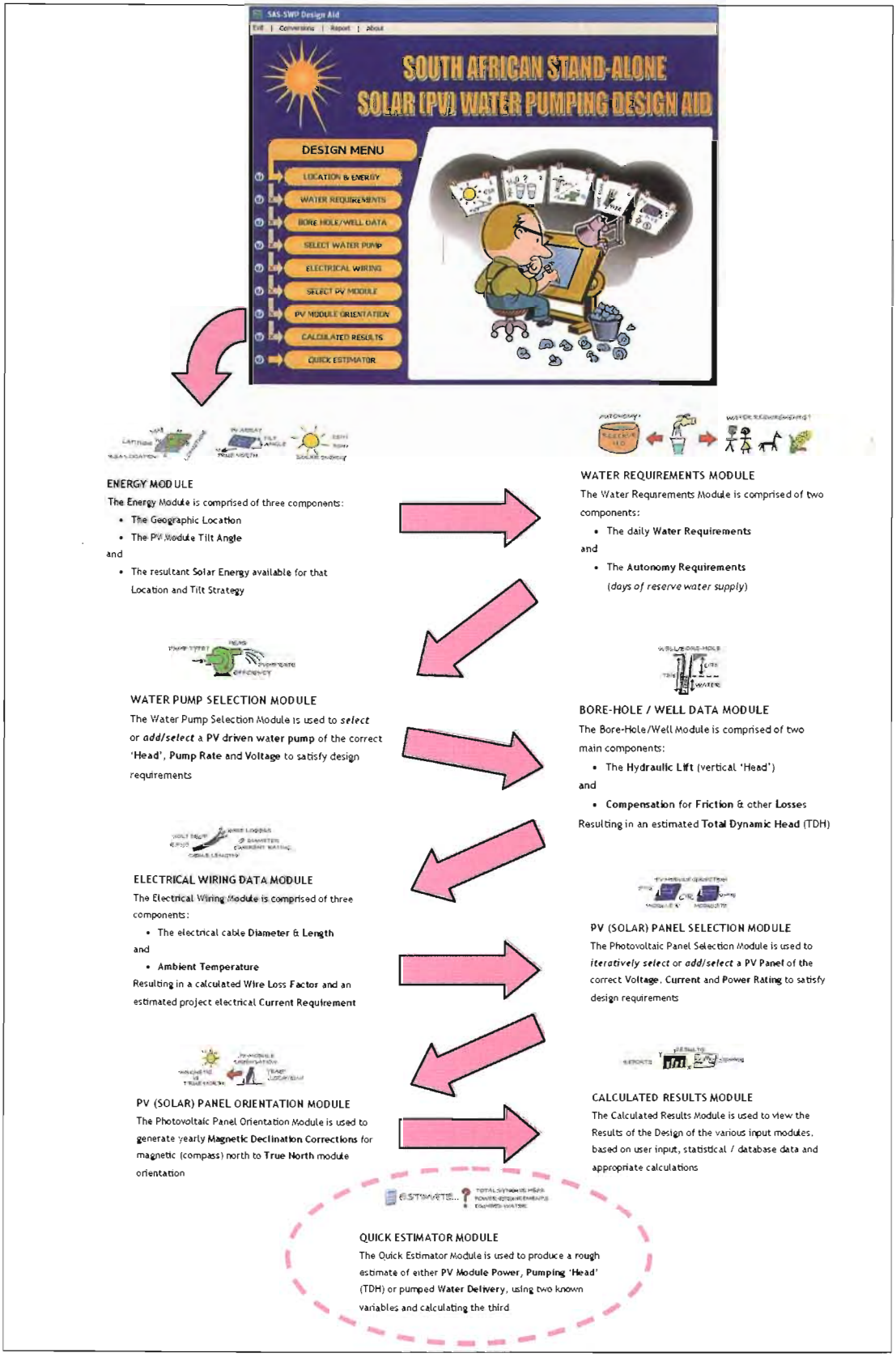

Figure 1 **SAS-SWP Functional overview**

SOFTWARE AND SUPPLEMENTARY DATA COMPACT DISK

COMPANION CD

SUPPLEMENTARY DATA &

SAS-SWP APPLICATION SOFTWARE

TABLE OF CONTENTS **Page**

LIST OF FIGURES **Page**

LIST OF TABLES

ANNEXURE LIST

GLOSSARY OF TERMS

Acronym or Symbol	Description
AC	Alternating Current
A_L	Load current
AM	Air Mass (optical)
ASDC	NASA's Atmospheric Sciences Data Centre
a-Si	Amorphous Silicon
BOS	Balance Of System
BSRN	Baseline Surface Radiation Network
CD	Compact Disk
CdTe	Cadmium Telluride
°C	Degrees Celsius (metric temperature scale)
C_f	PV array tilt angle correction factor when not at optimum tilt
C_{HW}	Hazen-Williams roughness coefficient
CIS	Copper Indium Diselenide
CSIR	South African Centre for Scientific and Industrial Research
CSV	Comma-separated variable
D_A	Autonomy period
DC	Direct Current
Del_h	Sky brightness factor
d_i	Installed pipe inner diameter
DME	South African Department of Minerals and Energy
DNR	Direct Normal Radiation
D_{NS}	Monthly 'no sun' days
DOE	United States Department of Energy
DOS	Disk Operating System
$dP\%$	Percentage difference between name-plate power and data sheet warranted power
D_{val}??	Specific data value at specified coordinate point

DWAF	South African Department of Water Affairs and Forestry
dy	Day number of the year
E	Solar irradiance
E_A	PV Energy available to the load
E_{Array}	Preliminary PV array energy
ECN	Energy Research Centre of the Netherlands
E_{dif}	Diffused radiation
E_{dir}	Direct beam radiation
EDRC	Energy and Development Research Centre of UCT
E_g	Global irradiance
E_{Hyd}	Hydraulic energy requirements
E_P	Energy delivered by a PV array
Ep_h	Sky clearness factor
E_{ref}	Reflected irradiance
E_{SF}	Solar energy input variation 'Safety Factor'
ESH	Equivalent Sun Hours
ESRA	European Solar Radiation Atlas
E_{tilt}	Irradiance on a tilted plane
E_y	Yearly energy factor
$F_\#$	Number of like pipe fittings
F_{1h}	Circumsolar brightening coefficient
F_{2h}	Horizon brightening coefficient
F_{AM}	PV array mismatch factor
F_b	Fractional boost adjustment factor
F_{CDR}	Individual component de-rate factors
F_d	Fractional de-rate adjustment factor
F_{d_total}	Total PVPS de-rate fraction
F_{LF}	Fitting loss factor
F_{PVm}	Total PV module adjustment factor
F_S	Loss compensation 'Safety Factor'
F_{Td}	Temperature de-rate fraction

F_V	Flow velocity
F_{WL}	Wire loss factor
GCIS	Government Communication and Information System
GIS	Geographic Information System
GPS	Global Positioning System
GRA2	DWAF Groundwater Resource Assessment Project, Phase 2
GTZ	Deutsche Gesellschaft für Technische Zusammenarbeit
GUI	Graphical User Interface
H	Solar irradiation or insolation
$\overline{H}$	Monthly average daily solar radiation on a horizontal surface
$\overline{H}_0$	Monthly average daily extraterrestrial solar radiation on a horizontal surface
H_{bh}	The hourly horizontal beam surface irradiation
$\overline{H}_D$	Mean daily irradiation
H_{dh}	The hourly horizontal diffuse surface irradiation
H_{FL}	Friction head loss
H_h	The hourly horizontal surface irradiation
H_{th}	Hourly tilted surface irradiation
I	Electrical current
IBM	International Business Machines
I_{DES}	Final PVPS design current
I_{DesP}	Preliminary PVPS design current
IEC	International Electrotechnical Commission
I_{est}	Empirical electrical current estimate
IGRF	International Geomagnetic Reference Field Model
I_{MP}	Electrical current at maximum power
I_{MPP}	Maximum power point current
INT	Integer part of a mathematical argument
I_{SC}	Short circuit current
ITDG	Intermediate Technology Development Group
K_t	Clearness Index (ratio of measured to extraterrestrial radiation)

$\overline{K}_t$	Monthly average Clearness Index
LCB	Linear Current Booster
LCC	Life Cycle Costing
L_D	Pump discharge head
L_{DD}	Aquifer daily draw-down, from borehole/well data sheet
$L_{Fraction}$	Latitude or Longitude fraction value
$L_{Fraction}$??	Fractional data value for specified coordinate point
L_{PI}	Total installed pipe length
L_S	Static aquifer level
L_t	Geographic latitude for the location in degrees
L_V	Vertical delivery lift or pumping head
M	Latitude or Longitude: Minutes of arc (')
MDC	Magnetic declination correction
MDC_b	Magnetic declination correction Base Value
Mono-Si	Mono-crystalline Silicon
MPP	Maximum Power Point
MPPT	Maximum Power Point Tracker
M_{PT}	Total number of parallel module strings required
M_{ST}	Total number of series PV modules required per parallel string
M_{Total}	Total number of PV modules required for the array design
Multi-Si	Multi-crystalline silicon
NASA	National Aeronautical and Space Administration of the USA
NGDB	South African National Groundwater Data Bank
NGDC	American National Geophysical Data Centre
NOC	Nominal Operating Conditions
NOCT	Nominal Operating Cell Temperature rating
NREL	United States National Renewable Energy Laboratory
P_{Array}	PV array power
P_{comp}	Pressurisation Compensation
PDF	Portable Document Format
P_{in}	Input power

P_{MAX}	Maximum power
P_{MP}	Power at maximum power point
Poly-Si	Polycrystalline silicon
P_{out}	Output power
PPI	Plastics Pipe Institute
P_{Pump}	Rated pump power
P_{SG}	Peak power of the solar generator
PSH	Peak Sun Hours
PSI	Pounds per square inch
P_T	Pressurisation-tank pressure
PV	Photovoltaic
PVP	Photovoltaic Water Pumps
PVPS	Photovoltaic Water Pumping System
Q	Flow rate
Q_{Ar}	Autonomy replenishment rate
Q_{Dr}	Total daily water requirement
Q_{Dr_design}	PVPS 'Final Design' water pumped
Q_P	Required pump rate
Q_{P_design}	PVPS 'Final Design' pump rate
Q_{Pm}	Volume flow rate
R	Electrical (ohmic) Resistance
R_{Ta}	Resistance of copper at temperature T_{amb}
RAPS	Remote Area Power Supply
RSA	Republic of South Africa
S	Latitude or Longitude: Seconds of arc (")
SABS	South African Bureau of Standards
SAS-SWP	South African Stand-alone Solar (PV) Water Pumping Design Aid
SAUPEC	South African Universities Power Engineering Conference
SAWS	South African Weather Service
SCADA	Supervisory Control and Data Acquisition

SHS	Solar Home Systems
S_{Load}	Preliminary PV array system load
$S_{Load'}$	De-rated preliminary PV array system load current
S_m	Friction loss 'Safety Factor' multiplier
SOC	Standard Operating Conditions
SODA	The SODA Service for Knowledge in Solar Radiation: Data, Databases, Applications and Education
S_{PV}	PV array surface area
SSE	Surface meteorology and Solar Energy
ST	Solar Time
STC	Standard Test Conditions
T_a	Mean monthly ambient temperature
T_A	Recommended reservoir tank size
T_{amb}	Ambient system operating temperature
T_c	Average PV module temperature
TDH	Total Dynamic Head
TMY	Typical Meteorological Year
T_r	PV module efficiency at reference temperature
UCT	University of Cape Town
USA	United States of America
US-GPM	Gallons per minute (American)
US-NEC	National Electric Code of the USA
V	Voltage
V_A	Volumetric autonomy requirement
V_{MP}	Voltage at maximum power
V_{MPP}	Maximum power point voltage
V_n	Nominal load voltage
V_{OC}	Open circuit voltage
VDC	DC voltage
VUT	Vaal University of Technology
W_a	Cross sectional area of the installed copper wire

W_{Ag}	Agricultural water requirement
W_{HA}	Daily water requirements for humans and animals
W_L	Length of installed copper wire
WS-NIS	Water Services National Information System
y	Year
Y_c	Gregorian calendar century and year
Y_{offset}	Magnetic declination yearly offset correction
α_s	Solar azimuth
β_p	Temperature coefficient for PV module efficiency
γ_s	Angle of the sun above the horizon
η_P	PV array average efficiency
η_{Pump}	Pump efficiency fraction
η_r	PV module efficiency at NOCT
η_{sub}	Daily PVPS sub-system efficiency
θ	Tilt angle of a tilted surface
θ_{OPT}	Optimum PV array tilt angle
θ_{zh}	Solar zenith angle
λ_c	Power conditioning losses
λ_F	Fittings losses
λ_{FF}	Total friction and fittings losses
λ_{F_total}	Total water pipe fittings losses
λ_p	PV array losses
β_h	Hourly slope of the PV array relative to a horizontal surface
γ_h	Hourly surface azimuth of a tilted surface
γ_{sh}	Hourly solar azimuth
ϕ	Geographic latitude
δ	Solar declination
ρ_s	Global monthly average SSE data set albedo value
ω	Solar hour angle for each daylight hour relative to solar noon
ω_{ss}	Sunrise/sunset hour angle

CHAPTER 1 – Introduction and Overview

1.1 Purpose of study

The purpose of this research is to develop a structured design methodology for photovoltaic powered water pumping systems and to transcribe that methodology into an operational software application to aid in the design of such systems.

1.2 Context of the study

Water is one of the basic necessities of life. In addition to being essential for the maintenance of life, this basic resource is a crucial requirement for combating poverty, hunger and disease in communities.

The provision of water through traditional means such as utility (grid) or fossil fuel powered generators driving electrical pumps can be challenging in many geographically remote areas. Service delivery is complicated by the fact that large numbers of the rural population reside in individual scattered homesteads and not in concentrated villages (Karekezi 2002:1066). Be it for potable (drinking quality) water, water for small-scale agricultural irrigation or for watering livestock, a demand for an alternatively powered water pumping methodology exists in those areas where utility power is unavailable, prohibitively expensive or distant.

In many arid regions, including South Africa, the correlation between the need for water and an abundance of available sunlight (Stassen 1996, quoted from RSA 2004:20; Spalding-Fecher 2002:6; RSA 2007b:440), makes solar power obtained from photovoltaic arrays an obvious and attractive technical choice for reliable, low maintenance delivery of power to water pumping systems. This, together with subsequent satellite and meteorological data analysis (see summary in Figure 36), confirms that solar power is a viable and exploitable resource in Southern Africa.

The technical feasibility of photovoltaic powered water pumping is confirmed by numerous researchers and studies (Dunlop 1988:1182; Posorski 1993:11-16; Thomas 1996:22; Moraes-Duzat 2000:1; Brandt 2001:4; EMCON Consulting Group 2006,

etc.), who have shown that while it is application specific, solar water pumping systems are generally more cost effective than diesel powered systems in operating conditions of up to 100 m of pumping head and a hydraulic equivalent of 2000 m^4 of water per day. It terms of power requirements, photovoltaic water pumping is considered a viable option between approximately 0,7 kW and 4 kW (peak) (Van Campen, Guidi & Best 2000:25; IEA 2003:20).

Assembling a solar water pumping system from ordinary, commercially available components and equipment is not particularly difficult and is generally done by 'system integrators' (also known as value-added re-sellers). These system integrators generally 'add' value to solar modules by purchasing in bulk and integrating the PV modules with available water pump/motor combination, drive electronics and ancillary equipment to form proprietary solar water pumping systems. Unless certain fundamental design requirements are considered, the resulting solar water pumping system is bound to be of low efficiency and high cost. Furthermore, solar modules, usually the greatest single expense item in any solar design, convert sunlight into electricity quite inefficiently – less than fourteen percent on average. Consequently, any solar water pump has to be as frugal on power consumption as possible when used with PV arrays. This emphasizes the critical requirement for maximum efficiency from all the components making up a solar water pumping system. De Villiers (2003) defines an efficient, cost-effective solar water pumping system as requiring critical equipment selection in addition to the use of application-specific technology to underpin the synergies necessary for effective component matching, overall system performance and affordability. Collins and Jones (2002:1) prescribe an optimally designed system to be of paramount importance in order to improve the cost-to-performance ratio of solar powered pumping systems. Customers or equipment providers should preferably be able to accomplish this optimisation process without the need for specialist engineering input. Location and requirement specifications should be input to a system, which should then provide a design solution based on available energy data and equipment selection, with cognisance of the required performance criteria.

The availability of groundwater is deemed adequate in most areas of South Africa, with low volume areas occurring mostly in the northern and north-western Cape Province (See groundwater exploitation potential map in Figure 47). Holtzhausen (2005:15) quotes the second phase of the DWAF initiated Groundwater Resource Assessment Project (GRA2), as listing the Groundwater Resource Potential for South Africa at 49 billion cubic metres per annum, with potable groundwater exploitation potential at 14,8 billion cubic metres per annum.

The Water Services Act of South Africa (Act 108 of 1997) recognises a person's right of access to a 'basic water supply', defined as twenty-five litres of potable water per person per day, or six kilolitres per household per month (RSA 2001:4). While potable water supply in the home is generally perceived as a 'given', many South African households in poorer and rural areas still lack this basic necessity. The endeavour for social 'upliftment' demands that this be addressed, as evidence from implementation case studies suggest that making even relatively small amounts of water available to poor people for personal and productive use can transform their lives dramatically (Polak, Adhikari, Nanes, Salter & Surywanshi 2003; Lipton, Litchfield, Blackman, De Zoysa, Qureshy & Waddington 2003). While it is known that affordability of service delivery is a key issue, the diverse application base makes it difficult to define in detail. Saunders and Warford (1976:187-188) of the World Bank note that a frequently used 'rule-of-thumb' for rural or near subsistence households is that they "should never have to pay more than about five percent of their income for water." These factors are discussed at length by Goldblatt (1996:21-26), who notes that a key concern for suppliers is the level of cost recovery, tariff setting and income policy, in the context of a low-income consumer base.

The Department of Water Affairs and Forestry (DWAF) indicate via demographic data from their Water Services National Information System (WS-NIS), that there are 12.8 million households in South Africa (RSA 2007a). Statistics South Africa report from the July 2005 national census that 29,73 percent of South African Households (3 805 000 Households) do not have water in either their dwellings or on site (RSA 2006a:44). Additional detail on this is provided in Table 1. The huge

service backlog is indicative of the fact that conventional supply methods are not fulfilling the full spectrum of demand rapidly enough and clearly supports the need for an additional service delivery method.

Table 1 **Households without water on site – RSA 2005 (adapted from RSA 2006a & RSA 2007a)**

Households without water in the dwelling or on site, by time taken to reach the water source.	Households without Water	*Total Number of Households	Households without Water (%)
Less than 2 minutes (less than 200m)	675000		
2 minutes but less than 5 minutes (200m < 500m)	1066000		
5 minutes but less than 15 minutes (500m < 1.5km)	856000		
15 minutes but less than 30 minutes (1.5km < 3km)	488000		
30 minutes but less than 45 minutes (3km < 4.5km)	300000		
45 minutes but less than 60 minutes (4.5km < 6km)	151000		
60 minutes or more (6km or more)	205000		
Unspecified time/distance	64000		
Total:	3805000	12800000	29,73
Source: Adapted from Report P0318, Statistics South Africa, Page 44, Table 7.6		***Source**: DWAF: WS-NIS Accessed 01/05/2007	
Main source of water for the Household	**Households**		
Borehole on site	171000		
Rain-water tank on site	34000		
Public tap	2101000		
Water-carrier/tanker	128000		
Borehole off site/communal	320000		
Flowing water/stream/river	516000		
Dam/pool/stagnant water	42000		
Well	88000		
Spring	273000		
Balance made up by Unspecified, Other and Piped water.	--		
Source: Adapted from Report P0318, Statistics South Africa, Page 42, Table 7.4			

The identified need is acknowledged by the South African government on the Department of Minerals and Energy (DME) internet web site (RSA 2006b), where it is stated that "The majority of the population in South Africa have no access to clean drinking water; diesel and petrol water pumping systems are frequently out of order or run out of fuel and rural dwellers have to walk long distances to collect water, thus the need for renewable energy driven, low maintenance, water pumping systems such as photovoltaic (PV) driven water pumping systems, becomes more evident." This is supported by the gazetted White Paper on the Renewable Energy Policy of the RSA,

which cites the potential of water pumping schemes for households and communities as a typical photovoltaic application (RSA 2004:21).

WS-NIS state that it will require a capital investment of 4 051,21 million Rand to achieve the water infrastructure supply targets (RSA 2007a). In a Project Brief on rural electrification in South Africa released by the United States National Renewable Energy Laboratory (NREL), jointly coordinated by NREL and the Energy for Development Directorate of the DME in conjunction with the Energy and Development Research Centre (EDRC) of the University of Cape Town, Arent (1998:2) comments that relative to line extensions, renewable power options are an economically superior alternative for many connections. This view is supported by Spalding-Fecher (2002:28) in his analysis of energy sustainability indicators for South Africa. Commenting on expenditure and duration, Arent (1998:2) states "It is estimated that the rural electrification market lifetime will last 20 years, and the total value of installed hardware will be approximately $1 billion." Worldwide delivery of photovoltaic generators totalled 396 mega-watts (peak) in 2001, with production of solar cells increasing by an average of thirty percent per year (Jäger-Waldau 2002:4). An industry market report (Solarbuzz 2007:1) quotes 2006 world solar cell production at 2204 mega-watts (consolidated) and the installed base at 1744 mega-watts. At a local installed base of eight mega-watts (peak) in 2000 (RSA 2004:21) and steadily increasing each year, the earnings potential in photovoltaic's is anticipated to be sizable. This establishes a sound economic reason for business interest in alternate powered water pumping applications.

With technical and economic feasibility, social responsibility and product requirement established, holistic synthesis of the above information identified a need that called for the development of a software program to aid in the design of photovoltaic powered water pumping systems. Following discussions with specialist personnel at the Vaal University of Technology, a design specification for the software application was formulated. Design configuration would be confined to non-tracking, stand-alone, directly coupled photovoltaic systems, to provide for the most robust and least complex design possible. This configuration was chosen to

address problems identified by Nieuwenhout, Martens, Lasschuit, Lafleur and Cloin (2001:54-57), Brandt (2001:19) and Cox, Gys, Klunne, Purcell and Louineau (2002:86-97), who found that technical complexity and electronic failure (together with theft and vandalism), form the major reasons for photovoltaic power delivery project failure in Southern Africa.

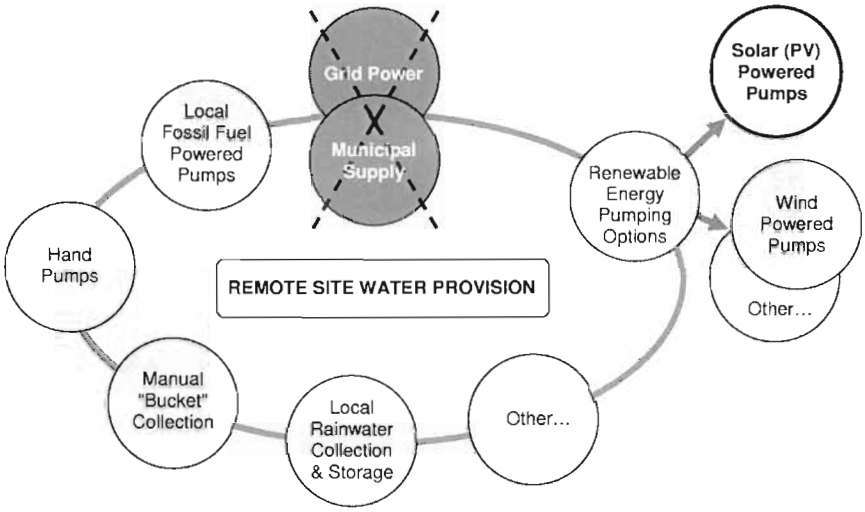

Figure 2 Context of the study: PV powered water pumping

The context of the study is illustrated in Figure 2, expanded into a system topology shown in Figure 3.

1.3 Problem statement

To engineer a structured photovoltaic powered water pumping design methodology that is able to leverage computer processing while limiting operational complexity.

1.3.1 sub-problems

- Provision of a robust design.
- Provision of comprehensive, accurate data sets for use in the design algorithms.
- Designing algorithms able to directly utilise database data.
- Designing algorithms and calculation methodologies that are able to provide design data over extended periods within reasonable calculation times.

- Designing a graphical user interface and operational methodology that facilitates operation by non-specialist users.

1.4 Scope of study

The system topology provided in Figure 3 gives an overview of process interaction and highlights the technology and research impact areas involved in this field of study.

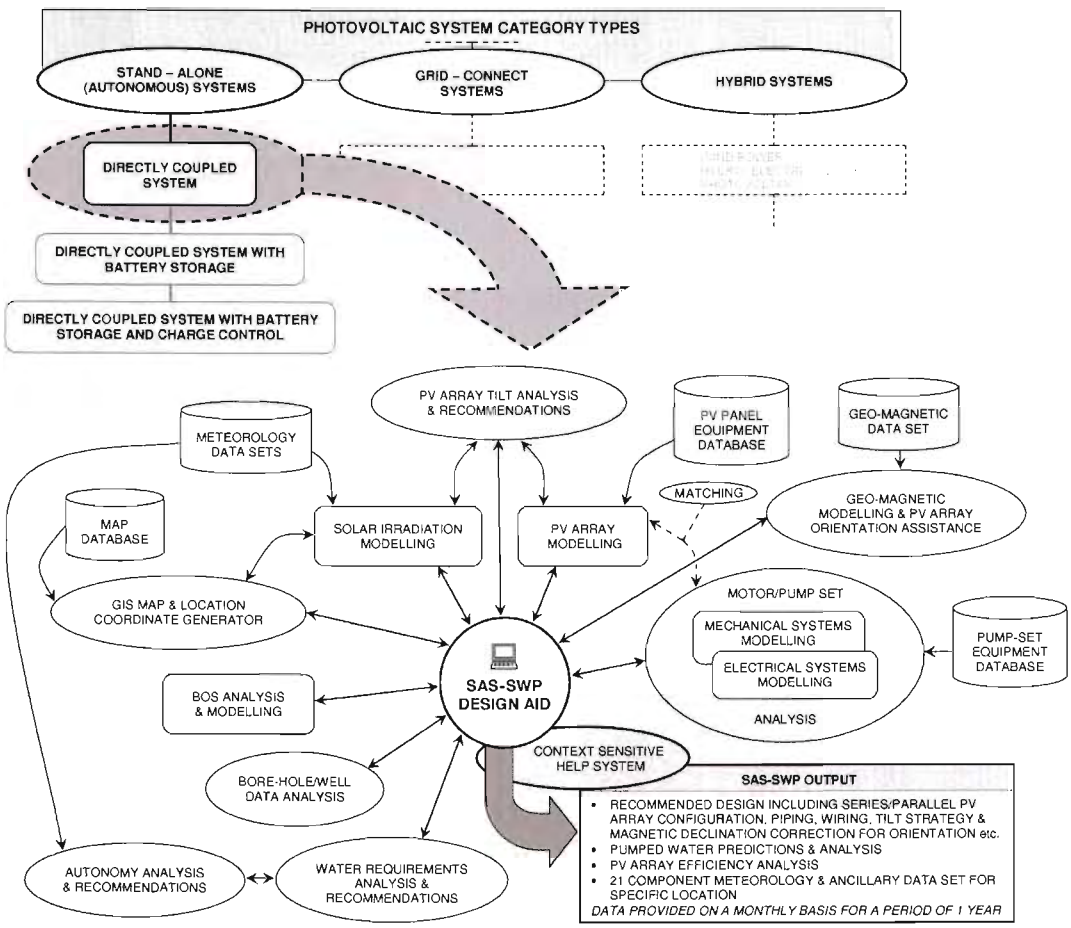

Figure 3 System topology

Following discussions with stakeholders and specialist personnel at the Vaal University of Technology, a software specification for a photovoltaic pumping system was drafted as detailed. The scope of study was bound by the specified design

criteria, which formed the basis of the research and subsequent software application development. Key specification requirements were defined as follows:

- Focus area for design, data and usage, is South Africa.
- User interaction to be via a Graphical User Interface, focussing on ease of use; suitable for non-technical users.
- An integrated database containing all surface meteorology and solar energy data.
- Generic water pump and solar panel database (no equipment manufacturer or vendor 'lock-in').
- Royalty and licence-free application programs.
- Software to run on an IBM compatible personal computer.
- Computation times to be optimised as far as possible.
- Stand-alone operation, *i.e.* not required to couple to the internet to source data.
- Inclusion of defined design requirements:
    - Site solar irradiation and supplementary data (temperature, cloud, *etc.*).
    - Site water requirements and usage data (including autonomy requirements for bad weather days).
    - Site bore-hole/well data (including aquifer data such as draw-down and static water level).
    - PV array orientation and tilt.
    - PV array configuration (component choice, as well as voltage and current options from combinational series and parallel module strings).
    - PV cell temperature compensation.
    - Choice of PV modules and motor/pump set.
    - Dynamic component matching analysis.
    - Component efficiency compensation.
    - Compensation for system losses such as volt drop (wire losses) and pipe friction, *etc.*

1.5 Delimitations and limitations

1.5.1 delimitations

The research was delimited by the following:

- To minimise system complexity, maintenance requirements and cost, the system design was constrained to non-tracking, standalone, and directly coupled photovoltaic (PV) water pumping systems that are oriented to true North.
- Financial analysis was excluded from the design due to the difficulty of maintaining a 'stand-alone' component price database.

1.5.2 limitations

The following limitations applied to this research:

- The research and resultant design was limited to the design specifications as detailed in the text.
- Equipment database composition was limited by the availability and accuracy of manufacturer/vendor data sheets.
- Meteorological data accuracy is limited to the composite effect of the different algorithms and methodologies used, as detailed in the text.
- Application software comparative testing was limited to the use of available data from the Vaal University of Technology solar laboratory.

1.6 Methodology and calculations

The research begins with a literature and empirical review of the physical and meteorological system components that influence, impact or prescribe design parameters and requirements for a photovoltaic powered water pumping system. Data sources are evaluated and relevant usage motivated. This is followed by a review of existing design methodologies, leading to a rationale for the adopted design strategy. Methods, calculations and data sources are detailed, progressively building up to the algorithms presented in the final design structure.

The various design algorithms and data-sets are validated using comparative and qualitative methods. Coded algorithms in the application software are subjected to comparative testing with hand calculations or reference software/data, culminating in a full software design test relative to a physical pumping trial data-set.

The full detail of the research, design methodology, calculations, testing and validation are as detailed in proceeding chapters of this text.

1.7 Significance of the research

This study documents an engineering solution to the problem of water provision as outlined in the context of study, utilising renewable energy (solar power) and readily available pumping hardware, configured via a structured design process.

Resultant from the research, a software application has been developed that facilitates the design of solar (photovoltaic) powered water pumping applications. The selected design configuration provides for the most robust and least complex design possible, making it imminently suitable for operation and application in rural African conditions.

The South African radiation/meteorology database and operational methodology that has been developed has potential for use in any application that utilises solar power. Likewise, the autonomy calculation methodology (reliant on the meteorology database) has application beyond directly coupled solar water pumping applications.

The magnetic declination correction algorithm and database that has been developed provides results to an accuracy of better than one half of a degree, lending itself to use for magnetic declination determination and correction where 'map and compass' navigation or alignment is used.

CHAPTER 2 - Solar Water Pumping Theory

This chapter reviews some of the components and methodologies related to solar/photovoltaic water pumping that are considered to be cardinal to understanding the program model requirements for the design of a software application.

2.1 The solar energy resource

Solar Energy reaching the earth drives almost every known physical and biological cycle in the earth system – It is the source of life on our planet.

This section details some of the concepts related to solar resource energy engineering that is considered fundamental to the photovoltaic process.

2.1.1 the sun

The radiant power emitted by the sun is approximately equal to 63,1 mega-watts per square metre (Quaschning 2003:90), with about 1,2 x 10^{17} watts of this energy reaching the earth's surface at any given time. Solar irradiance decreases with the square of the distance to the sun (inverse square law). Since the distance from the earth to the sun changes fractionally during the year, solar irradiance outside the earth's atmosphere varies between 1325 W/m² and 1420 W/m² (Quaschning 2003:90). Extraterrestrial solar irradiance (not subjected to atmospheric influences), has only a direct component – all solar radiation is considered to be on a parallel plane. This direct irradiance is also called direct normal or beam irradiance. Only an extraterrestrial surface that is perpendicular to the incoming sun's rays receives this level of irradiance. Under these conditions, a surface oriented parallel to the sun's rays, receives no irradiance, while an inclined surface receives reduced irradiance depending on the cosine of the angle of incidence of the solar flux.

The surface temperature of the sun is the main characterisation parameter that defines the spectral irradiance for all wavelengths of sunlight. Visible light (wavelengths between 0,4 μm and 0,75 μm) contributes 46 percent, infrared light 47

percent and ultraviolet light 7 percent of the spectrum, respectively (See Figure 4). The difference between the extraterrestrial and terrestrial spectrum in the ultraviolet and infrared ranges is primarily due to absorption, while in visible range it is due to reflection and scatter while passing through the earth's atmosphere.

In meteorology terms, radiation occurring between 0.29 µm and 4 µm is referred to as solar radiation, while radiation in the spectral range greater than 4 µm is defined as terrestrial radiation (Quaschning 2003:91).

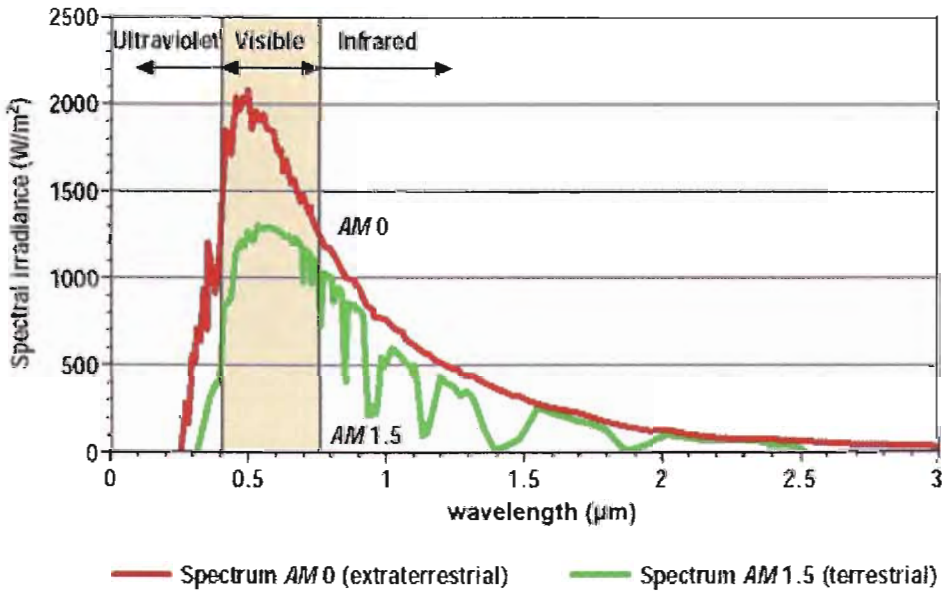

Figure 4 **Extraterrestrial and terrestrial spectrum of sunlight (Quaschning 2003:91)**

2.1.2 solar constant

The annual mean amount of energy received at the top of the earth's atmosphere on a surface orientated perpendicular to the suns rays, at the mean earth/sun distance, is known as the 'solar constant'. This annual mean solar irradiance value is a satellite measured value and is currently generally accepted as being 1367 ± 2 W/m² (Quaschning 2003:90).

2.1.3 irradiation (insolation)

This term is often misunderstood. Clarification on its usage in this text is given in the proceeding paragraphs.

2.1.3.1 irradiance and irradiation

The definition of the terms irradiance and irradiation is subject to confusion. According to Quaschning (2003:90), the terms are often used incorrectly, even by specialists. The terms are defined below according to an article in the International Journal of Solar Radiation (Dogniaux, Grueter, Kasten, Page, Perrin de Brichambaut, Treble & Palz 1984: 249-255):

- Irradiance is defined as power received per unit area. It is expressed in W/m^2 (watt per square metre).
- Irradiation is the energy received per unit area. It is expressed in J/m^2 (joule per square metre). Other units are J/cm^2 (joule per square centimetre) and the commonly used Wh/m^2 (watt-hours per square metre).

From the above it is clear that the total specific radiant power, or radiant solar flux, per area, that reaches a receiver surface, is called irradiance. It is measured in W/m^2 and has the symbol *E*. When integrating irradiance over a defined time period, it becomes solar irradiation. Irradiation is measured in either J/m^2 or Wh/m^2 and is represented by the symbol *H*.

Solar irradiation has also been referred to as solar insolation in many (predominantly American) references. For the purposes of this text, the two terms are assumed to have the same meaning and are use interchangeably.

Measurable terrestrial irradiance fluctuates according to climatic conditions (weather) and the location of the sun in the sky. Sun location changes on a daily time-basis with respect to altitude angle and azimuth angle. Altitude angle is also affected by seasonal change.

Daily irradiation depends upon many factors, the predominant parameters being cloud cover, daylight duration and the sun elevation (angular height of the sun above horizon). Daylight duration and the sun elevation is calculated using earth-sun (solar) geometry. They are functions of geographic latitude, physical 'day-of-the-year' number and solar time. The cloud cover parameter is more variable and depends on local meteorological conditions, which influence and create micro-climatic (local) variations in the irradiation received, with the exception of shadow effects that can be observed in areas of steep relief, such as mountain ranges. Intervening parameters such as atmospheric aerosols and relative humidity also influence radiation. Aerosols scatter the radiation and may increase or decrease the radiation available at ground level, while water vapour absorbs radiation. The greater the relative humidity, the smaller the resultant irradiance will be.

The combination of these parameters produces the variability of irradiation in space and time. The climatology of the daily irradiation depicts these variations on a macro scale.

Daily irradiation exhibits sensitivity to seasonal variations. On a regional scale, this is predominantly due to changes in solar declination. The change in distance between the centre of the earth and the sun centre, due to the elliptical orbit, also has a small influence. On a macro-scale, irradiation varies with latitude and is generally greater in the north, decreasing southward. This suggests that the main cause of changes in solar radiation level is the change in sun elevation that creates these latitudinal variations. On average, the influence of cloud cover is of lesser importance, as it tends to exhibits local effects that disturb the latitudinal distribution, often in the vicinity of mountain ranges, where spatial distribution has a strong local component that is linked to the geographic relief (local micro-climatic effects).

2.1.3.2 irradiance components

Quaschning (2003:91) explains that while direct beam radiation E_{dir} is the largest irradiance component to reach the surface of the earth, it is not the only one. The presence of the atmosphere and associated climatic effects both attenuate and change

the nature of the solar energy resource. Particles in the atmosphere reflect or scatter a portion of the beam irradiance into diffused and reflected components. Figure 5 illustrates these atmospheric effects on solar energy reaching the earth. Concentrating solar systems can only use direct irradiance, but non-concentrating systems such as those used for solar water pumping use the additional scattered and diffused radiation E_{dif} to supplement their input energy. This is generally called global irradiance E_g (equals $E_{dir} + E_{dif}$) and is measured on a terrestrial horizontal surface (horizontal plane). Solar collectors that are mounted at a tilt (tilted plane) have an additional irradiance component that originates from reflection E_{ref}, predominantly from the ground surface. The average reflected irradiance component is about 20 percent of the global irradiance. The irradiance on a tilted plane E_{tilt} therefore consists of three components, $E_{tilt} = E_{dir} + E_{dif} + E_{ref}$. A surface perpendicular to the incident direct sunlight is usually subjected to the greatest possible irradiance. This is normally less than 1 kW/m² - higher values only being possible due to situations such as concentrating reflection from snow or cloud (Quaschning 2003:91).

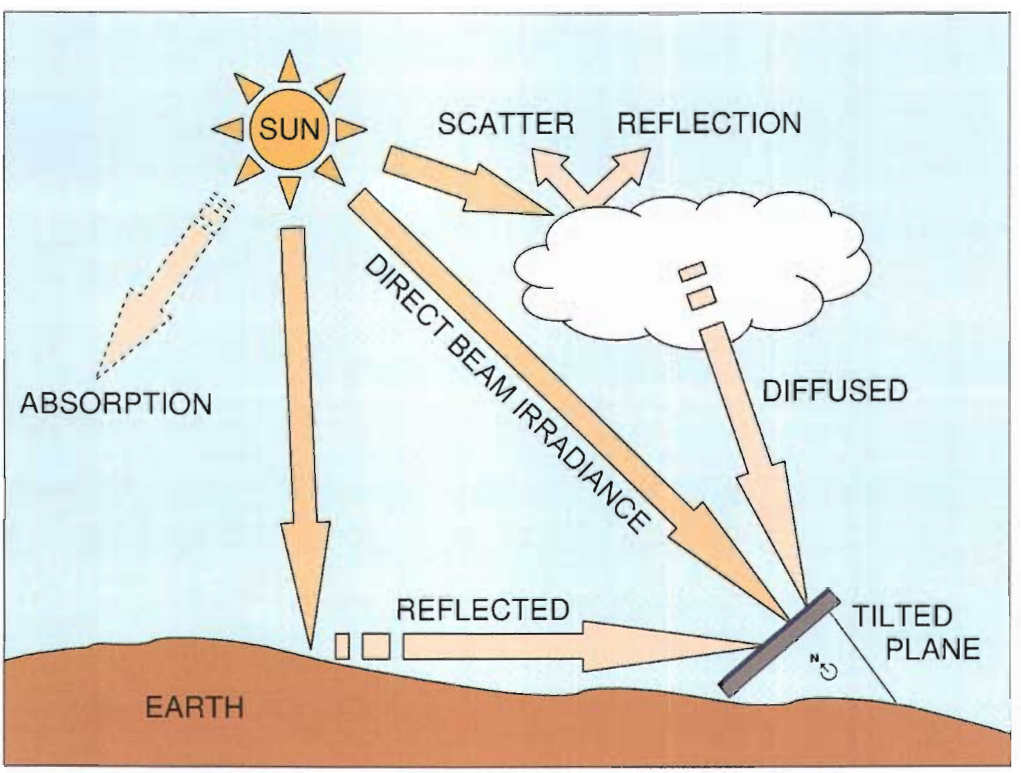

Figure 5 **Sunlight passing though the atmosphere**

2.1.3.3 irradiance measurements

Different types of instruments exist to measure solar irradiance, the most common of which are described in the following paragraphs.

A pyranometer is used to measure global irradiance. It uses silicon sensors, with a small photovoltaic cell that generates an electrical current that is approximately proportional to the solar irradiance. This type of sensor measures only part of the solar spectrum, as it cannot sense infrared light. The annual accuracy of these sensors is limited because the solar spectrum changes with the air mass. A more precise pyranometer design uses a black receiver plate that is mounted below a double glass dome, in its sensor circuit. The plate heats up according to the incident irradiance and a thermocouple converts the heat difference between the plate and its surroundings into a voltage signal that is proportional to the irradiance. To measure the direct normal or beam irradiance, the sensor of the measuring instrument is end-mounted inside an absorber tube, thereby isolating it from diffuse irradiance. This configuration is called a pyrheliometer and requires precise two-axis solar tracking. The addition of a shading ball or ring that permanently shades a pyranometer isolates the instrument from direct irradiance and thereby allows it to measure diffused irradiance Quaschning (2003:91-93).

Ground measurement of total broadband solar radiation can be accomplished in two different ways: Directly, or by using a radiation component summation technique (Carnicero Domínguez 2001:2-3). The first method consists of using a pyranometer, an instrument initially designed to measure total broadband solar radiation incident on the surface of the earth. A problem with the pyranometer approach is that its output manifests a dependence on the angle of incidence of the incoming radiation. This dependence, generally termed cosine error, can produce a significant error in the measurement output of the instrument. Cosine errors can be minimised by careful instrument design and compensating calibration procedures from manufacturers. It should be noted that although the cosine error can be minimized, it cannot be completely eliminated from the measurement (Carnicero Domínguez 2001:2).

A study by the Baseline Surface Radiation Network (BSRN) (Ohmura, Dutton, Forgan, Fröhlich, Gilgen, Hegner, Heimo, König-Langlo, McArthur, Müller, Phillipona, Pinker, Whitlock, Dehne & Wild 1998) suggests that improvements in the total solar irradiance measurement can be achieved by using an indirect measurement technique that can negate the directional response problem. This method consists of measuring the two components of the global surface solar irradiance separately, *i.e.* using independent direct beam and diffuse irradiance measurements.

Diffuse irradiance is difficult to measure accurately (Dutton, Stoeffel & Michalsky 2001: 297-314). Cosine response error is reduced when pyranometers are used to measure diffuse irradiances, because the incident radiation is not collimated. The preference has therefore been to use pyranometers to measure diffuse irradiances, blocking the direct beam solar radiation from the instrument field of view. Pyranometers do, however, present another type of error reported since their conception. The temperature gradient through the pyranometer (dome to body) results in an offset in the output of the instrument. This error is generally called thermal offset. This type of instrument response error was reported by Gulbrandsen in 1978 (Gulbrandsen 1978: 899-904). It was considered negligible when measuring total broadband solar irradiance because of its small magnitude relative to the total instrument output. Likewise, it was not considered significant in the original application of pyranometers for diffuse irradiance measurement.

A study by Kato, Ackerman, Clothiaux, Mather, Mace, Wesely, Murcray and Michalsky in 1997 reported a disagreement between calculations of extinction of the direct solar beam and the quantities measured during clear-sky days during the execution of the Atmospheric Radiation Enhanced Shortwave Experiment. Additionally, they reported that in some cases the amount of diffuse radiation for a clear sky day was less than the amount scattered by a clear atmosphere with no aerosols, a condition that is not possible. Kato *et al.* (1997:25881-25898) deduced that there were two scenarios that could account for the discrepancy between modelled output and actual measurements, namely:

- The presence of a gas not included in the model, that is able to absorb an amount of radiation equal to the discrepancy, or
- Measurement errors in any of the instruments used.

They surmised that the error would be something considered negligible, but that actually had a significant impact on measured data accuracy.

The Kato study (Kato *et al.* 1997) provoked a response in the solar resource community, initiating a process to review the accuracy and measurement uncertainties of several types of radiometer instruments. The pyranometer came under scrutiny and it was concluded that thermal offset generated because of temperature differences between the dome and body of the instrument, previously considered negligible when measuring total irradiance, had an effect on the output of the instrument when measuring diffuse irradiance (Haeffelin, Kato, Smith, Rutledge, Charlock & Mahan 2001: 472-484, *etc.*).

The solar resource community then proceeded to characterise and quantify the thermal offset in pyranometers. An example of this is the investigation by Dutton *et al.* (2001:297-314) regarding thermal offset errors in diffused solar radiation measurements with a selection of commercially available pyranometers. Additionally, a means was sought to not only eliminate the error in future measurements but also to correct existing diffused irradiance data. Methods adopted include modelling pyranometer response functions (Lester & Myers 2006:322-331), using thermistors in the dome of a pyranometer to characterise the thermal offset (Haeffelin, Domínguez, Rutledge & Kato 2001:1-6) and active compensation using thermistors mounted in the body and dome of a pyranometer (Carnicero Domínguez 2001:9). Carnicero Domínguez (2001:63-76) also presents a methodology for the correction of thermal offset in historical data by means of two derived relationships, using atmospheric infrared radiation measurements and a cloud cover fraction determined using the Long/Ackermann algorithm (Long, Ackerman, De Luisi & Augustine 1999:1-7).

It is important to note that pre-1998 diffused solar radiation data gathered using pyranometers and by implication global solar irradiance data, inherently contain the pyranometer thermal offset error encapsulated in the data, unless specifically corrected or compensated for.

Figure 6 illustrates a range of typical irradiance measurement instruments in operation.

Careful maintenance of all sensors and regular instrument calibration is necessary to obtain high measurement accuracy levels. Physical factors such as dust on the sensors and tracker inaccuracy, as well as calibration issues such as cosine error compensation and thermal offset can reduce measurement quality significantly.

Figure 6 **Sensors for solar irradiance measurement**
Top Left: Pyranometer – for Global Irradiance measurement
Bottom Left: Two-axis tracked pyrheliometer - Direct Normal Irradiance
Right: Pyranometer with shading ball – for Diffused Irradiance
(Quaschning 2003:93)

Total broadband solar irradiance at the surface of the earth can also be measured by remote sensing techniques using satellite instrumentation. Dedicated meteorological satellites are typically used to provide irradiance data. This is done by comparing satellite generated meteorological images with clear sky pictures, resulting in a cloud index for the image (see Figure 7 and Figure 8 for examples). Complex computer models then analyse the image data, in conjunction with the position of the sun, aerosols, gasses, water vapour and a number of other parameters in order to calculate the reduction in extraterrestrial irradiance on its way through the atmosphere. Satellite data validation is generally achieved by comparison with detailed ground measurement data (Pinker & Laszlo 1992:207).

2.1.3.4 irradiance modelling

While quality surface measurement of irradiance is the optimum data source in solar energy application design, it is not always available for a particular site. This is generally due to limited meteorological stations equipped for continuous irradiance measurement, irregular calibration, lack of qualified personnel and funding aspects. The 'SOLATILT' program for Southern Africa, written by Geerdts and described in the Remote Area Power Supply (RAPS) Design Manual (Cowan (ed.) 1992:8), used the data of only 12 meteorological stations to represent the entire Southern African region.

Other than isolated industry and university test sites, the main source of ground measurement irradiation data in Southern Africa is from the South African Weather Service (SAWS). High accuracy pyranometers are reputed to be used by SAWS in the major cities in the country (Bekker 2007:3). Eberhard (1990) published a book on solar radiation data for South Africa, based on two decades of SAWS data. Tests and simulation analysis by Bekker (2007:2-6) from the University of Cape Town using the SunSim simulation package, found the accuracy of SAWS data to be questionable; - attributable to irregular calibration of measurement instrumentation.

The availability (or lack thereof) of solar irradiation data is discussed at length by Cros, Mayer and Wald (2004:29), who conclude that in most cases, the accuracy of

interpolated surface solar radiation data is less than required and that satellite derived assessments represent an accurate solution to the problem.

Geostationary satellites monitor the state of the atmosphere and the earth's cloud cover on a space-and-time continuous basis, with a resolution approaching one kilometre in the visible range. This information can be used to generate time and site specific irradiance data, as well as high resolution solar radiation maps (Perez, Ineichen, Moore, Kmiecik, Chain, George & Vignola 2002:307). According to a study by Zelenka, Perez, Seals and Renné (1999:199-207), satellite derived data has been shown to be the most accurate modelling option when operating beyond a twenty five kilometre radius of a ground station, when compared to low density ground measurement interpolation. Based on the Cros and Zelenka studies, it may be concluded that a viable and acceptable alternative to surface data is to use satellite data.

Figure 7 and Figure 8 illustrate typical satellite imagery for composite hourly data and monthly composite maps respectively.

The information generated from satellite imagery data is generally hemispherical irradiation on a horizontal surface (Pinker & Laszlo 1992:194-211). To calculate the solar irradiation on a tilted surface, which a solar receiver generally is, requires complex modelling and computation of the source data. The global irradiation needs to be separated into the individual irradiance components (as discussed in Section 2.1.3.2). Various prediction models are available for each of the irradiance components (or combinations thereof) and care should be taken in choosing a particular model, as many models are targeted (and verified) for a particular geographic and/or climatology region. In addition, Quaschning (2003:93) warns that data sets used in modelling predictions should cover a period of at least seven to ten years in order to ensure a representative sample, as annual variation in measured irradiation can exceed twenty percent.

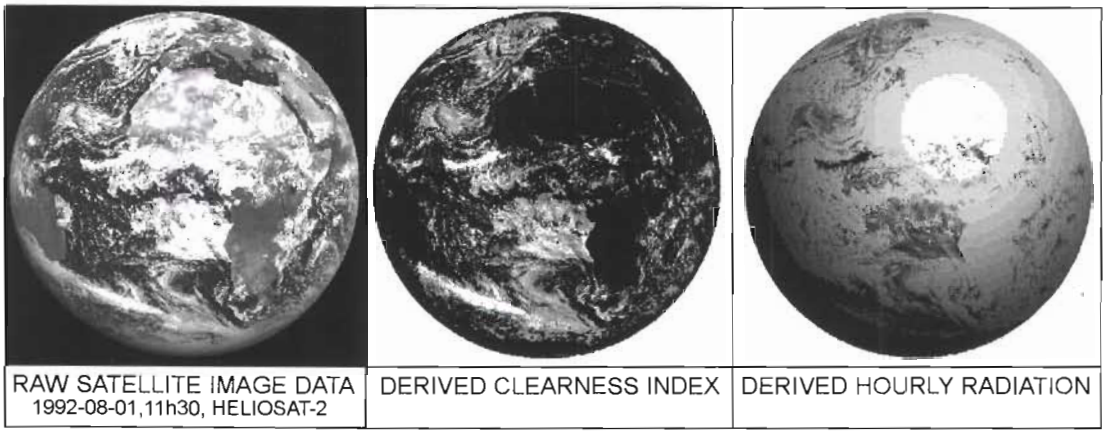

Figure 7 **Satellite image data for Africa**
(compiled from: Heliosat Project 1992)

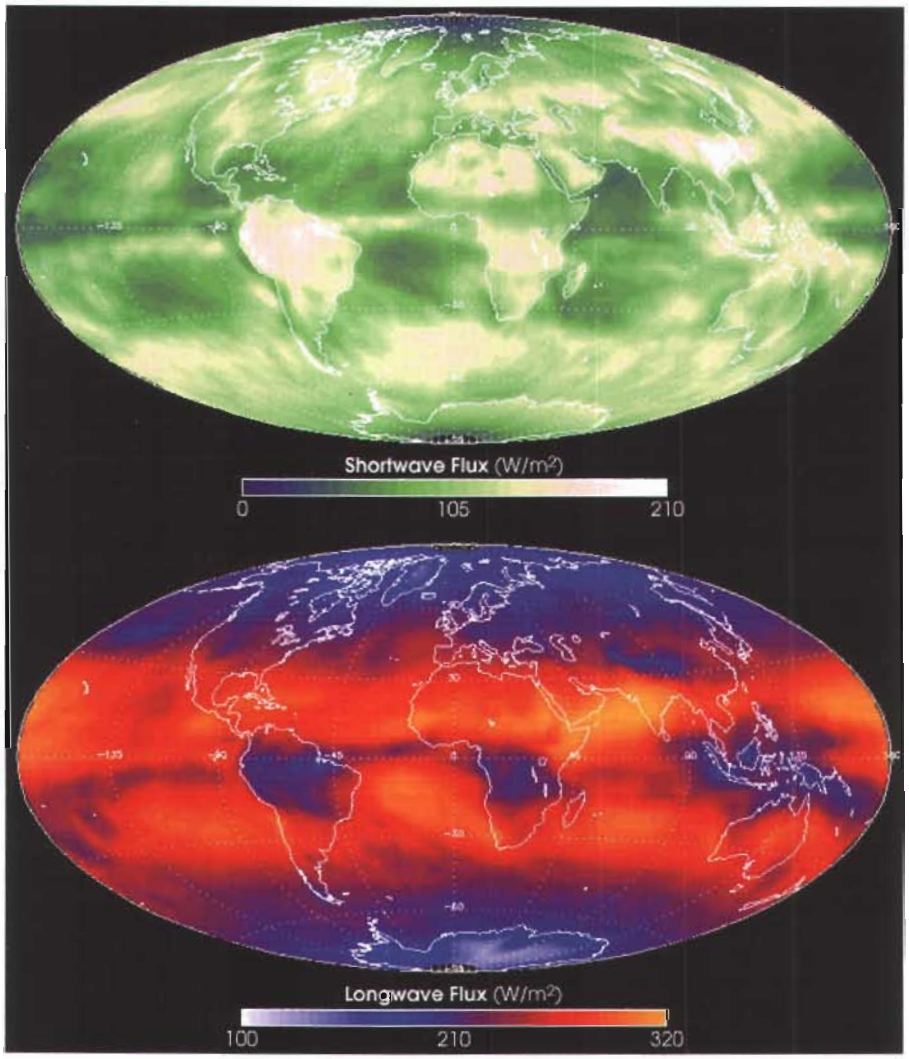

Figure 8 **Satellite composite monthly short- & long-wave radiation map**
(NASA CERES 2000)

Converting hemispherical data to direct beam irradiance is generally done by developing relationships between clearness indices (ratios of measured to extraterrestrial radiation values) denoted by the term K_t (clearness index), after research by Liu and Jordan (1960:1-19). The monthly average clearness index ($\overline{K}_t$) is calculated as follows:

$$\overline{K}_t = \frac{\overline{H}}{\overline{H}_0} \qquad (1)$$

where

$\overline{H}$ = The monthly average daily solar radiation on a horizontal surface.

$\overline{H}_0$ = the monthly average extraterrestrial daily solar radiation on a horizontal surface.

The value of K_t depend on location and season and is generally constrained within the limits $0,3 < K_t < 0,8$ (Whitlock 2004:4), where 0,3 is very overcast and 0,8 is perfectly sunny. Other climatology or meteorological parameters such as temperature, humidity, and cloud cover are also sometimes used to augment the clearness index approach.

Empirical correlations of diffuse to global ratios and diffuse to direct radiation can also be used to try and reduce errors in computing hemispherical radiation from estimates of direct and diffuse radiation, especially under overcast sky conditions. The Perez Anisotropic Diffuse Model (Perez, Ineichen, Seals, Michalsky, & Stewart 1990:271-289) is an example of an extensively used (RAPS, NASA SSE, SODA, METEONORM, *etc.*) and validated model (Perez, Stewart, Seals & Guertin 1988; Feuekmann & Zemel 1992:59; Myers 2003:11, *etc.*) for converting hemispherical data on a horizontal surface, to equivalent data for a tilted surface, by computing diffused irradiance on the tilted surface.

By way of example, the Perez Non-Isotropic/Extended Page Horizontal Diffuse Method as proposed by NASA (Whitlock 2004:8-9) is detailed in the following paragraphs. The anisotropic diffuse method of Perez *et al.* (1990:301-305) is used with ten year average NASA surface meteorology and solar energy (SSE) insolation and extended Page horizontal diffuse data sets as inputs. The Collares-Pereira and Rabl (1979:15-164) insolation equation (5) and Liu and Jordan (1960:1-19) diffuse equation (11) are used to obtain hourly values for the 'monthly average day' as listed in Table 2 (Klein 1977:325-329). The Perez tilt equation, '*Fx*' factors, *etc.* are applied to 'monthly average day' parameters in an hourly equation (2) using solar beam and surface/sky reflectance components, with the diffuse component based on the non-isotropic diffuse method of Perez *et al.* (1990:301-305). The resultant hourly tilted surface equation is:

$$H_{th} = (H_h - H_{dh})R_{bh} + H_{dh}\,[((1 - F_{1h}) \cdot (1 + \cos\beta_h)/2) + F_{1h}(a_h/b_h) + F_{2h}\sin\beta_h] + H_h \cdot \rho_s[(1 - \cos\beta_h)/2] \quad (2)$$

where

ρ_s is taken from global monthly average, satellite-based SSE data set albedo values (for preliminary estimates).

β_h = hourly slope of the PV array relative to a horizontal surface and is a constant for fixed panels or panels in a vertical axis tracking system.

$$a_h = \cos\theta_h \text{ or zero, whichever is maximum.} \quad (3)$$

$$b_h = \cos\theta_{zh} \text{ or } 0{,}087\text{, whichever is maximum.} \quad (4)$$

The hourly horizontal surface insolation, H_h; horizontal diffuse, H_{dh}; and horizontal beam, H_{bh}, are calculated as:

$$H_h = r_t H \quad (5)$$

$$H_{dh} = r_d H_d \quad (6)$$

$$H_{bh} = H_h - H_{dh} \quad (7)$$

$$r_t = (\pi/24) \cdot (A + B\cos\omega) \cdot [(\cos\omega - \cos\omega_s)/(\sin\omega_s - \omega_s \cos\omega_s)] \quad (8)$$

with

$$A = 0{,}409 + 0{,}5016 \sin[\omega_s - (\pi/3)]$$

$$B = 0{,}6609 + 0{,}4767 \sin[\omega_s - (\pi/3)]$$

from Collares-Pereira and Rabl (1979:155-164).

$$R_{bh} = \cos\theta_h/\cos\theta_{zh} \quad (9)$$

$$H_d/H = [a + (b \cdot \overline{K}_t)] \quad (10)$$

where

H = the monthly average horizontal irradiation impinging on the Earth's surface, from the SSE data set

$\overline{K}_t$ = the monthly average clearness index

H_d is derived from the extended Page method (Page 1964:378). The a and b values for a particular cell are determined from comparison with a group of reference sites.

$$r_d = (\pi/24) \cdot [(\cos\omega - \cos\omega_s)/(\sin\omega_s - \omega_s \cos\omega_s)] \quad (11)$$

from Liu and Jordan (1960:1-19).

$$\cos\theta_{zh} = (\cos\phi \cdot \cos\delta \cdot \cos\omega) + (\sin\phi \cdot \sin\delta) \quad (12)$$

where

θ_{zh} = solar zenith angle (in radians)

δ = solar declination

ϕ = geographic latitude

$$\cos\theta_h = (\cos\theta_{zh} \cdot \cos\beta_h) + (1 - \cos\theta_{zh}) \cdot (1 - \cos\beta_h) \cdot [\cos(\gamma_{sh} - \gamma_h)] \quad (13)$$

$$\gamma_{sh} = \sin^{-1} [(\sin\omega \cdot \cos\delta)/\sin\theta_{zh}] \quad (14)$$

Equation (14) returns the hourly solar azimuth angle, *i.e.* the angle between the line of sight of the sun into the horizontal surface and the local meridian. Azimuth is zero facing the equator, positive west, and negative east. The section on Solar Geometry provides more detail on this. γ_h = hourly surface azimuth of the tilted surface *i.e.* the angle between the projection of the normal to the surface into the horizontal surface and the local meridian. γ_h is a constant for fixed surfaces. $\gamma_h = \gamma_{sh}$ for both vertical and two-axis tracking systems. ω = solar hour angle for each daylight hour relative to solar noon, between sunrise plus 30 minutes and sunset minus 30 minutes. The sun is displaced 15 degrees from the local meridian for each hour from local solar noon (Whitlock 2004:6).

Coefficients which lead to the F_{1h} and F_{2h} (circumsolar and horizon brightening coefficients, respectively) are based on experimental measurements. Climate regions include steppe/semi-arid, desert/arid, temperate continental and subtropical land, temperate ocean as well as highly polluted environments (Perez *et al.* 1990:271-289). The experiment consisted of simultaneous measurements of global, vertical surface, tilted surface (various azimuths), and direct-normal values for both solar radiation and illuminance. The solar radiation measurements were synthesized with hourly parameters Ep_h, Del_h, and θ_{zh} , where:

$$Ep_h = (((H_{dh} + H)/H_{dh}) + [1{,}041\theta_{zh}^3])/[1 + (1{,}041\theta_{zh}^3)] \quad (15)$$

= sky clearness, range = 1,0 (overcast) to 6,2 (clear sky)

$$Del_h = H_{dh}/(\cos\theta_{zh}) \quad (16)$$

= sky brightness

Given hourly values of Ep_h, Del_h, and θ_{zh}, values for coefficients *F11* through *F12* are determined from Table 3. Hourly values for F_{1h} and F_{2h} are determined from:

$$F_{1h} = F11 + (F12 \cdot Del_h) + (F13 \cdot \theta_{zh}) \quad (17)$$

$$F_{2h} = F21 + (F22 \cdot Del_h) + (F23 \cdot \theta_{zh}) \quad (18)$$

Monthly average tilted surface radiation, H_t, is estimated by summing H_{th} over the 'monthly average day' from Table 2.

Table 2 Monthly average day
(Klein 1977:325-329)

Month	Day in Month	Declination	Month	Day in Month	Declination
January	17	-20,9	July	17	21,2
February	16	-13,0	August	16	13,5
March	16	-2,4	September	15	2,2
April	15	9,4	October	15	-9,6
May	15	18,8	November	14	-18,9
June	11	23,1	December	10	-23,0

The 'monthly average day' is the day (in the month) whose declination is closest to the average declination for that month

Table 3 Perez irradiance coefficients
(Perez *et al.* 1990:271-289)

Ep Range	*F11*	*F12*	*F13*	*F21*	*F22*	*F23*
1,000 - 1,065	-0,008	0,588	-0,062	-0,060	0,072	-0,022
1,065 - 1,230	0,130	0,683	-0,151	-0,019	0,066	-0,029
1,230 - 1,500	0,330	0,487	-0,221	0,055	-0,064	-0,026
1,500 - 1,950	0,568	0,187	-0,295	0,109	-0,152	-0,014
1,950 - 2,800	0,873	-0,392	-0,362	0,226	-0,462	0,001
2,800 - 4,500	1,132	-1,237	-0,412	0,288	-0,823	0,056
4,500 - 6,200	1,060	-1,600	-0,359	0,264	-1,127	0,131
6,200 →	0,678	-0,327	-0,250	0,156	-1,377	0,251

The intended use of a solar energy model dictates its complexity and precision requirements. Myers (2003:8) classified solar/meteorological data type requirements with respect to application usage as indicated in Table 4, simplifying the required data selection process relative to the type of application.

Table 4 Radiation model data type relative to application (Myers 2003:8)

Type of Data	Time Resolution	Application
Hemispherical, vertical surface, cardinal dir.	Seasonal/Daily	Glazing energy balance (energy or power)
Illuminance, vertical surfaces, cardinal dir.	Seasonal/Daily	Day-lighting
Hemispherical tilt	Monthly/Annual	Fixed Flat Plate
Hemispherical tracking	Monthly/Annual	Tracking Flat Plate
Direct normal	Monthly/Annual	Focusing/concentrating systems
Sun shape (disk + circumsolar) variation	Varies	Concentrating tracking collector
Monthly mean daily total	Monthly/Daily	Sizing and design specification, economics
Monthly mean	Monthly	Sizing and design specification, economics
Daily profiles	Hourly	System simulation modelling and rating
8760 Hourly data for year hemispherical and/or direct	Hourly	System simulation, economic analysis (multiple years for min/max performance)
10 to 30 year hourly power	Hourly	Performance and economics, system lifetime
Daily profiles power	Sub Hourly	System responses to clouds, *etc.*

2.1.4 peak sun hours

Peak Sun Hours (PSH) is an energy unit bounded by irradiance and time, *i.e.* it is a unit of irradiation (or insolation) usually expressed in daily terms (kWh/m²/day). The number of peak sun hours per day is equal to the daily irradiation at the location (kWh/m²) divided by peak irradiance (1000 W/m²) (McNutt, Kroposki, Hansen,

DeBlasio, Thomas, Durand, Rosenthal & Hutchinson 1999:2). It is best explained by way of an example: If 1 m² of the earth's surface receives 1 kW of irradiance for one hour, this would be equal to one PSH. If the same 1 m² of surface receives 0,5 kW of irradiance for 2 hours, this would also be equal to one PSH. The hourly irradiance time equivalence to 1 kWh/m² for a day is said to be the PSH for that day. This is illustrated in Figure 9. For fixed plate solar receivers it is usually a mean monthly, seasonal or yearly value and is typically the value indicated on solar surface plot contours as found on irradiation/insolation maps.

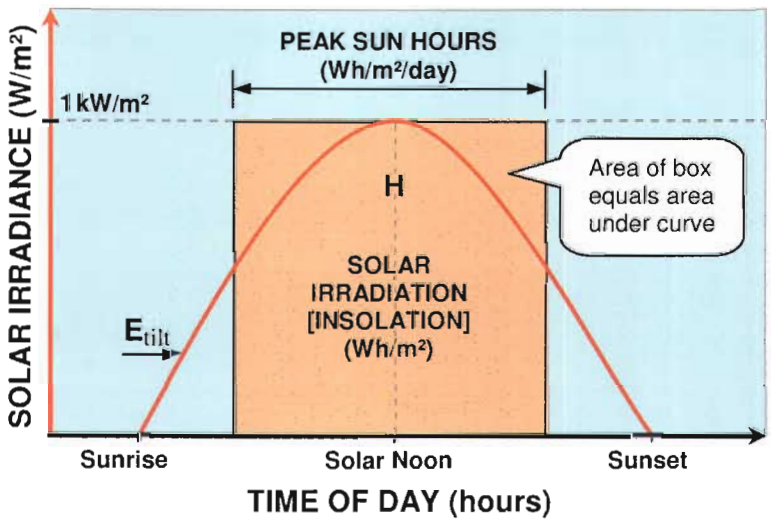

Figure 9 **Peak sun hours**

Equivalent Sun Hours (ESH) is a more conservative representation of PSH, using monthly historical values for the year that had the least, or minimum, monthly averaged value in a ten-year period. This is the prudent and therefore recommended energy parameter to use when designing 'delivery-critical' solar powered applications.

2.1.5 air mass

Optical air mass (AM) is a useful quantity when dealing with atmospheric effects. It indicates the relative distance sunlight must travel through the atmosphere to reach a given location. As there are no atmospheric effects outside the earth's atmosphere, this condition is referred to as air mass zero (AM 0). Quaschning (2003:91) describes

air mass one (AM 1) as corresponding to the sun being directly overhead (solar noon – sun's rays perpendicular to the earths surface), with sunlight only having to pass through the air mass of the atmosphere once. The value of the air mass decreases with an increase in solar altitude and increases with a decrease in solar altitude, where solar altitude (γ_S) is the angle of the sun above the horizon. An air mass two (AM 2) value would therefore indicate that sunlight has travelled twice the distance in the atmosphere than that of an air mass one (AM 1) value. Air mass 1,5 (AM 1,5) is considered to be the most representative of average daily terrestrial conditions and is commonly used as a reference condition when rating photovoltaic modules (Argaw 2004:6; RS 1999:3). Figure 10 illustrates the relative air mass distance that the suns rays pass through in the atmosphere.

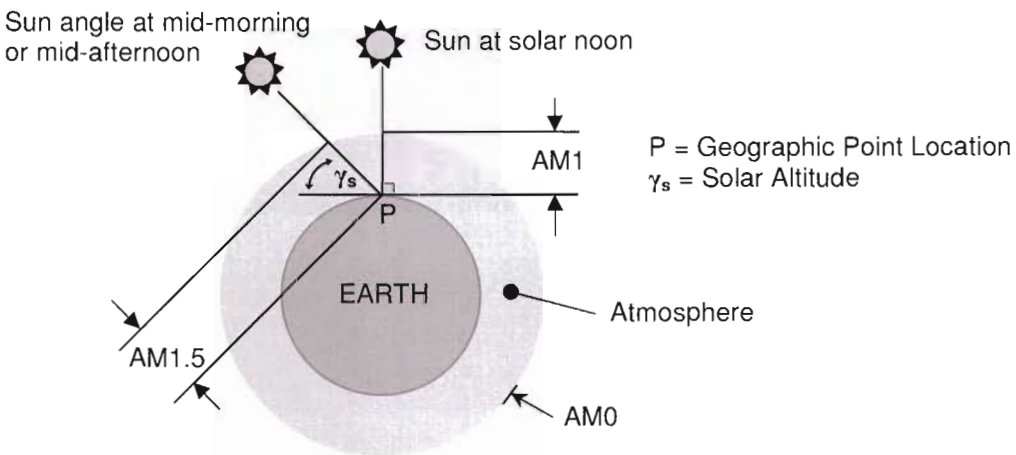

Figure 10 Air mass (AM) and sun incidence angle

In general, the definition of air mass is as stated in equation (19), although, being a trigonometric equation, other derivations are often used.

$$AM = \frac{1}{\sin(\gamma_S)} \tag{19}$$

The air mass calculation can be detailed in a more complex manner by factoring in refraction, altitude and the like, as given, for example, by the METEONORM optical

air mass equation by Remund and Kunz (2003:36), who note that "the value of the optical air mass declines with increasing altitude, and increases with declining solar altitude". The more complex calculation forms are often required for precision systems modelling.

2.2 Solar geometry

In solar energy applications, knowledge of the geometrical parameters of the solar trajectory is required. The major parts of the formulae for the solar trajectory calculations have been taken from the European Solar Radiation Atlas (ESRA) (Greif & Scharmer 2000:23-26). Angles used in the solar geometry formulae are given in radians, unless otherwise stated.

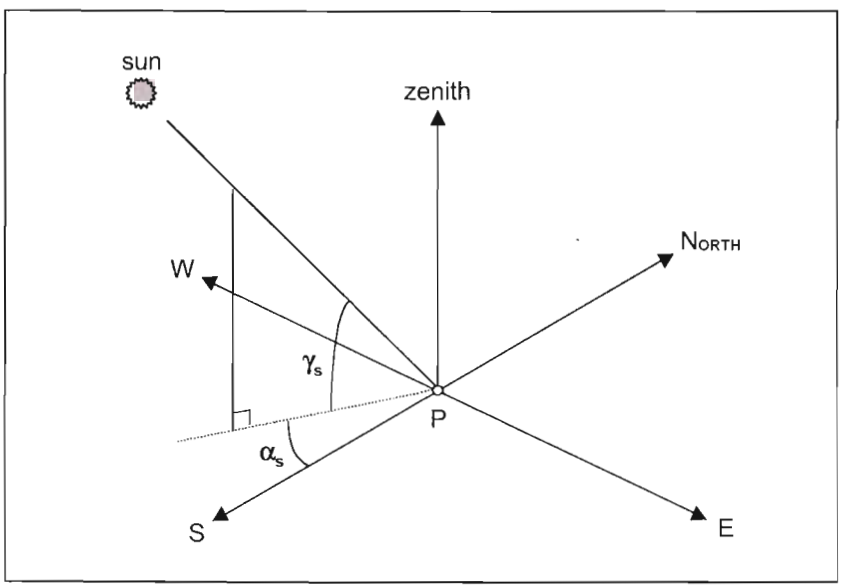

Figure 11 **Solar position viewed from a point P on the earth's surface (ESRA 2000)**

Viewed from a fixed point on the earth's surface (P), the solar position is defined by two angles (see Figure 11 and Figure 12), namely:

- Solar altitude (γ_s): Angle between horizontal plane and line joining the centres of the earth and the sun (solar elevation).
- Solar azimuth (α_s): Angle between the projection of a straight line joining the centres of the earth and the sun on the horizontal plane and due south. $\alpha_s > 0$ in a positive solar direction *i.e.* west of the North/South meridian, $\alpha_s < 0$ in a negative solar direction *i.e.* east of the North/South meridian.

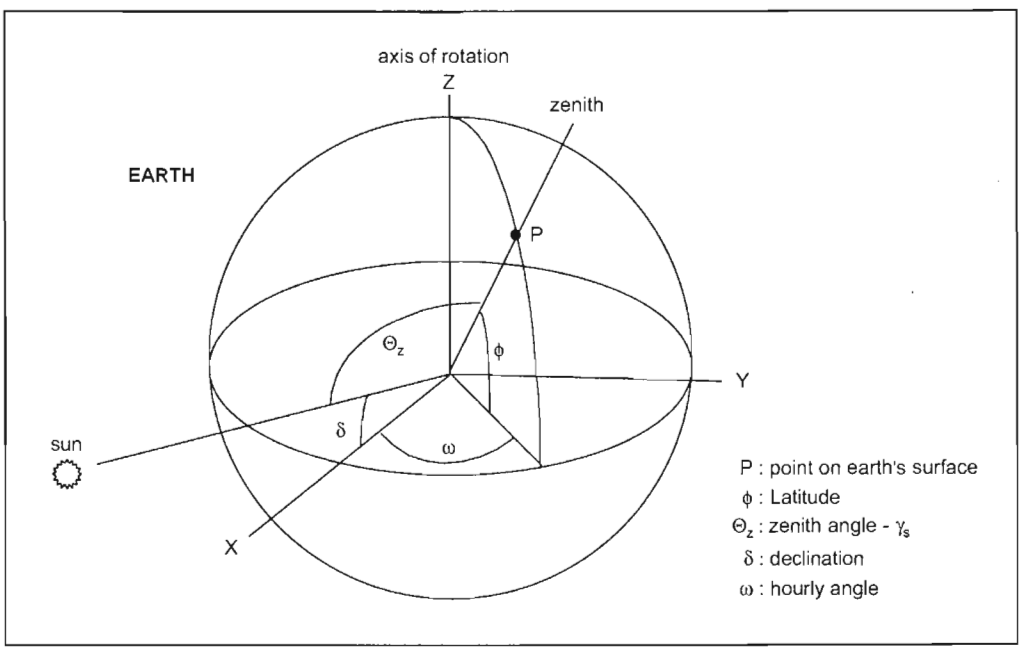

Figure 12 **Solar position (declination, zenith angle and hourly angle) (ESRA 2000)**

The two angles may be expressed as a function of latitude (ϕ), solar declination (δ) and hourly angle (ω):

$$\gamma_s = [\sin\phi \cdot \sin\delta + \cos\phi \cdot \cos\delta \cdot \cos\omega] \tag{20}$$

$$\alpha_s = \text{Arcsin}\left[\frac{\cos\delta \cdot \sin\omega}{\cos\gamma_s}\right] \tag{21}$$

The declination (δ) is the angle between the equatorial plane and the straight line joining the centres of the earth and the sun. It is determined by the laws governing the solar trajectory. The noon declination can be calculated accurately using equation (22).

$$\delta = 0.0064979 + 0.405906\sin\omega_t + 0.0020054\sin 2\omega_t - 0.002988\sin 3\omega_t - 0.0132296\cos\omega_t + 0.0063809\cos 2\omega_t + 0.0003508\cos 3\omega_t \quad (22)$$

where

$$\omega_t = \omega_0(dy + t_1)$$

$$t_1 = -0{,}5 - \frac{\lambda}{2\pi} - n_0$$

$$\omega_0 = \frac{2\pi}{365{,}2422}$$

$$n_0 = 78{,}8946 + 0{,}2422\cdot(y - 1957) - INT\left[\frac{(y-1957)}{4}\right]$$

where *INT* stands for integer part of the argument, y for year and dy for day number of the year. The declination is zero at the Equinox, positive 23,45 degrees at the summer solstice and negative 23,45 degrees at the winter solstice (refer to Figure 13). It is this variation that is responsible for the seasons of the year.

The hour angle (ω) in radians, is equal to the solar time (ST) also in radians. It is calculated using the solar time (ST) in hours:

$$\omega = (ST - 12)\frac{\pi}{2} \quad (23)$$

An astronomical day begins and ends when the centre of the sun's disk is precisely on the (flat) horizon, ignoring atmospheric refraction. The sunrise/sunset hour angle (ω_{ss}) is calculated by solving equation (20), with $\gamma_s = 0$.

2.2.1 sun elevation

The angular elevation of the sun above horizon is commonly called sun elevation, solar elevation or solar altitude angle. It is the angle between the centre of the solar disc (sun) and the horizontal plane. This angle is zero at sunrise and sunset and maximum when the sun is at its zenith. The zenith of the sun is defined as the position in the sky at which the sun at its highest for a given geographical location. Zenith is always reached at 12 o'clock (noon), local solar time.

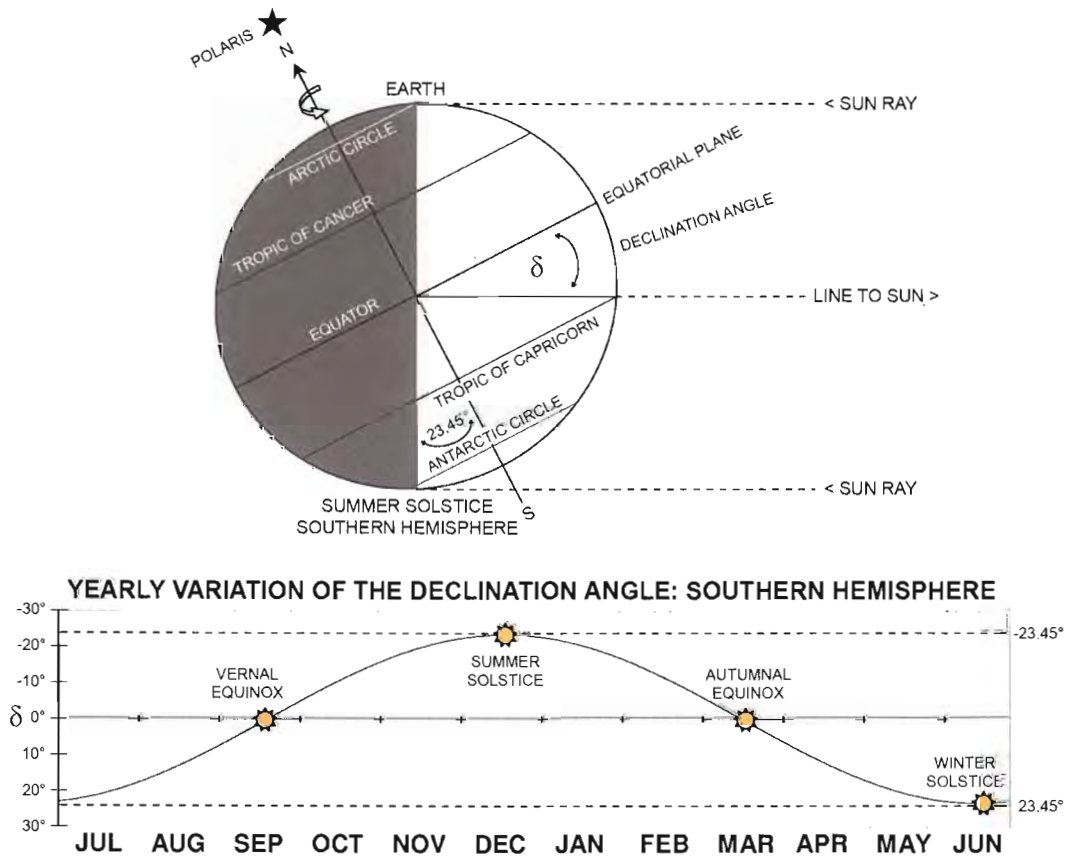

Figure 13 Declination angle variations for the earth

The sun elevation is a function of the season and the geographic latitude of the location. The higher the latitude, the smaller the maximum degree of sun elevation will be. For example, at 30° south latitude (the latitude of Durban), the maximum solar elevation is approximately 37° at the winter solstice in June (southern hemisphere), while it is only 7° at 60° south latitude. At the summer solstice in

December, maximum solar elevation is 83° at 30° south latitude and 53° at 60° south latitude. The seasonal declination of the earth at the summer solstice for the southern hemisphere is illustrated in Figure 13.

The duration of the day is also a function of the geographic latitude and season of the year. In the southern hemisphere, the length of the day is longest at the summer solstice on 21 December and shortest at the winter solstice on 21 June. The influence of latitude on day duration is reasonably constant for a given geographic latitude. On 21 June, the duration of a day is approximately 10 hours at 30° south latitude, while it is less than 6 hours at 60° south latitude. The duration of a day on 21 December for 30° south latitude is 14 hours. This equates to an increase of 4 hours with respect to the winter solstice. At 60° south latitude the increase is much larger, with the duration of a day equal to 19 hours. That is an increase of approximately 13 hours between winter and summer day duration.

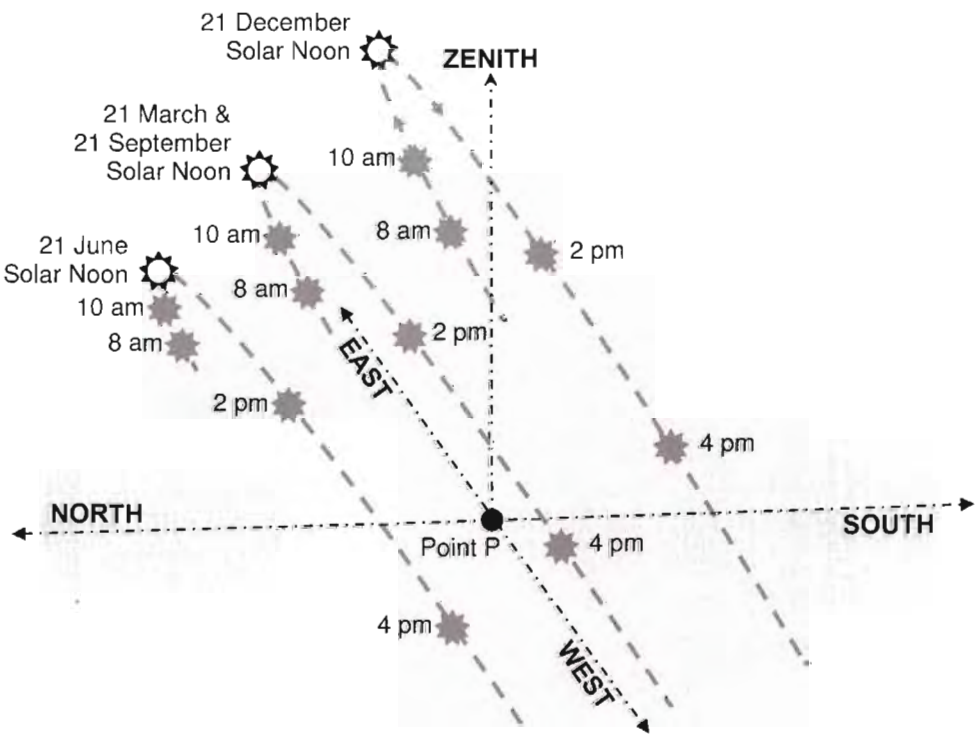

Figure 14 **Seasonal sun paths for 30° South latitude**

Figure 14 illustrates various sun paths relative to a point P on the earth's surface at 30° south latitude. The seasonal changes in the suns path are clearly visible. This example shows that for the given location in winter, the sun rises in the northeast, sets in the northwest, has a short daily path and rises to a shallow angle above the horizon. In summer the sun rises in the southeast, sets in the southwest, has a longer daily path and peaks at a much higher angle above the horizon at midday.

2.2.2 solar window

The seasonal variation in apparent sun path relative to a stationary object on the surface of the earth creates a solar availability window. This 'solar window' (illustrated in Figure 15) represents the effective area through which useful levels of sunlight pass throughout the year for a specific location.

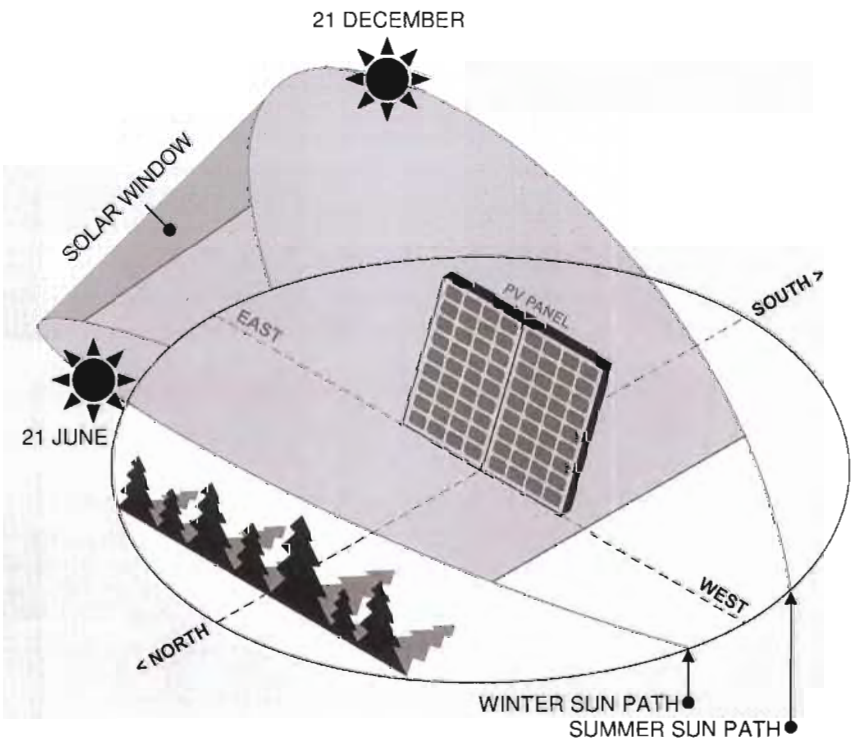

Figure 15 Solar window

When doing a design, the solar window should be kept free of shading (typically from trees or buildings) from 9 a.m. to 3 p.m. solar time, when maximum solar

radiation occurs. The solar altitude of the sun on 21 December and 21 June (the summer and winter solstices) determine the upper and lower boundaries of the solar window. It is generally the lowest altitude of the sun, reached on the winter solstice, which is most important for protecting solar energy delivery. If the longer winter shadows do not shade the solar collector or photovoltaic module, it is usually safe to assume that shorter summer shadows will not shade the collector either.

The differing effect of the seasonal change in plant foliage is another factor that determines the amount of sunlight that will reach the solar collector or photovoltaic module. It should be noted that even the shading provided by the bare winter branches of a deciduous tree can cause significant shading on a solar collector, and particularly on a photovoltaic module. Shading of only one cell within a PV module can reduce the module's power output as much as 75 percent. It should also be noted that at low solar altitudes the atmosphere, clouds, smog and air pollutants can absorb or deflect considerable amounts of solar radiation. So much solar radiation can be lost at low solar altitudes that altitudes below twelve degrees are essentially regarded as ineffective for the collection of solar energy.

The energy available for solar powered applications as defined by the solar window for a specific location is encapsulated in the 'Peak Sun Hour' (or equivalent) rating given for that location, all local conditions being at optimum *i.e.* no shadows, *etc.*

2.2.3 solar collector orientation

A solar collector gathers the most sunlight when it is perpendicular to the suns rays. Ideally, it should be tilted to follow the sun's change in elevation during the course of the year, and turn to follow the sun's apparent path from east to west during the day. Tracking can be applied to photovoltaic installations via active or passive tracking systems; however the hardware, machinery and controls needed to achieve this are usually not cost-effective when used in small rural applications.

2.2.3.1 tilt angle

The energy available to a solar receiver on the earth's surface is dependant on many factors, the two predominant variables when considering tilt being the season and daily sun path. Figure 16 illustrates that the energy available to a solar receiver is at a maximum when the receiver is perpendicular to the incident irradiance. This is a general guideline, although it must be noted that local diffused and reflected irradiance (albedo) components also play a role in determining the optimum tilt angle of a receiver (Ineichen, Perez & Seals 1987:301-305) and should be taken into consideration for final-design tilt estimates.

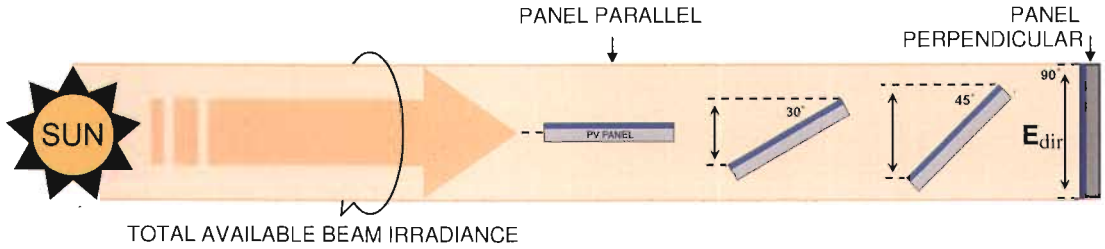

Figure 16 **Solar receiver surface area vs. Tilt, for direct beam irradiance**

In order to maintain a perpendicular angle between the solar receiver and the incident irradiance, solar tracking devices are often used. This adds an extra dimension of complexity, cost and maintenance that is best avoided in remote rural areas.

The alternative is to maintain a solar receiver at a fixed position with a set tilt angle and facing due North (true/solar North, for the southern hemisphere (RS 1999:7)). The required tilt angle for this configuration then becomes a function of the geographic latitude, season and position of the sun at solar noon. The tilt angle (θ) is often set at a 'rule of thumb' value equal to latitude (yearly) or latitude plus (summer) or minus (winter) 15 degrees (Kyocera Solar 2002:33), but can be calculated for any day of the year with simple trigonometry and the solar declination angle (δ), according to the following equation:

$$\theta = \left| L_t - \delta \right| \qquad (24)$$

where

θ = Tilt angle in degrees from the southern horizontal, in a south-north vertical plane

L_t = Geographic latitude for the location in degrees

δ = Solar declination (in degrees); from equation (22) converted to degrees ($\times 180/\pi$)

Alternatively, the simple equation of Cooper (Duffie & Beckman 1991:13) given in equation (25) may be used.

$$\delta = 23.45 \cdot \sin\left[\frac{284 + dy}{365} \cdot 360\right] \qquad (25)$$

where

dy = day number of the year, 1st January being one, 1st February being 32 and so on.

The tilt angle concept for the southern hemisphere is illustrated in Figure 17.

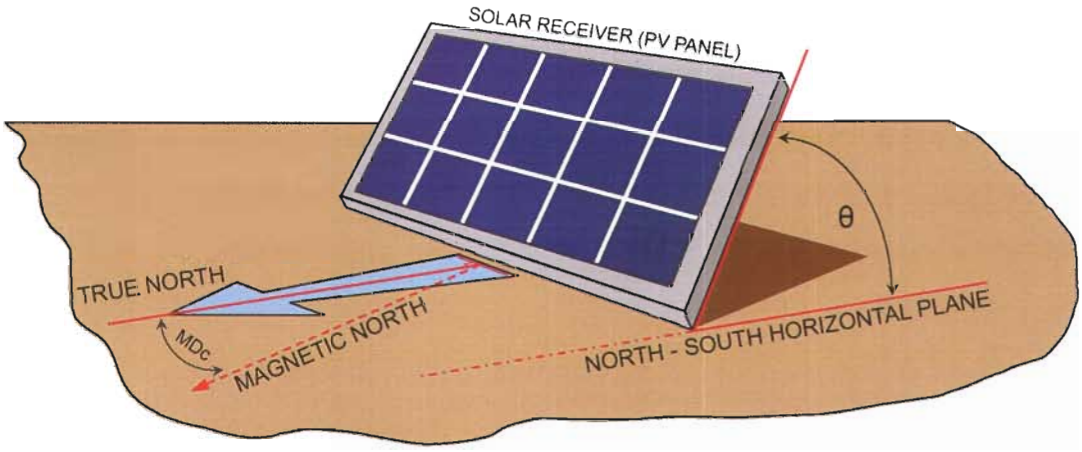

Figure 17 **Tilt angle for a solar receiver (adapted from Denny 2006)**

For optimal utilisation of available solar irradiance, a non-tracking, fixed installation's tilt angle should be adjusted as frequently as possible, typically monthly. This frequent adjustment requirement is sometimes problematic due to

factors such as seasonal usage, remoteness of location or resources. To overcome this, seasonal, half-yearly and even yearly, mean tilt values are commonly used.

2.2.3.2 magnetic declination correction

Non-Tracking solar receivers should be orientated to true (solar) North. This can be achieved using a global positioning system (GPS), but is commonly set via a simple compass bearing in remote rural areas.

True North is not the same as magnetic North at most locations on the earth's surface. Because of the earth's magnetic field, a compass reading of North varies by as much as 24 degrees from true North in some parts of Southern Africa. This variance is called magnetic declination and is usually represented as the number of degrees that compass (magnetic) North varies from true (solar) North at a specific point in time. In Southern Africa, magnetic North is west of true North. This implies that any magnetic declination correction (MDC) is added to the compass reading in an easterly (clockwise) direction.

Magnetic declination changes slowly over time, so caution should be exercised when using the correction value found on topographic maps, as a yearly compensation must be factored into the published declination correction figure.

A commonly accepted 'rule of thumb' (NOVA 2002:12) is that an azimuth orientation error of 10 degrees will result in a loss of 2 percent of a photovoltaic modules output. The actual value may be estimated from the direct solar irradiance that reaches the inclined surface, attenuated depending on the cosine of the angle of incidence (Quaschning 2003:90). Losses increase the greater the applied aiming error, *e.g.* 10° = 1,5 percent, 20° = 6 percent, 30° = 13,4 percent, *etc.* A 90° aiming error will not however, result in a photovoltaic module giving a zero output, due to the localised albedo components described previously.

This illustrates that a simple error in orientation of only the magnetic declination value can reduce the output of a photovoltaic module by up to ten percent; something that is totally avoidable with correct orientation.

2.3 Principles of a photovoltaic system

Photovoltaic (PV) cells are semiconductor devices that convert light directly into electricity. Because the source of the light (irradiance) is invariably the sun, they are often referred to as solar cells. The term photovoltaic derives from a combination of the Greek word 'phos', meaning light and the electromotive force descriptor 'volt' (after Alessandro Volta). The output of a PV cell (or connected array of cells) is direct current (DC) electricity.

The history of photovoltaic devices is described by Masters (2004:445) and Nelson (2003:2-4) and dates back to 1839, when French physicist Alexandre-Edmond Becquerel discovered the photovoltaic effect while illuminating a metal electrode in an electrolytic solution. Thirty-eight years later, British physicist William Adams and student Richard Day observed a photovoltaic effect in solid selenium. Other researchers such as Fritts, Lange, Grondahl and Schottky also did pioneering work on selenium and cuprous oxide PV cells. This resulted in the first practical application of a solar cell, as a light meter for photographic applications. Following the world's entry into the semiconductor age with Schottky's development of the p-n junction model, Chapin, Fuller and Pearson of Bell Laboratories exploited the PV effect as an energy conversion process by producing the first generation of crystalline silicon based solar cells in 1954, with an efficiency of around five percent.

2.3.1 operating principles of a solar cell

A typical silicon solar cell is a thin wafer consisting of an ultra-thin layer of phosphorus-doped (n-type) silicon on top of a thicker layer of boron-doped (p-type) silicon. An electrical field is created near the top surface of the cell where these two materials are in contact, called the p-n junction. When sunlight strikes the surface of a solar cell, this electrical field provides momentum and direction to light stimulated

electrons, resulting in a flow of current when the cell is connected to an electrical load.

From Quaschning (2004:81), the operating principles of a solar (PV) cell can be described in simplistic terms using the analogy of electrons and 'holes'. Electrons and the 'holes' they leave behind are negatively and positively charge carriers respectively and usually appear in pairs within solid matter. Semiconductor materials are used to produce solar cells, using the characteristics of the material to make it easy for incoming light photons to release electrons from the electron-hole pair binding. Leaving the holes behind them, the released electrons can move freely within the solid. This movement has no clear direction, so in order to derive benefit from it, the collection of electrons is required. To facilitate this aim, the semiconductor material is doped (polluted) with 'impure' atoms, typically phosphorous for n-type and boron for p-type layers in polycrystalline cells. The two different kinds of atoms produce an n-type and a p-type region inside the semiconductor. These two neighbouring regions generate an electrical field that can collect electrons, drawing free electrons released by the sunlight photons to the n-type region. The holes 'move' in the opposite direction, into the p-type region.

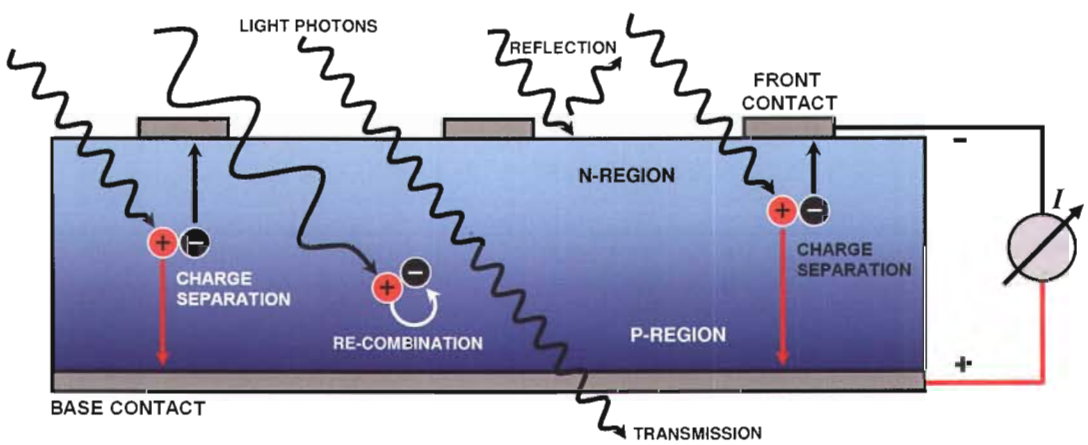

Figure 18 **Processes occurring in a solar cell subjected to light (adapted from Quaschning 2004:82)**

Not all of the energy from the sunlight can generate free electrons, due to various factors. Part of the sunlight is reflected from the surface of the solar cell, some even passing through the cell. In some cases, electrons and holes recombine before arriving at the n-type and p-type regions. Additionally, if the energy of the photon is too low, as is the case with light at longer wavelengths (such as infrared), there is insufficient energy available to release an electron. On the other hand, if the photon energy is too high, only a part of its energy is needed to release the electron, the remainder being converted into (and lost to) heat. Figure 18 illustrates these processes in a solar cell.

Detailed information on photovoltaic cells is available from many literature sources, *e.g.* Townsend (1989), Eckstein (1990), Zweibel (1990), Duffie *et al.* (1991), as well as from professional organisations, manufacturers and internet sources.

From Quaschning's description of solar cell materials (Quaschning 2004:82), it may be deduced that various semiconductor materials are suitable for solar cell production, silicon currently being the most prolifically used. It is the second most common chemical element in the earth's crust (after oxygen). Silicon is found mainly in quartz sand (SiO_2) and is extracted using a high temperature reduction process. Impurities are then removed, resulting in a polycrystalline silicon product. Polycrystalline silicon crystals are oriented in multiple directions, separated by grain boundaries that introduce efficiency losses. Seeding a single crystal at high temperatures can transform the polycrystalline silicon into mono-crystalline silicon. With no grain boundaries present in the resulting material, losses within a mono-crystalline solar cell are reduced. The drawback to producing mono-crystalline silicon lies in the fact that it requires more energy to produce, thus making it more expensive.

Besides crystalline silicon, thin-film modules show promise as a viable option in the near future. They can be made from amorphous silicon and other materials such as cadmium telluride (CdTe) or copper indium diselenide (CIS or $CuInSe_2$). Thin-film modules can be produced using only a fraction of the semiconductor material

necessary for crystalline cells and their development potential is therefore high. It is not clear which material will drive future markets but it appears that crystalline solar cells will continue to dominate in the near future. Other materials could become more prominent, provided they can be produced and processed more economically.

2.3.1.1 solar cell parameters

Photovoltaic data sheets present many parameters, with the most common terms relating to crystalline solar cells being detailed below.

Light striking a solar cell generates a current that varies with the cell voltage. Current–voltage characteristics usually show this correlation. When the load (voltage) of a solar cell is short-circuited, it is possible to measure the 'short circuit current' I_{SC}, proportional to irradiance on the solar cell. The I_{SC} rises with increasing temperature, although the standard temperature for reporting short circuit current is usually 25 °C. If the cell current is equal to zero (no load connected), the solar cell is described as 'open-circuit'. The cell voltage then becomes the 'open circuit voltage', V_{OC}. The dependence of V_{OC} on the irradiance is logarithmic and decreases at a faster rate than the I_{SC} increases, with rising temperature. This results in a solar cell's maximum power and efficiency decreasing with rising temperature. These principles are illustrated in Figure 19. Generally a temperature rise of 25 °C will cause a drop in PV cell output power of about ten percent (RS 1999:5).

Figure 20 illustrates solar cell characteristics, showing the current–voltage and power–voltage relationships. From this it can be seen that a solar cell generates its maximum power at a certain voltage. It is also clearly evident that the power curve has a point of maximum power. This is called the 'maximum power point' or MPP. The maximum power point voltage (V_{MPP}) is less than the open circuit voltage, and the MPP current (I_{MPP}) is lower than the short circuit current. At the MPP, current and voltage have the same relation to irradiance and temperature as the short circuit current and open circuit voltage. In terms of dependence on irradiance, the electrical current dominates the device's behaviour, so that MPP power is nearly proportional to the irradiance *i.e.* it is predominantly regarded as a current source.

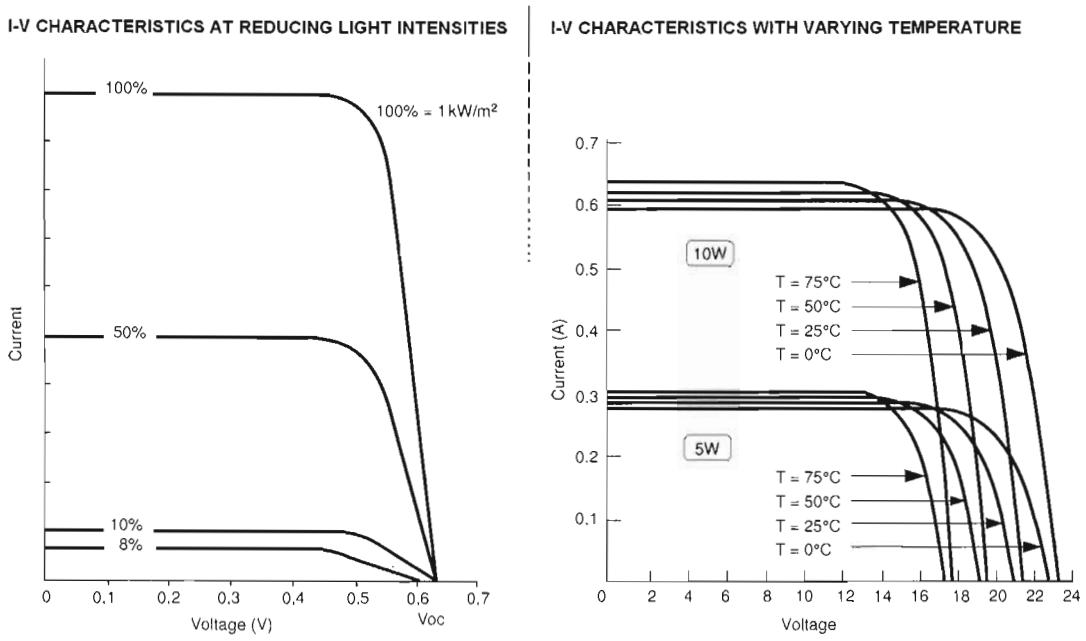

Figure 19 **Light & temperature characteristics of a polycrystalline solar cell (RS 1999:5)**

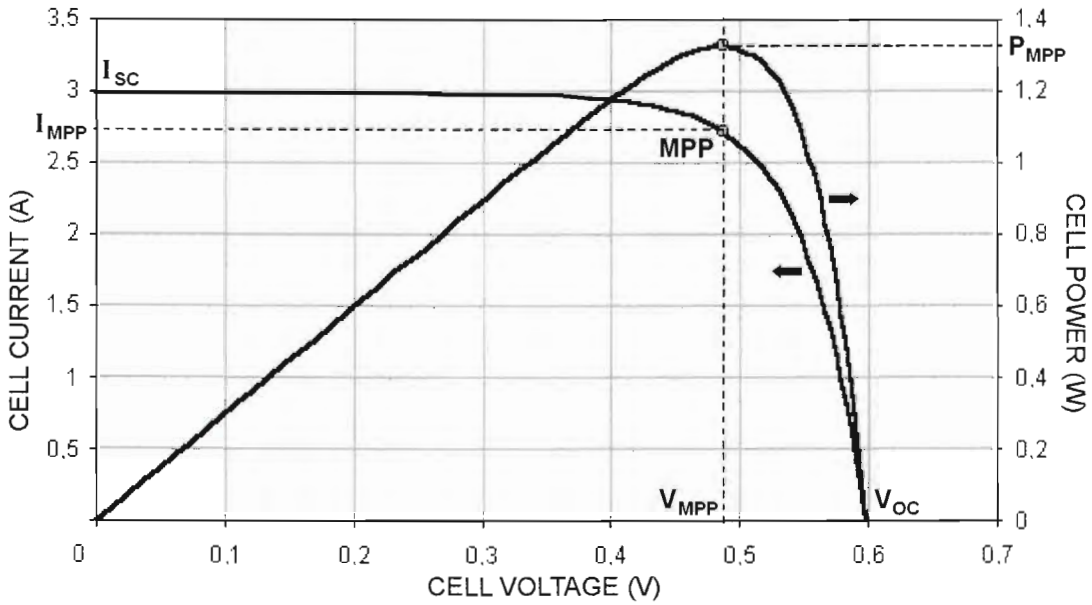

Figure 20 **Solar cell I-V & P-V characteristics, showing MPP (adapted from Duffie & Beckman 1991:750; Quaschning 2004:83)**

Module output parameters such as V_{OC}, I_{SC}, V_{MP}, I_{MP}, P_{MAX} and the MPP parameters only have meaning when the rating conditions for these outputs are specified (McNutt *et al.* 1999:2; RS 1999:2-4), *i.e.* In order to make solar cells and modules comparable, the measurements are taken under predefined rating conditions, the most common of which are noted in the following paragraphs.

Standard Test Conditions (STC):

- Irradiance at 1000 W/m²
- Cell temperature of 25 °C
- Air mass of AM1,5
- Wind speed not greater than 1,0 m/sec

Standard Operating Conditions (SOC):

- Irradiance at 1000 W/m²
- Cell temperature = NOCT
- Air mass of AM1,5

Nominal Operating Conditions (NOC):

- Irradiance at 800 W/m²
- Cell temperature = NOCT
- Air mass of AM1,5

Nominal Operating Cell Temperature (NOCT):

NOCT is measured under the following conditions:

- Irradiance on surface of array = 800 W/m²
- Ambient air temperature of 20 °C
- PV array electrically open-circuit (no load)
- Wind speed not greater than 1,0 m/sec

The power generated by solar modules in 'real world' climatic conditions is usually lower; hence STC power has the unit *W*p (Watt peak). Solar cell efficiency is defined

as the ratio of the maximum electrical solar cell power to the radiant power on the solar cell area, as measured at STC. Silicon solar cells now reach efficiencies of 24,7 percent for crystalline, 19,8 percent for multi-crystalline and 16,6 percent for thin film transfer (Green, Emery, King, Igari & Warta 2003:347). These values are not the norm however, with a common average being around 8 to 12 percent (material dependant). Table 5 lists some common PV module characteristics for standard photovoltaic technologies.

Table 5 **PV module characteristics for standard technologies (adapted from: Leng, Meloche, Monarque, Painchaud, Thevenard, Ross & Hosette 2004:PV.22)**

PV Module Type	η_r (%)	*NOCT* (°C)	β_p (%/°C)
Mono-Si	13,0	45	0,4
Multi-Si	12,0	45	0,4
Poly-Si	11,0	45	0,4
a-Si	5,0	50	0,11
CdTe	7,0	46	0,24
CIS	7,5	47	0,46

The PV module efficiency at *NOCT* is given as η_r, with β_p indicating the temperature coefficient for module efficiency.

2.3.2 cells, modules, panels and arrays

Solar cells are not normally operated on an individual basis, due to their low output voltage. Polycrystalline cells, for example, each give approximately 0,45 volts when illuminated, dependent on light intensity and attached load, but independent of surface area (RS 1999:5). The electrical current however, is directly proportional to light intensity and surface area. Cells are therefore connected into a number of series (voltage component) and parallel (current component) string combinations to achieve desired module ratings (typically in 6 volt increments). The same procedure can be followed with modules and panels to build arrays of any practical power (current and

voltage) rating, although care should be taken when coupling components from different manufacturers, in order to ensure correct load matching. Figure 21 illustrates the cell-module-panel-array concept.

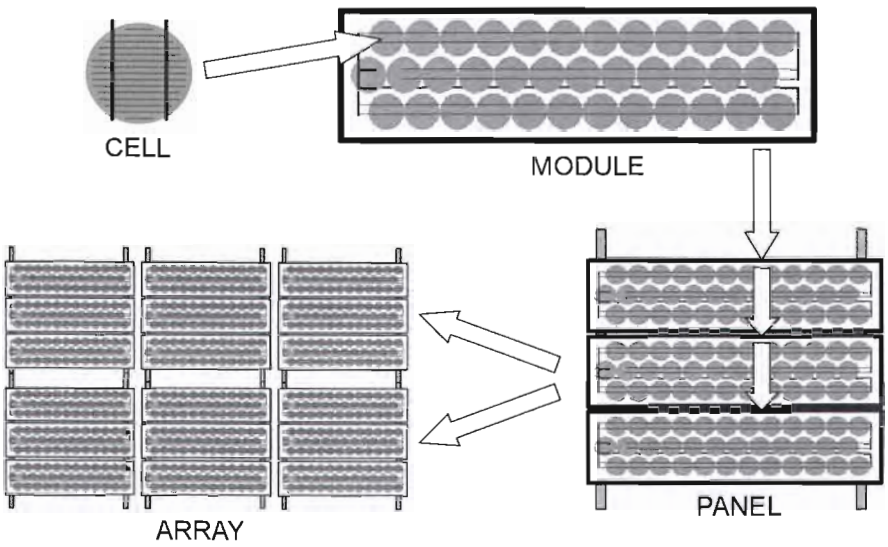

Figure 21 Cells, modules, panels and array composition

When unmatched devices are connected in series, the resulting voltage is still a summation of the two voltage outputs, but the current through the circuit is limited by the weakest delivery device in the series. In parallel circuits, the electrical current is summed, while the open circuit voltage is approximately equal to the average of the component voltages.

Other factors that affect (de-rate) the performance of solar panels are temperature, reflection, refraction, incorrect alignment and orientation, surface dirt, spectral distribution, shadowing or shading and production tolerances. Solar cells are especially vulnerable to power output loss due to shading. If just one cell of a large number of series-connected cells becomes shaded, it forms a current restriction and the whole string stops generating power. Bypass diodes are added to prevent possible damage to the shaded cells, but cannot stop the disproportionate power loss. Partial shading of PV generators should therefore be avoided whenever possible.

It is appropriate to consider the many factors that can de-rate the performance of a solar module prior to completing any simulation or sizing calculations (RS 1999:10). Simple maintenance and location functions such as keeping the array clean and entirely free from shading helps maximize PV module power output.

2.3.3 photovoltaic system components

Although a photovoltaic array produces electricity directly from sunlight, this energy must be properly controlled, stored, converted and distributed in order to be useful. Depending on the application and configuration, several additional components to the array may be required to perform these functions.

2.3.3.1 photovoltaic applications

Photovoltaic systems are generally divided into two major categories: Stand-alone systems and utility-interactive or grid-connected systems.

A stand-alone system, as the name implies, is a PV system that operates independently of utility grid power. Due to its practicality and cost-effectiveness for a variety of remote power needs, stand-alone PV systems form a large part of the PV market. The most common configurations of a stand-alone PV system are direct coupled, direct coupled with battery storage and direct coupled with battery storage and charge control (refer to Figure 3 for a system topology). The focus of this research is on the stand-alone directly coupled system, shown in block diagram form in Figure 22 and described as follows: Direct-coupled systems are the simplest type of stand-alone PV system and are configured with a DC load connected directly to the positive and negative terminals of a PV module or array. They have no electrical storage and can only be used where the load requirements and the power produced by the PV array coincide. Common direct-coupled applications include water pumping (with the option of a reservoir tank to provide storage) and circulation or ventilation fans. A crucial factor in direct-coupled PV system design is the matching of load requirements with the power output of the PV array under typical operating conditions (Kolhe, Joshi & Kothari 2004:617).

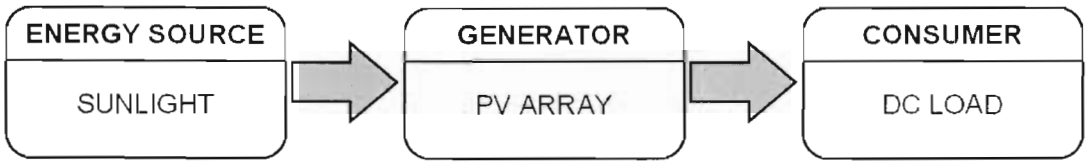

Figure 22 Directly coupled stand-alone PV system

2.3.3.2 balance of system components

Balance-of-system components, or BOS, is a term used to classify equipment, materials and hardware other than the PV array. Typical BOS components for a directly coupled system include disconnect and over-current protection devices, diodes, surge suppressors and grounding equipment. Mechanical BOS hardware includes items such as the array support structure, enclosures, *etc*.

2.3.3.3 electrical load

An electrical load is defined as the end-use appliance, device or equipment that requires electricity to operate. For the purposes of this work, it is defined as a direct current (DC) powered pump/motor combination hereafter referred to as a water pump, pump or pump-set. The magnitude and duration requirements of the electrical load determine the size and performance requirements of the PV system powering it. Considerable variations exist in the energy consumption and efficiency of electrical loads, making the load selection an important part of a design process. Because the electrical load dictates the overall size (and therefore cost) of the PV system required, it should be as energy efficient as possible. The use of direct-coupled DC powered electrical loads eliminates the need for an inverter and usually results in a more energy efficient and simplified system design.

2.3.3.4 characteristics of an electrical load

The electrical load in a PV pumping system generally takes the form of an electrical motor, which converts electrical energy into rotational mechanical energy. In a simple two-pole DC electrical motor, the direction of the current in the armature is switched each half rotation by means of a split-ring commutator and brushes in order to maintain the same armature rotation direction. Permanent magnets are used for the

magnetic field in small DC motors, while electromagnets are used in larger designs. Series and shunt are two types of DC motors, the series type being more common as it performs better over a greater speed range than a shunt motor. Brushless DC motors are also becoming popular because of their lower maintenance requirements, despite having an initial cost premium and complexity due to switching electronics. Water pumping systems using DC motors are one of the most common examples of a directly coupled system, where the matching of the pump/motor load with the PV array 'power delivery' ability is an important part of an effective system design (Kolhe *et al.* 2004:613).

Directly coupled PV powered pump motors are effectively in a stalled mode during pre-shutdown conditions, as dictated by lowering ambient irradiance. At stall conditions, a DC motor produces maximum rotational shaft torque at maximum current. An electrical current (I) flowing through a resistance (R) results in power loss (in the form of heat), equal to the product of the square of the total current and the resistance (I^2R losses). In the case of DC motors, this is a function of the motor current and the armature resistance (Hughes 1987:8,51). The heat resulting from I^2R losses in the armature coil is dissipated by conduction through various motor components and air flow in the air gap, while the ease with which this heat can be dissipated is a function of the motor type, construction and ambient conditions. Motor manufacturers typically provide an indication of the motor's ability to dissipate heat by providing thermal resistance specification values. Thermal resistance is a measure of the resistance to the passage of heat through a given thermal path. DC motors have a thermal path from the motor windings to the motor casing, as well as between the casing and the local environment (ambient air, water, *etc.*). In the case of submerged pump-sets, the water assists in dissipating heat more rapidly, providing a measure of protection assistance. Additionally, a directly coupled, photovoltaic powered DC motor that enters a stall condition is partially protected by the PV panel source impedance.

PV powered water pump-sets are designed to use solar power efficiently, with design characteristics allowing them to work effectively during low solar irradiance

conditions and at reduced voltage, without stalling or overheating (Buschermohle & Burns 2000:4). This is an important motor design consideration, as a stalled motor could burn out its windings even when supplied with a lower than nominal voltage.

2.3.4 module sizing

Determining the PV module (or array) size is a factor of the local irradiation, the load requirements and compensation for various system losses and inefficiencies (wire losses, mismatch, *etc.*). A common generic worksheet method (RS 1999:10) is listed in equation (26), while an empirical method developed by the GTZ (Deutsche Gesellschaft für Technische Zusammenarbeit) (Hahn 2000:2) for stand-alone water pumping systems is given in equation (27). This methodology is adequate for rough estimates, but lacks the accuracy required for detailed modelling.

$$P_{SG} = \frac{A_L \cdot F_S}{\overline{H}_D} \cdot V_n \qquad (26)$$

where

P_{SG} = Peak power of the solar generator (W_p)

A_L = Load current (Ah/day)

F_S = Safety factor to compensate for losses, generally 20 %, gives an F_S = 1,2

$\overline{H}_D$ = Mean daily or monthly irradiation (kWh/m²/day); (ESH or PSH)

V_n = Nominal voltage of the load (V)

$$P_{SG} = 11{,}6 \cdot \frac{L_V \cdot Q}{\overline{H}_D} \qquad (27)$$

where

P_{SG} = Peak power of the solar generator (kW_p)

L_V = Total vertical delivery lift or pumping head (m)

Q = Required flow rate (m³/day)

$\overline{H}_D$ = Mean daily or monthly irradiation (kWh/m²/day); (ESH or PSH)

Modules/panels are configured in series/parallel string combinations to attain the required P_{SG} value.

2.3.5 array modelling

An initial distinction needs to be made as to whether the model needs to perform simulation over frequent (typically hourly) intervals (for detailed models) or if simulation is done over a longer normalised period (simplified models). The detailed models require extensive meteorological data, in either measured or derived, *e.g.* Typical Meteorological Year (TMY) format (Argaw 2004:10). Some of the models also require detailed PV cell/panel information generally not supplied by the manufacturer, *e.g.* the SANDIA model as described and implemented by King, Boyson and Kratochvil (2004). Lack of manufacturer data for modelling is a problem also reported by Duffie and Beckman (1991:749). Simplified models generally only require long term monthly averaged meteorological data and manufacturer supplied panel specifications. The choice of a suitable model is application dependant and can be made with the assistance of analysis done by Myers (2003:8) given in Table 4. The detailed versus simplified model type choice dictates the frequency of the irradiance data used as an input to the array model. For stand-alone directly coupled systems, the simplified model is adequate for most applications.

Townsend (1989:17) comments that calculating direct-coupled PV output requires a complete description of the current-voltage (*I-V*) characteristics of the PV array under all operating conditions. He provides detailed analysis of various existing models and methods, as well as the development of a dynamic model of his own.

Modelling a PV system is generally a complex, time consuming and computationally intensive exercise, which is simplified by Evans (1981:555-560) in his method to predict the long term, monthly average electrical output of a fixed-plate PV array. The Evans procedure combines basic parameters characterizing the array with the local monthly mean temperature and clearness index (see Irradiance Modelling, section 2.1.3.4) to yield a monthly average array efficiency that is multiplied by the

monthly array irradiation to give the electrical energy output. This methodology is adopted commercially by RETScreen (Leng *et al.* 2004:PV21).

From an equation adapted from Leng *et al.* (2004:PV22), an array can be characterised by its average efficiency, η_P, which is a function of average module temperature T_c:

$$\eta_P = \eta_r \cdot \left[\left[1 - \frac{\beta_p \cdot (T_c - T_r)}{100} \right] \right] \tag{28}$$

where

η_r is the PV module efficiency at reference temperature T_r (25 °C), and β_p is the temperature coefficient for module efficiency (in % per °C). T_c is related to the mean monthly ambient temperature T_a through use of the Evans formula (Evans 1981:557):

$$T_c = \left[\left(219 + 832 \overline{K}_t \right) \cdot \frac{NOCT - 20}{800} \right] \cdot C_f + T_a \tag{29}$$

where

NOCT is the Nominal Operating Cell Temperature and $\overline{K}_t$ the monthly clearness index. *NOCT*, η_r and β_p depend on the type of PV module considered. This information can be gained from manufacturer data sheets or from default information as tabulated in Table 5. The factor C_f is equal to one when the array's tilt is set at optimal (θ_{OPT}).

If the actual tilt angle (θ), in degrees, differs from the optimum, then the C_f correction factor becomes:

$$C_f = 1 - 1{,}17 \times 10^{-4} \left(\theta_{OPT} - \theta \right)^2 \tag{30}$$

The energy delivered by the PV array (E_P) is then:

$$E_P = S_{PV} \cdot \eta_p \cdot \overline{H}_t \tag{31}$$

where

$\overline{H}_t$ is the monthly mean irradiation and S_{PV} is the surface area (m^2) of the array. Array power must be attenuated by various array losses (λ_p)(mismatch, diodes and connections, *etc.*) and power conditioning losses (λ_c)(wire losses, connections, *etc.*):

$$E_A = E_P(1-\lambda_p)\cdot(1-\lambda_c) \tag{32}$$

where E_A is the energy available to the load.

2.4 Photovoltaic water pumping systems

Photovoltaic markets are commonly classified based on the end-use application of the technology. The most common PV projects are off-grid applications, of which water pumping is an important market segment, particularly in developing countries.

Water pumping has a history dating back to the earliest civilizations and many methods have been developed over the years to realize this task with the minimum of effort. A variety of power sources have been utilised to accomplish this, including human energy, animal power, wind and hydro-power, electrical (grid) power and fossil fuel powered generator/pump pumping sets. Photovoltaic powered pumping systems are a relatively recent addition to this list, with the first systems being installed in the 1970's (Van Campen, Guidi & Best 2000:25).

Initial PV pumping system installation was for village drinking water in remote rural areas, although later usage analysis showed that most systems also provide water for livestock and subsistence farming. Van Campen *et al.* (2000:26) suggest that this factor be catered for when designing new projects.

Photovoltaic water pumping applications are one of the most common uses of PV power throughout the world, with thousands of solar powered water pumps installed both in industrialised and developing nations (Leng *et al.* 2004:PV13). Due to their inherent low maintenance and high reliability, they are also increasingly being used as a replacement for mechanical windmill and diesel powered pumps (EMCON 2006).

As a rule, hand-operated pumps are the least-cost option for low consumption rates and low pumping heads. If hand pumps cannot satisfy the demand, diesel powered pumps are commonly used for drinking and irrigation water supply. These pumps stand in competition with PV powered water pumps, which present themselves as a reliable and environmentally friendly alternative water delivery method. A study by GTZ (2002:4) found that this type of system was technically feasible and economically competitive between 0,7 kW and 4 kW, when compared to its main competitor, a small diesel pump. Posorski (1993:11-16) analysed PV powered drinking water systems and developed an economic evaluation in terms of hydraulic equivalent (head [m] × flow rate [m^3] = hydraulic equivalent [m^4]), concluding that solar water pumping is economically advantageous in remote areas up to a hydraulic equivalent of 2000 m^4 of water and at pumping heads up to 100 m. Similar results were reported by Thomas (1996:1, 22), who suggested various pumping regimes as a function of pumping head and flow rate, depicted graphically in Figure 23. In an evaluation done by Argaw (2004:15), a much lower value of 600 m^4 was defined.

A study by EMCON Consulting Group (2006:57) for the Namibian Government shows that Namibian water supply needs stand to benefit from converting to solar PV water pumping in cases where water depth is less than 120 m and the hydraulic load is less than 4000 m^4 per day; or where water depth is less than 200 m and the hydraulic load is less than 500 m^4 per day. The study also evaluated costing of photovoltaic pumping systems and concludes that the years required to achieve cost 'breakeven' between photovoltaic water pumping systems and diesel pumping systems, using a net discount rate of four percent and a LCC of 20 years as the reference case, are as follows:

- With immediate effect for systems operating below 250 m^4 per day,
- Less than one year when operating below 500 m^4 per day,
- Less than 2.5 years when operating below 1000 m^4 per day,
- Less than 6 years when operating below 2000 m^4 per day, and
- Less than 8 years when operating below 4000 m^4 per day and below 120 m head.

The EMCON study is deemed particularly valid for use as a reference because of geographic similarity (Southern Africa) and financial equality (Namibian Dollar is pegged to Rand value on a 1:1 basis at time of writing).

The variations in hydraulic equivalent load values reported above are expected because of the country, site and equipment specific variability and nature of any given installation.

Several types of pumps are available for use in water pumping applications. They can be categorised according to their design type (rotating or positive displacement pumps), to their location (surface or submersible) or to the type of motor they use (AC or DC). From the Thomas study (Thomas 1996:22) it can be deduced that rotating pumps (*i.e.* centrifugal pumps) are usually preferred for deep wells or boreholes and large water requirements, whereas the use of displacement pumps is usually limited to low volume and/or high pumping head applications. Positive displacement pumps such as diaphragm, piston and progressive cavity pumps usually have good lift capabilities but are less accessible than surface pumps and can be more sensitive to fouling from dirty water. The choice between using a DC or AC motor to drive the pump depends on factors such as system configuration, availability, price, reliability and technical support. DC motors are usually quite efficient and are easier to match with a photovoltaic array, while AC motors tend to be cheaper and more readily available, but require an inverter to enable connection to the array. For stand-alone directly coupled water pumping system drives, the choice is confined to a correctly sized DC motor.

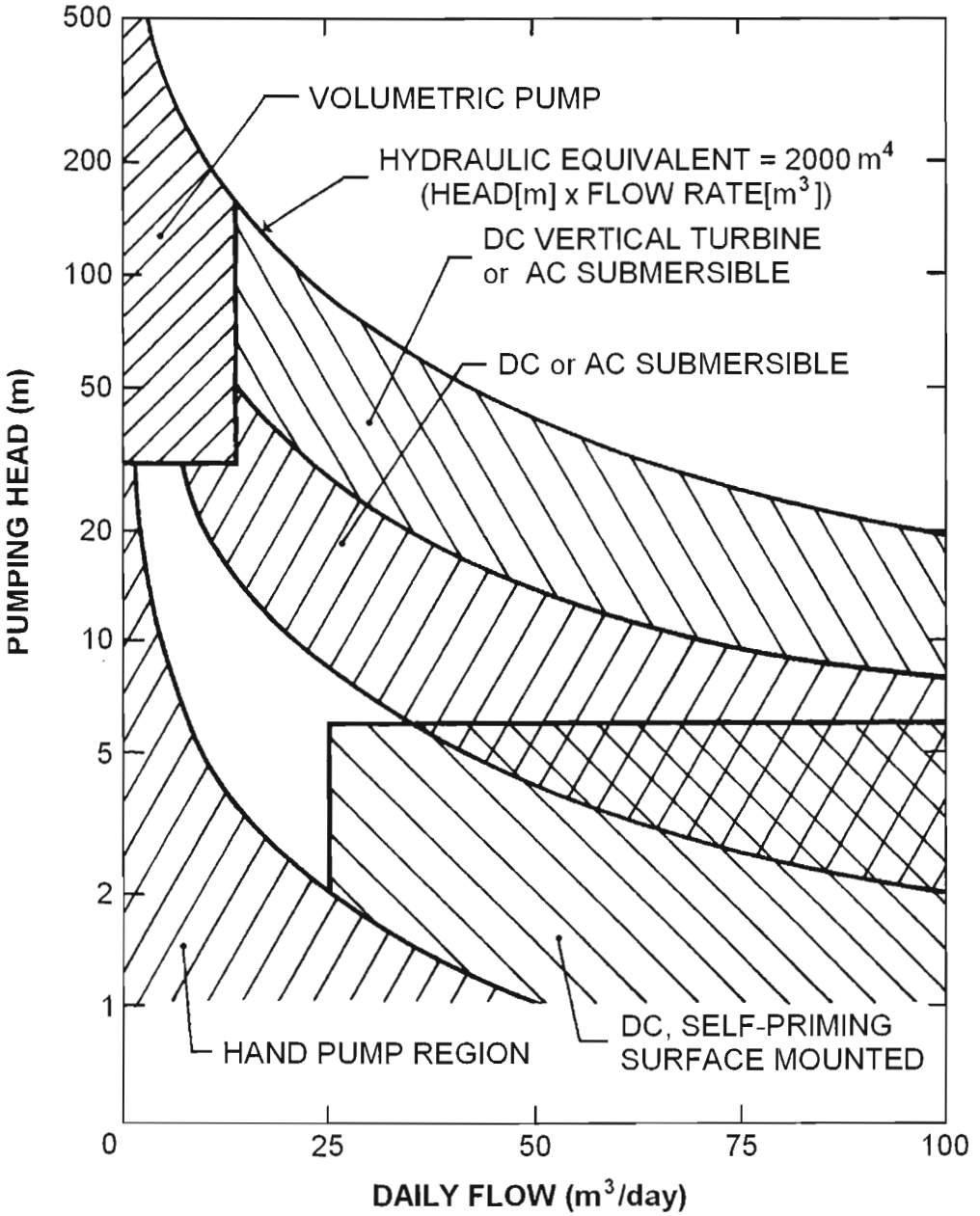

Figure 23 **Pump set type vs. Pumping regime**
(adapted from Thomas 1996:22)

Stand-alone photovoltaic water pumping systems (PVPS) are a focused application of photovoltaic system components as discussed in previous sections. A PVPS in block diagram format is illustrated in Figure 24.

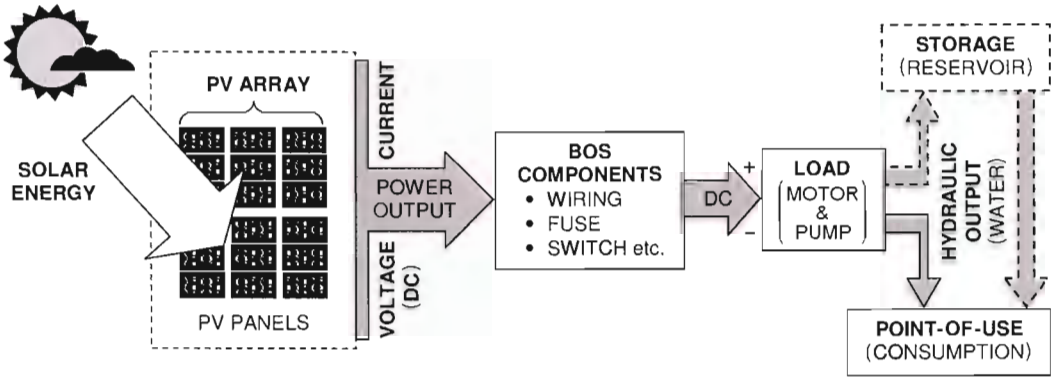

Figure 24 **Block diagram of a photovoltaic water pumping system (Denny & Case 2007:8)**

This system configuration and components have been extensively researched by others, as shown in the literature study summarised below:

Chapman (1989:71) presented a nomogram sizing methodology. Appelbaum and Bany (1979a:27-30; 1979b:439-445) analyzed a direct coupled PV pumping system under steady state conditions. Singer and Appelbaum (1993:47-53) examined the starting characteristics of PV powered DC motors and pumps, both with and without maximum power point trackers (MPPT). Roger (1979:193-198) showed that a DC motor driving a centrifugal pump represented a well-matched load for a PV array because the system utilised most of the DC power generated by the array. Anis, Mertes and Van Overstaeten (1985:27-42) reported that a load composed of a DC motor driving a constant volume pump represented a unmatched load to a PV array because the motor driving a constant volume pump required a nearly constant current. The matching of a DC motor to a PV generator to maximize daily gross mechanical energy is reported by Saied and Jabori (1989:459-465). Salameh and Taylor (1990:57-61) analyzed the effect of PV array configuration on the performance of PVPS. Hsiao and Blevins (1984:489-498) and Koner, Joshi and Chopra (1992:301-313) analyzed the performance of PVPS by varying the motor constant. In the study by Hsiao *et al.* (1984:489-498), hourly radiation data for a year was required, leading to extensive use of computer simulation time, a factor also reported by Townsend (1989:13) and Moraes-Duzat (2000:130). A general method

for estimating the long-term performance of direct-coupled PVPS's was devised by Kou, Klein & Beckman (1998:33-40), while McNutt *et al.* (1999) detailed a procedure for determining the performance of stand alone PV systems. Klein and Beckman (1984:393-402) developed equations for the 'utilizability' of solar radiation at high critical levels (low utilizability). Expanding on the solar radiation utilizability concept, Loxsom and Durongkaveroj (1994:215-219) used two straight-line segments to represent the nonlinear flow rate versus solar irradiation relationship in a PVPS. Van Dyk, Meyer, Scott, O'Connor and Wessels (1997:1197-1200) found great variability in their test and analysis of PV modules under South African conditions. Sarkar, Obaidullah, Mahmud and Martinac (2002) showed a system efficiency of four percent for a direct-coupled submersible water pump without a MPPT, while Kolhe *et al.* (2004:613-618) analysed a directly coupled PVPS powered by a permanent magnet motor coupled to a centrifugal pump and found it to be a good match between the array and the electromechanical system, observing that the torque speed curve should be as steep as possible in the operating region with low starting torque. This is by no means a comprehensive list of papers, but serves to illustrate that there is a large amount of ongoing investigation into photovoltaic pumping systems and components.

Similarly, many universities have done research on the subject: Townsend (1989), Eckstein (1990), and Al-Ibrahim (1996) developed a comprehensive four parameter PV cell model for the TRNSYS simulation program developed at the University of Wisconsin – Madison (TRNSYS 2006). They also developed motor, pump and MPPT models for the program. There are, however, complicated nonlinear relationships among the models that require numerical skill from the operator in order to simulate systems successfully (Kou *et al.* 1998:34). Kou *et al.* also mention that pump and motor input parameters required for simulation were difficult to obtain from available data (a problem also reported by Moraes-Duzat (2000:130) for other simulation programs). The TRNSYS program is often cited as the reference for software developed in the Americas. Similarly a simulation and design program developed by the German Universität der Bunde-Bundeswehr in Munich, called DASTPVPS (DASTPVPS 2006), is often the reference for programs in Europe

(GTZ 2002:5). Limitations to the DASTPVPS system are that it is DOS based and has specialised data sets focussed on the European continent.

Theses/dissertations from various parts of the world: Wolete (1998), Moraes-Duzat (2000), Hadi (2003) and Betka (2005), *etc.* provide a wealth of information pertaining to various aspects and approaches to solar powered water pumping, while a number of books: Cabraal, Seiss, Slominski, Buresch and Kenna (1987), Risser and Post (1991), Thomas (1987/1996), Van Campen *et al.* (2000), Argaw, Foster and Ellis (2003) and Argaw (2004), *etc.* all provide information on PVPS selection, design and implementation methodologies.

Although commonalities and similarities exist, none of the above references can be said to have a generic methodology, each adopting their own perspective and developing a 'fit for purpose' solution accordingly. This demonstrates that there is no single solution to designing a PVPS and that several methodology and strategy routes exist for a designer. The challenge is to ensure an optimised, robust, design solution. King, Hund, Boyson and Kratochvil (2002:1428) called direct-coupled systems "deceptively simple", while Kolhe *et al.* (2004:613) state that "The directly-coupled PV electromechanical system necessitates a complete study, from a mechanical load to the PV array, but it leads to a very simple and reliable solution."

The dominant problems associated with this type of design (direct-coupled PV) are the nonlinear supply of power and the resultant complexity in providing an optimised load match Kolhe *et al.* (2004:613). The output from a PV array is a nonlinear and time dependant source of power that changes according to the variation in solar irradiance throughout a day, as well as due to the attenuating effects of PV cell temperature. This directly influences the performance characteristics of a DC motor, which is generally designed for; and operated from, a fixed voltage constant current source. In a PVPS system, a pump driven by a DC motor performs optimally at a specific PV array configuration and pumping head profile (Dunlop 1988:1182). PV array configuration is a function of the electrical load requirements, which in turn is a function of the motor/pump set and related BOS efficiencies. The motor/pump set is

chosen based on hydraulic load requirements, derived from the site water requirements and bore-hole/well parameters such as the static and dynamic head. Hydraulic efficiency is reduced by mechanical BOS factors such as piping friction and pressure losses over fitting, *etc.* All these factors are interrelated and must be considered when doing a PVPS design. A typical PVPS system layout is illustrated in Figure 25, showing some of the major design parameters.

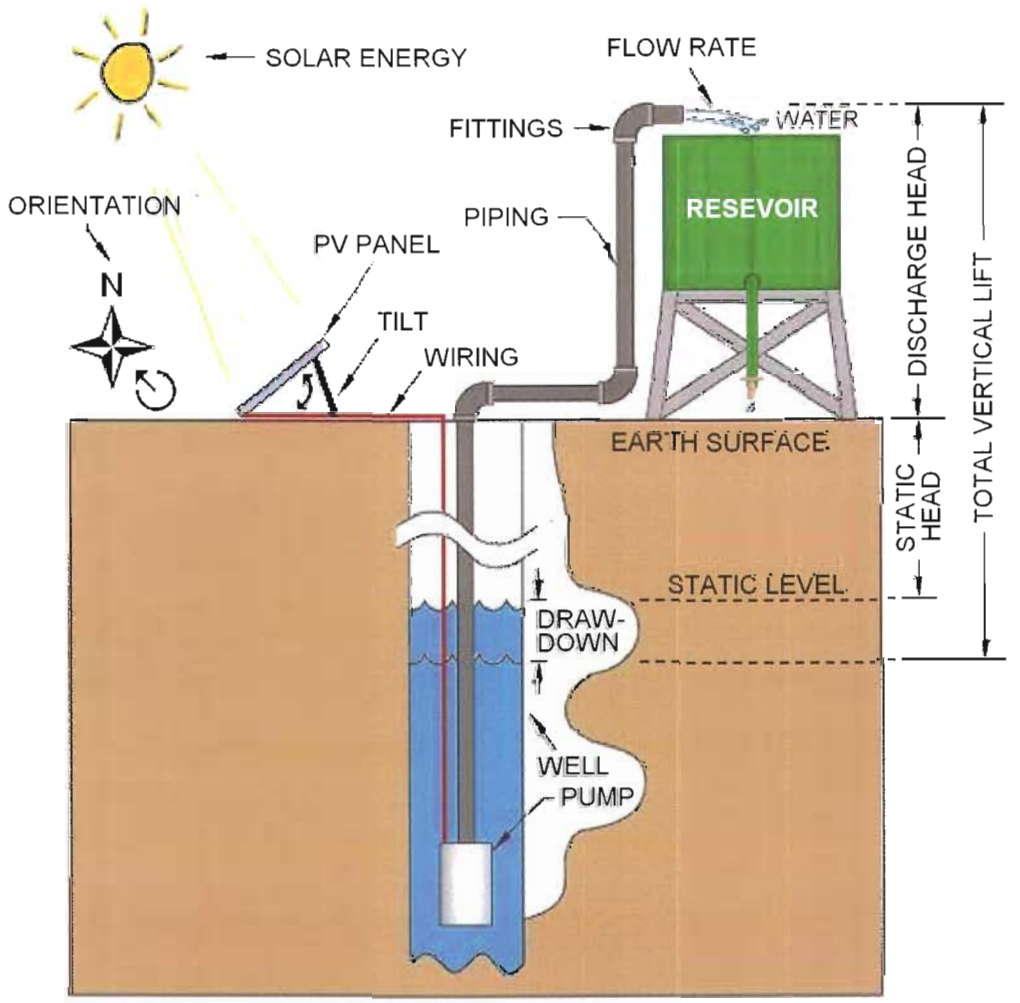

Figure 25 **Typical PVPS layout**
(adapted from Denny 2006:1 & Kyocera Solar 2002:9)

2.4.1 design requirements

From the aforementioned text, it may be deduced that in the absence of batteries and a load matching device such as an MPPT, the critical design requirements and parameters for a PVPS may be summarised as follows:

- Site solar irradiation and supplementary data (temperature, cloud, *etc.*).
- Site water requirements and usage data (including autonomy requirements for bad weather days).
- Site bore-hole/well data (including aquifer data such as draw-down and static water level).
- PV array orientation and tilt.
- PV array configuration (component choice, as well as voltage and current options from combinational series and parallel module strings).
- PV cell temperature compensation.
- Choice of motor/pump set.
- Dynamic component matching analysis.
- Component efficiency compensation.
- Compensation for system losses such as volt drop (wire losses) and pipe friction, *etc.*
- Economic evaluation (Note: Excluded from this study).

An additional consideration is raised by Risser *et al.* (1991), who motivate that designs should be done for 'worst case' scenarios. This is an important consideration and should be implemented if the design is for a 'life dependant' commodity such as remote area water supply.

2.4.2 existing design methodologies

Existing methodologies used for solar water pumping design include the following:

- The classic 'back of an envelope' design
- Work-sheet methods (*e.g.* Sunwize Technologies 2006:99-104), that tend to make use of generalised data and factoring
- Nomograms, both in general (*e.g.* Argaw 2004:44; Thomas 1996:16-17) and manufacturer specific (*e.g.* Kyocera Solar 2002:26-32) formats
- Specialised software (*e.g.* Grundfos: CASS / WinCAPS; Maui Solar Software: Solar Design Studio, *etc.*), that is complex, expensive, and usually proprietary to a specific equipment manufacturer.

Figure 26 shows an example of a nomogram used to estimate PV array size and daily water production.

2.4.3 standards for directly-coupled photovoltaic pumping systems

A literature search was conducted but returned no direct design standards. The following list of international standards published by Technical Committee 82 (TC82) of the International Electrotechnical Commission (IEC) clarifies representation, testing and monitoring of stand-alone directly coupled photovoltaic water pumping systems as indicated by the relevant descriptors:

- IEC 61836 Solar photovoltaic energy systems - Terms and symbols.
- IEC 60904-1 Measurement of photovoltaic current-voltage characteristics.
- IEC 61194 Characteristic parameters of stand-alone photovoltaic systems.
- IEC 62124 Photovoltaic stand-alone systems – Design qualification and type approval.
- IEC 61702 Rating of direct coupled photovoltaic pumping systems.
- IEC 61724 Photovoltaic system performance monitoring - Guidelines for measurement, data exchange and analysis.

The only document of South African origin that could be found is a 'Rationalized User Specification' printed by the South African Bureau of Standards (SABS) on behalf of the NRS Project and is not a standard as contemplated in the Standards Act, 1993 (Act 29 of 1993). The document is a specification pertaining to Solar Home Systems (SHS) and contains no reference to directly-coupled stand-alone water pumping systems:

- NRS052-1:1999 SPECIFICATION: Photovoltaic systems for use in individual homes; Part 1: Standardized requirements applicable to individual homes remote from the electricity grid.

Wiles (2001) from Sandia National Laboratory provides useful basic guidelines to photovoltaic system wiring and installation as interpreted from the United States National Electric Code (US-NEC).

2.5 Environmental impact aspects of photovoltaic systems

The environmental impact aspects of photovoltaics was not directly researched, but remains an important consideration in any responsibly applied engineering design. Production of photovoltaic cells elicits debate with respect to required power for manufacture relative to PV cell power delivery and payback time. Typical lifetime of a well maintained PV panel is now known to be in excess of twenty years (Quaschning 2004:84). The physical use of photovoltaic systems is generally accepted as being environmentally friendly, with PV considered a 'green' energy source. Photovoltaic's operate silently and produce no by-products during operation, with their only operational consumption being available sunlight. A perceived negative aspect in the use of PV is of an aesthetic nature, due to the physical area required for array deployment. This aspect can be managed with careful site consideration and innovative construction. Defunct panels should be recycled or disposed of as per manufacturer recommendations and regulatory requirements.

Detailed information on this topic is available in literature, *e.g.* Handbook of Climate Change Mitigation Options for Developing Country Utilities and Regulatory Agencies (South, Camp, Siegel & Meade 1999:8-14 – 8-16); Environmental Aspects of PV Power Systems (Nieuwlaar & Alsema 1997:1-27), *etc.*

2.6 Supplementary information

- Bore-hole drawdown estimation and analysis is beyond the scope of this document. A good starting point for such research is the article "A Generalised Solution for Step-Drawdown Tests Including Flow Dimension and Elasticity", published in Water SA (Van Tonder, Botha & van Bosch 2001:345-354).
- As with any standard electro-mechanical system, a PVPS installation requires periodic inspection and maintenance. This topic has not been covered in this text. Sandia National Laboratories in the USA provide a practical guide for the operation, inspection, troubleshooting, repair and maintenance of PV systems (Sandia 1991) that can be used in conjunction with manufacturer recommendations.
- Solar installations are susceptible to damage from lightning, which is commonplace in many areas of Southern Africa. Protection issues have not been covered in this text. Moine, Marcel and Charoy (2003:31) of the IEA provide guidelines on lightning protection for PVPS installations.
- PV Component and system modelling in packages external to the coded SAS-SWP application was only done on a research and comparison basis. Townsend (1989), Eckstein (1990) and Al-Ibrahim (1996) provide useful TRNSYS models and methodologies to accomplish this, should it be required. Wolete (1998) used MATLAB to create a simple PVPS model, while Oi (2005), provides details and examples of a PVPS modelling and simulation strategy using SIMULINK and MATLAB software.

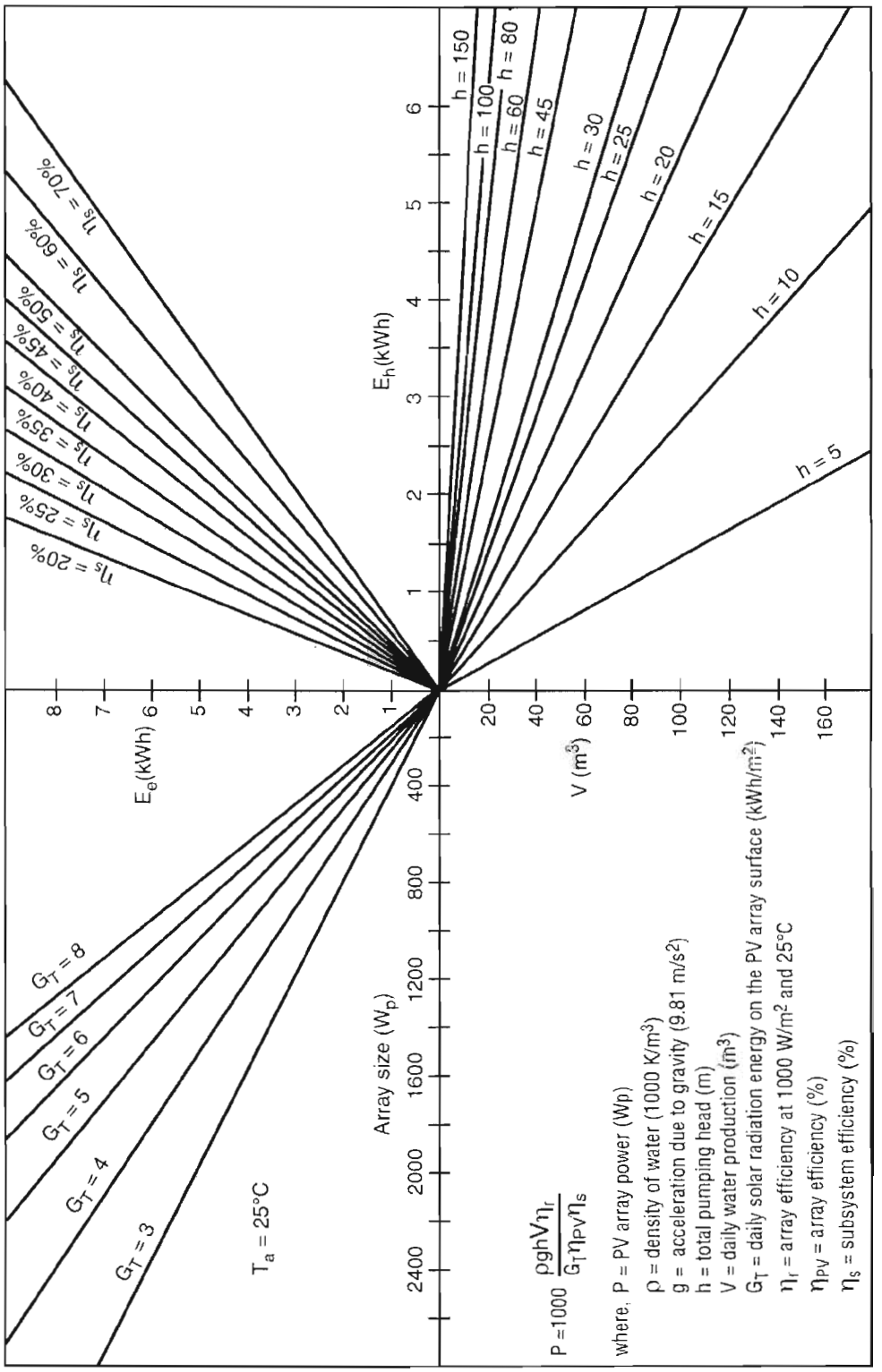

Figure 26 **Nomogram for estimating PV array size & daily water production (Argaw 2004:44)**

CHAPTER 3 - Application Software Model Development

3.1 Application software specification

The major design criteria and constraints forming the specification are as scoped in sections 1.4 and 2.4.1.

3.2 Application program development

A development process was initiated to deliver a design aid package according to specification. The process entailed evaluation of software packages, human-computer interface design, application design and coding, on-line application help coding and integration, functionality testing and de-bugging and product delivery.

3.2.1 evaluation of software packages

Various software programming packages were evaluated for use in the development of the Stand-alone Solar (PV) Water Pumping Design Aid Application. This included traditional programming packages such as C++, Visual Basic and Delphi, together with custom packages such as TestPoint. All the evaluated packages were capable of producing the required application, with varying degrees of complexity and effort. The custom object-oriented TestPoint package (TestPoint 2005) was eventually selected because the development suite produces royalty and license free, compiled, autonomous run-time applications (a design requirement), together with the programmers familiarity with the package.

3.2.2 graphical user interface

A functional design process translates a users needs into a task model. This represents the work to be done, which is then converted into a functional model incorporating a user interface. The most dominant means for humans to receive information is through vision, making the Graphical User Interface (GUI) the foremost method for human-computer interaction (Olsen 1998:1-4). The objective of a GUI should be to simplify the user's access to application software functionality, without compromising processing and operability. A simple, intuitive, front-end GUI that presents the operator with menu driven design steps has been developed. Context sensitive on-line help is available in all menu steps, with overall help being accessed

via menu selection or use of the 'F1' function key. An overview of the GUI and application interaction is illustrated in Figure 1 and Figure 27 respectively.

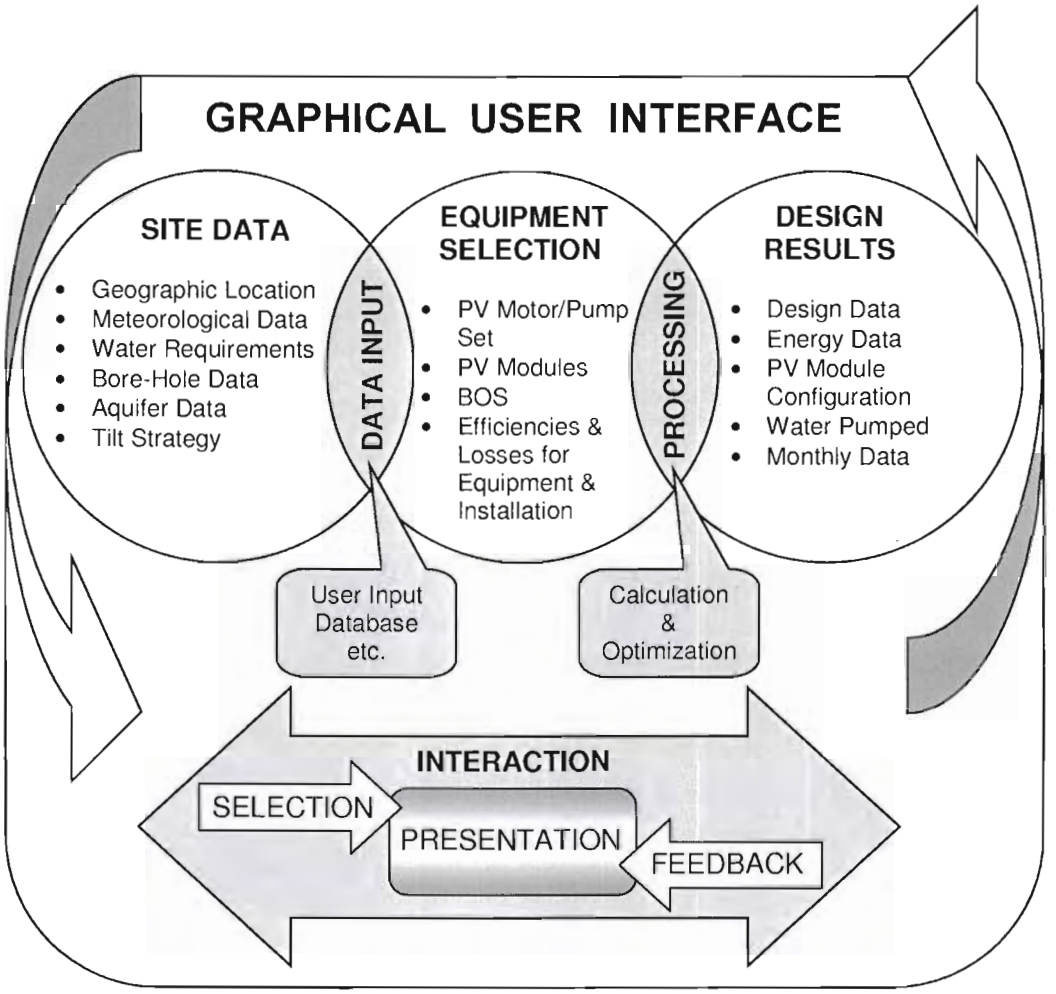

Figure 27 **Graphical user interface & processes**

The design menu steps (modules) in the program are all characterised by event-triggered GUI operations, *i.e.* input, calculations, database operations, help system and output, as seen in the program model bounce diagram given in Annexure 1. The bounce diagram, together with the software listing in Annexure 3, should be used as a reference for all software functionality.

Modules other than the 'Quick Estimator' have pre- and post calculation dependencies and are interlocked to ensure correct operational sequence. A top-down approach is followed in the menu layout. The front-end GUI, together with all other

menus, applets, windows, panels, data entry and operation are illustrated in the system help file listing provided in Annexure 2.

3.2.3 module development

The program has nine major design menu steps, grouped into modules: Location & energy, water requirements, bore-hole/well data, water pump selection, electrical wiring, PV module selection, array orientation, calculated results summary and an independent 'Quick Estimator'. Various sub-modules also exist and may require completion during the execution of a major module. The modules originate from logical functional and operational groupings developed during the functional design stage. A simplified calculation chain is provided for reference in Figure 32.

3.2.3.1 location and energy module

This module is the first step in the PVPS design process. In this module the user is prompted to input geographic location coordinates or to select a location on a map. Either of these actions generates database vectors that are used to extract location specific surface meteorology, solar energy and ancillary data.

Figure 28 **Database coverage map – RSA**

Input coordinates are limited to the Southern African region, which includes the entire Republic of South Africa. It is defined as the rectangular area illustrated in Figure 28, bounded by the following coordinates:

- Longitude: 16 Degrees to 33 Degrees East
- Latitude: -22 Degrees to -35 Degrees South

The user is then presented with five default tilt strategies, together with a user defined tilt option. All information is presented graphically, as well as in tabular format, in monthly intervals for a period of one year.

The default tilt strategies presented by the application are: Monthly optimum, summer/winter average, geographic latitude plus and minus 15°, yearly average and seasonal (spring/summer/winter/autumn) average tilt. Tilt strategy selection is facilitated by the provision of a yearly energy factor indication (E_y), per tilt strategy. The E_y factor is derived from the integral of the monthly averaged daily *ESH* irradiation for a specific tilt strategy, over a one year period divided by a factor 1000. Numerical integration is coded in the software using the trapezoidal rule.

Correct tilt strategy selection is important because it influences the amount of energy available to the design (plane-of-array energy), as indicated by the E_y factor, as well as the physical effort required to set the array tilt at the selected strategy frequency and tilt angle.

3.2.3.2 water requirements module

In this module the user is prompted to enter the water usage base for the design calculation. This includes consumption for humans, animals and irrigation usage. The total daily water requirements are then calculated and presented, together with autonomy recommendations (reserve water supply, stored in a reservoir tank) and supplementation. The results delivered from this module include total daily water required, required pump rate and a recommended water tank size.

Water usage is calculated on a per capita basis, *i.e.* number of people, animals or square metres under irrigation, multiplied by the individual daily requirements. The calculation uses normalised daily water usage requirement quantities developed by Thomas (1996:8) and given in Table 6. This forms the basic requirement, to which

additional requirements for autonomy and supplementation are added. Autonomy provision is required for night-time usage, as well as for cloudy periods when direct-coupled PV pumping systems are sluggish or totally dormant.

Table 6 Typical daily water consumption (adapted from Thomas 1996:8)

Water Consumption (per consumer)	Quantity (litres per day)
People (Rural Environment)	40
People (Urbanised Environment)	100
Horses	50
Dairy Cattle	40
Cattle	20
Pigs	20
Sheep	5
Goats	5
Chickens	0,1
Subsistence Agriculture	60 m^3/hectare = 6 litres/m^2

Autonomy recommendations are made based on site meteorological data (from database). The greatest monthly 'no sun' days (D_{NS}) in a year is used to calculate a recommended autonomy period (D_A, in days), according to equation (33), using a constant value of 30 as the average number of days in a month.

$$D_A = 7 \cdot \frac{D_{NS}}{30} \tag{33}$$

The autonomy period is converted to a volumetric requirement (V_A, in litres) using equation (34), which basically multiples the autonomy days with the daily water requirements for humans and animals (W_{HA}, in litres/day). An assumption is made that agricultural requirements can be neglected for short periods of time, *i.e.* when the typical duration of the required autonomy period is less than three days (Thomas 1996:7). Autonomy stockpile requires supplementation/replenishment during normal

operation in order to create or maintain the reserve water supply. According to international research by Auer and Viel (1996:1437), the longest anticipated autonomy period is six consecutive days. This period is much less for South Africa, with a maximum number of monthly 'no sun' days at 8,56 days (area east of Trompsburg in the southern Free State Province; from analysis of the meteorology database that has been created – refer to Figure 36 for monthly maximum values for Southern Africa). Database analysis indicates that weekly 'no sun' days for most South African locations is two days or less. Based on this, an operational window period of seven days was selected. The implication of the operational window is that replenishment takes place in the differential period between weekly 'no sun' days (site specific) and seven days, as illustrated in Figure 29.

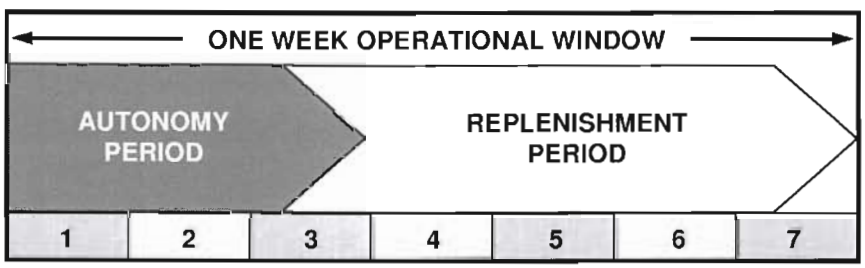

Figure 29 **Autonomy & replenishment operational window**

The supplementation or replenishment rate (Q_{Ar}, in litres/day) is calculated using equation (35).

$$V_A = D_A \cdot W_{HA} \tag{34}$$

$$Q_{Ar} = \frac{V_A}{(7 - D_A)} \tag{35}$$

While the calculated value is recommended, an industry 'rule of thumb' three day autonomy (Thomas 1996:7; Kyocera Solar 2002:7) selection is also included in the in the software. This feature is activated via a 'tick box' and sets D_A equal to a value of three for calculation purposes.

The application also makes a 'Safety Factor' (E_{SF}) recommendation based on energy input variation possibility and is defined as the difference between the mean yearly (denoted by the subscript 'y') *PSH* and *ESH* solar irradiation values, relative to the *PSH* for the location, applied to water requirements and calculated according to equation (36).

$$E_{SF} = \frac{\overline{PSH}_y - \overline{ESH}_y}{\overline{PSH}_y} \tag{36}$$

Note: Any recommendations provided by the application software can be included, excluded or modified for the overall calculation process, at the discretion of the operator.

The total daily water requirement (Q_{Dr}, in litres/day) is then calculated using equation (37).

$$Q_{Dr} = \left(W_{HA} + W_{Ag} + Q_{Ar}\right) \cdot \left(1 + E_{SF}\right) \tag{37}$$

where

W_{Ag} = Agricultural water requirements (litres/day)

The recommended reservoir tank size (T_A, in litres) is calculated from the daily water requirements and the autonomy period and is given in equation (38).

$$T_A = Q_{Dr} + V_A - Q_{Ar} \tag{38}$$

Once total daily water requirements have been determined, it is possible to calculate pump rate requirements (Q_P, in litres/hour) using equation (39).

$$Q_P = \frac{Q_{Dr}}{H_t} \tag{39}$$

where

$\overline{H_t}$ = Mean monthly irradiation per day (kWh/m²/day); (ESH or PSH)

3.2.3.3 bore-hole/well data module

In this module, site specific aquifer and bore-hole/well data is input into the system. Typical data required includes static level, draw-down and discharge head, together with installed pipe diameter, pipe length, and fittings used. This is illustrated in Figure 26, with similar graphical assistance provided to the operator in the help file and directly by the application program. Compensation for friction and other losses is then computed and combined with other data to determine the total dynamic head (TDH) for the design.

The calculation process for this module starts by calculating the total vertical lift of the system under design, done according to equation (40).

$$L_V = L_S + L_{DD} + L_D \tag{40}$$

where

L_V=Total vertical lift (metres), as calculated

L_S = Static aquifer level (metres), from borehole data sheet or physical tests

L_{DD} = Aquifer daily draw-down (metres), from borehole data sheet or physical tests

L_D = Discharge head (metres), as measured

The next step is to determine compensation for friction losses caused by pipes and fittings. A PVPS piping installation consists of lengths of straight pipe, bends, elbows, tees, valves and various other flow impediments, each requiring consideration in the calculation of TDH.

A number of empirical formulae have been developed to solve problems involving pressure drop and friction losses in pipes. The most commonly accepted approximations for water flow applications are the Darcy-Weisbach formula and the Hazen-Williams equation (Plastics Pipe Institute 2000:1).

Energy losses for flow through pipes are generally categorised into major and minor loss factors. Major losses are due to friction between the moving fluid and the inside walls of the pipe, while minor losses are due to losses over fittings such as valves and pipe elbows. Major losses can be computed using either the Darcy-Weisbach formula, which utilizes the Moody friction factor and is a function of the piping system Reynolds number, or the Hazen-Williams friction loss equation. The Darcy-Weisbach method is generally considered more accurate than the Hazen-Williams method, but is cumbersome to use due to the iterative nature of it execution (Plastics Pipe Institute 2000:2). Standard practice is therefore to use the less accurate but acceptable Hazen-Williams Equation (Plastics Pipe Institute 2000:2). The Hazen-Williams friction loss equation is considered valid for water at temperatures between four degrees and twenty-five degrees Celsius (LMNO Engineering, Research and Software 1998; The Engineering Toolbox 2005) and is therefore expected to function adequately for South African operating conditions. The equation delivers friction loss results in metres of water head loss per metre of installed pipe.

The Hazen-Williams formulae as used in the software application are given in equations (41) and (42). These are metric adaptations of formulae extracted from Technical Report TR-14 (Plastics Pipe Institute 2000:8), supplemented by information from 'The Engineering Toolbox' (2005) and Thomas (1996:14).

$$H_{FL} = Q_{Pm}^{\ 1,852} \cdot \left(\frac{67,03455}{C_{HW}^{\ 1,852} \cdot d_i^{\ 4,8655}} \right) \tag{41}$$

$$F_V = 122,179 \times 10^{-3} \cdot \left(\frac{10,648 \times 10^{-4} \cdot Q_{Pm}}{1,55 \times 10^{-3} \cdot d_i^{\ 2}} \right) \tag{42}$$

where

H_{FL} = Friction head loss (metres per metre of installed pipe)

Q_{Pm} = Volume flow rate (litres per minute; *i.e.* $Q_p/60$)

C_{HW} = Hazen-Williams roughness coefficient (dimensionless; from Table 7)

d_i = Installed pipe inner diameter (mm)

F_V = Flow velocity (metres/second)

Table 7 Hazen-Williams roughness coefficient for piping

Pipe Material	C_{HW}
Galvanised Iron	120
Steel	130
Copper	135
Polyethylene	140
Thermo-Plastic	145
Polyvinyl Chloride (PVC)	150

Equation (42) is used by the application software to check design flow velocity and generates a visible warning when F_V exceeds 1,524 metres (5 feet) per second (Plastics Pipe Institute 2000:6). This limit should generally not be exceeded for non-metallic pipes, which are the predominant choice in small directly coupled PVPS. A typical corrective action for an F_V warning would be to increase the pipe diameter used in the design.

A common method to express energy loss through a pipe fitting is in linear metres of equivalent pipe that would sustain the same loss (Plastics Pipe Institute 2000:4; Kyocera Solar 2002:8). The equivalent lengths of straight pipe for various fitting, expressed as a function of pipe diameter, is presented in Table 8. The total losses for fittings can be calculated by executing equation (43) for each type of fitting and then summing the results in equation (44).

$$\lambda_F = F_{\#} \cdot F_{LF} \cdot d_i \tag{43}$$

$$\lambda_{F\_total} = \lambda_{F1} + \lambda_{F2} + \lambda_{F3} + \lambda_{FN...} \tag{44}$$

where

λ_F = Fittings loss in equivalent metres of pipe

$F_{\#}$ = Number of like fittings

F_{LF} = Fitting loss factor (fitting equivalent diameter loss ratio; from Table 8)

d_i = Pipe inner diameter (mm)

The F_{LF} values in Table 8 are a metric adaptation of data contained in the TR-14 report (Plastics Pipe Institute 2000:10) and Kyocera Solar (2002:9-10) data and assumes a fitting bend radius equal to 1,5 times the pipe diameter.

Table 8 Loss factor for pipe fittings

Type of Fitting	F_{LF}
Insert Coupling	0,012
Male-Female Inset Adapter	0,018
Tee, Flow Through, Main	0,02
Tee, Flow Through, Branch	0,06
Elbow, 90°, Moulded	0,03
Elbow, 90°, Mitred	0,024
Elbow, 60°, Mitred	0,016
Elbow, 45°, Moulded	0,016
Elbow, 45°, Mitred	0,012
Elbow, 30°, Mitred	0,008
Gate Valve	0,02

Total friction and fittings losses (λ_{FF}) are then calculated with equation (45).

$$\lambda_{FF} = \left[\left(L_{PI} \cdot H_{FL}\right) + \lambda_{F\_total}\right] \cdot S_m \qquad (45)$$

where

λ_{FF} = Total friction and fittings losses (equivalent pipe length, in metres)

L_{PI} = Total installed pipe length (metres)

H_{FL} = Friction head loss (metres per metre of installed pipe)

λ_{F_total} = Total fittings losses (in metres of equivalent pipe length)

S_m = Safety Factor (Multiplier; Default = 126 [large]; small = 6; none = 1)

Analysis of various commercial friction loss tables showed common use of the Hazen-Williams equation, with an element of conservatism added by incorporating a safety multiplier. The multiplier values varied greatly, so two broad ranges were defined and the average multiplier value for the ranges obtained. Provision is made in the application software for a safety multiplier on the λ_{FF} value, with the default Safety Factor selection (S_m) set to 'large'. This sets the multiplier to a value of 126. Additional settings are 'small', and 'none', which set the multiplier to six and one respectively. Additionally, an industry default 'five percent' selector (Kyocera Solar 2002:8-9) is provided that forces a five percent of total vertical lift compensation for friction and fittings losses, which can be selected for small systems design (tank within approximately 10 m of bore-hole), should the operator so desire.

The last factor to consider before the TDH can be calculated is the inclusion of a pressurised water tank in the PVPS loop. While this is not expected, it may occur in the more affluent homestead applications. The software makes provision for this by providing compensation in the TDH calculation, according to equation (46) from Kyocera Solar (2002:8). A proviso is that the pressurisation-tank operating pressure is known and made available to the software application.

$$P_{comp} = P_T \times 0{,}102 \tag{46}$$

where

P_{comp} = Pressurisation compensation (in metres of head; default = 0)

P_T = Pressurisation-tank pressure (kPa)

Total dynamic head may now be calculated according to equation (47).

$$TDH = L_V + \lambda_{FF} + P_{comp} \tag{47}$$

where

TDH = Total dynamic head (metres)

L_V = Total vertical lift (metres)

λ_{FF} = Total friction and fittings losses (equivalent pipe length, in metres)

P_{comp} = Tank pressurisation compensation (metres of head)

At this point enough data is available to enable calculation of the hydraulic energy required for the design, which is done using equation (48).

$$E_{Hyd} = \frac{Q_{Dr} \cdot TDH}{366{,}972} \tag{48}$$

where

E_{Hyd} = Hydraulic energy required for the project (Wh/day)

Q_{Dr} = Total daily water requirement (litres/day)

TDH = Total dynamic head (metres)

366,972 = Energy conversion factor (Constant; The hydraulic energy calculation results in an answer in Joules. The unit required by the software program is Wh/day. Conversion to Wh, given that 1 J = 1 W/s , is a time factor 1/3600, assuming water at a constant density of 1000 kg/m³ and gravity a constant 9,81 $m.s^{-2}$. Simplification of all the 'constants' results in combined factor of 366,972. The adoption of density as a constant is justified in that it changes by one percent or less between 4 °C and 35 °C, salinity being negligible - as is the case with potable water)(Bucher 1996:10).

3.2.3.4 water pump selection module

This module is used to select or add/select an applicable PV powered water pump from a database in order to satisfy design requirements with respect to voltage, water pump rate and head. Pump selection is done via scroll, point and click actions. A pump must exist in the database before it can be used in the design calculations. Adding a pump is via an integrated input applet that requests pump data such as manufacturer, model, head, flow, power, voltage and pump efficiency. All data, with the exception of efficiency, is commonly supplied with the pump. If pumping efficiency is not provided by the manufacturer, the operator may select a value from

a range of default values depending on pump type and operating head, with reference to Table 9.

Table 9 **Default pumping efficiency values (adapted from Risser *et al.* 1991)**

TDH (m)	Pump Type	Efficiency η_{Pump} (%)
5	Surface Centrifugal	25
20	Surface Centrifugal	15
20	Submersible Centrifugal Single Step	25
20 to 100	Submersible Centrifugal Multiple Step	35
50 to 100	Positive Displacement	35
> 100 m	Positive Displacement/Jack Pump	45

A system calculated efficiency option (Equation 49) is also available, which is the recommended choice in the absence of manufacturer data.

$$\eta_{Pump} = \frac{P_{out}}{P_{in}} = \frac{TDH \cdot Q_P \cdot 27{,}249 \times 10^{-4}}{P_{Pump}} \qquad (49)$$

where

η_{Pump} = Pump efficiency fraction ($\times 100$ = percent)

TDH = Total dynamic head (metres)

Q_P = Required pump rate (litres/hour)

P_{Pump} = Rated pump power (watts)

The application software assumes an integrated motor/pump combination and calculates a 'wire-to-water' efficiency factor.

3.2.3.5 electrical wiring module

This module is used to recommend the gauge of wire to install. It also provides an estimate of wire losses for a given voltage, cable length, diameter and ambient temperature, resulting in an estimated electrical current requirement for the design. Design calculations are configured to ensure that wire gauge recommendations only

allow a three percent or less wire loss factor. Because of the variability of, and low power available to a PVPS application, the system should be as frugal as possible on power, with losses kept to a minimum. While the application software only makes recommendations and does not block inefficient design or costing tradeoffs, the operator should strive to limit wire losses to less than five percent.

Enough data is available at this point to enable calculation of preliminary PV array energy (E_{Array}, in Wh/day) and system load (S_{Load}, in Ah/day), calculated with equations (50) and (51) respectively.

$$E_{Array} = \frac{E_{Hyd}}{\eta_{Pump}} \tag{50}$$

$$S_{Load} = \frac{E_{Array}}{V_n} \tag{51}$$

where

η_{Pump} = Pump efficiency fraction

V_n = Nominal system voltage (Volts; generally in multiples of 6, starting at 12)

In order to calculate the wire loss factor, an intermediate estimate of electrical current is required. This is calculated according to equation (52), using the system load current and an empirical multiplier of 1,06 to account for miscellaneous system losses. The wire loss factor is then calculated using ambient temperature, wire resistivity (for copper), cross sectional area, bi-directional length and Ohms law (Hughes 1987:10-11), according to equations (53) and (54).

$$I_{est} = S_{Load} \cdot 1{,}06 \tag{52}$$

$$R_{Ta} = \left[\frac{0{,}01725 \cdot (W_L \cdot 2)}{W_a}\right] \cdot \left[1 + \frac{T_{amb}}{234{,}5}\right] \tag{53}$$

$$F_{WL} = 1 - \frac{\text{voltdrop}}{V_n} = 1 - \frac{I_{est} \cdot R_{Ta}}{V_n} \quad (54)$$

where

I_{est} = Empirical electrical current estimate (ampere)

S_{Load} = System load (Ah/day)

R_{Ta} = Resistance of copper at temperature T_{amb}

W_L = Length of installed copper wire (metres; single way, pump to PV array)

W_a = Cross sectional area of the installed wire (mm^2)

T_{amb} = Ambient system operating temperature (degrees Celsius)

F_{WL} = Wire loss factor (fraction)

V_n = Nominal system design voltage (volts)

The system load should now be de-rated by the wire loss factor, using equation (55), thus allowing calculation of an estimated design current according to equation (56).

$$S_{Load'} = \frac{S_{Load}}{F_{WL}} \quad (55)$$

$$I_{DesP} = \frac{S_{Load'}}{\overline{H_t}} \quad (56)$$

where

$S_{Load'}$ = De-rated system load (Ah/day)

F_{WL} = Wire loss factor (fraction)

I_{DesP} = Preliminary design current (ampere)

$\overline{H_t}$ = Mean monthly irradiation per day (kWh/m²/day), *i.e.* ESH or PSH (Equivalent or Peak) sun hours per day.

3.2.3.6 PV panel selection module

This module is used to iteratively select or add/select a PV panel to use in the design. This selection, together with all the other module results, culminate in a load

matching calculation that gives an indication of the PV array, voltage, current and power delivery rating to satisfy design requirements. Monthly array efficiency and pumping analysis is performed on the design results, which is presented both graphically and in tabular format and presents the designer with an opportunity to optimise the design in an iterative manner. A PV panel must exist in the database before it can be used in the design calculations. Adding a panel is via an integrated input applet which requests data such as manufacturer, model, material type, short circuit current (I_{SC}), open circuit voltage (V_{OC}), maximum power point current (I_{MP}), voltage (V_{MP}) and power (P_{MP}), nominal operating cell temperature ($NOCT$) and difference between name-plate power and data sheet warranted power ($dP\%$). This data is commonly available from the manufacturer via the data sheet supplied with the PV panel.

Table 10 PV module adjustment factors

Component De-Rate Factors	**Default Value (%)**	**Typical Range (%)**
Difference between warranted module minimum power & nameplate power rating	($dP\%$) From database	0 to 20
Module Mismatch	2	0,5 to 3,0
Diodes & Connections	0,5	0,3 to 1
Soiling	5,5	0,5 to 70
Shading	0 (= no shade)	0 to 100
Age	0 (= new)	0 to 30
Temperature	From calculation	87% to 92% of STC Power Rating
Component Boost Factors	**Default Value**	**Typical Range**
Cumulative Boost Factors	0	0 to 100

In order to calculate a final design current, the preliminary current obtained in equation (56) must be modified by PV panel and ancillary equipment efficiency. This modification factor is typically less than one and is therefore generally a de-rate factor. The factor, called the 'Panel Adjustment Factor' in the application software, accounts for various losses or enhancements incurred due to the PV array and ancillary equipment. These factors are summarised in Table 10 and originate from

cross referenced data between the California Energy Commission (2001:8), providing default values and PVWATTS System documentation (Renewable Resource Data Centre 2001), providing range values. Three exceptions are the temperature compensation algorithm, which is adapted from work by Evans (1981:555-560) and the boost factor and *dP%*, which are innovations of the application software.

Excluding Temperature and Boost, the component de-rate factors are processed according to equation (57) to obtain fractional values, which are then multiplied together to obtain a total de-rate fraction (F_{d_total}) according to equation (58).

$$F_d = 1 - \frac{F_{CDR}}{100} \tag{57}$$

$$F_{d\_total} = F_{d1} \cdot F_{d2} \cdot F_{dN...} \tag{58}$$

where

F_d = Fractional de-rate adjustment factor

F_{CDR} = Individual component de-rate factors

The fractional boost value is obtained using equation (59).

$$F_b = 1 + \frac{Cumulative\ boost\ factors}{100} \tag{59}$$

where

F_b = Fractional boost adjustment factor

Cumulative boost factors = Total efficiency increase gained from a linear current booster or equivalent electronic/mechanical system performance enhancer (percent).

The temperature de-rate fraction (F_{Td}) value is obtained using equation (60).

$$F_{Td} = 1 - \frac{F_{TDR}}{100} \tag{60}$$

where

$$F_{TDR} = \frac{\eta_r - \eta_p}{\eta_r} \cdot 100 \tag{61}$$

η_r = From Table 5

η_p = From Equation (28), with T_c modified to cater for $\overline{K}_t = 0$, as given in equation (62), adapted from Evans (1981:557) and obtaining the C_f factor from equation (30).

$$T_c = \left[\left(223{,}45 + 832\overline{K}_t \right) \cdot \frac{NOCT - 20}{800} \right] \cdot C_f + T_{amb} \tag{62}$$

where

T_c = PV cell operating temperature (degrees Celsius)

$NOCT$ = Nominal operating cell temperature rating (degrees Celsius)

$\overline{K}_t$ = Monthly maximum clearness index (dimensionless)

C_f = PV array tilt angle correction factor when not at optimum tilt (dimensionless)

T_{amb} = Ambient system operating temperature (degrees Celsius)

Note. All of the above data requirements are transparently sourced from database information.

The total PV module current modification factor can now be calculated according to equation (63).

$$F_{PVm} = F_{d\_total} \cdot F_b \cdot F_{Td} \tag{63}$$

where

F_{PVm} = Total PV module adjustment factor

Final design current is calculated using the preliminary current obtained in equation (56), adjusted by the total PV module adjustment factor, using equation (64).

$$I_{DES} = \frac{I_{DesP}}{F_{PVm}} \tag{64}$$

where

I_{DES} = Final design current (ampere)

I_{DesP} = Preliminary design current (ampere)

F_{PVm} = Total PV module adjustment factor

The modules needed to fulfil design requirements can now be calculated according to equations (65), (66) and (67). An assumption is made in the application software that all the modules to be used are of the same type and rating.

$$M_{PT} = \frac{I_{DES}}{I_{MP}} \tag{65}$$

$$M_{ST} = \frac{V_n}{V_{MP}} \tag{66}$$

$$M_{Total} = M_{PT} \cdot M_{ST} \tag{67}$$

where

M_{PT} = Total number of parallel module strings required, rounded up to the next integer number, *i.e.* $Ceiling(M_{PT})$

I_{MP} = Peak module current (ampere)

I_{DES} = Final design current (ampere)

M_{ST} = Total number of series modules required per parallel module string, rounded up to the next integer number, *i.e.* $Ceiling(M_{ST})$

V_n = Nominal system voltage (volts)

V_{MP} = Peak module voltage (volts)

M_{Total} = Total number of modules required for the PV array

The array power for the design is required by subsequent calculations and is given by equation (68). The maximum power point voltage for the design can also be obtained and is defined as 79 percent of the cumulative open circuit voltage of the system (Case, Joubert & Harrison 2002:T5-005), calculated according to equation (69).

$$P_{\text{Array}} = (I_{\text{MP}} \cdot M_{\text{PT}}) \cdot (V_{\text{MP}} \cdot M_{\text{ST}}) \tag{68}$$

$$V_{\text{MPP}} = 0{,}79 \cdot M_{\text{ST}} \cdot V_{\text{OC}} \tag{69}$$

where

P_{Array} = PV array power (watts)

I_{MP} = Peak individual module current (ampere)

M_{ST} = Number of series connected PV modules per parallel string in the array

V_{MP} = Peak individual module voltage (volts)

M_{PT} = Total number of parallel module strings in the PV array

V_{MPP} = Maximum power point voltage for the array (volts)

V_{OC} = Open circuit voltage of the individual modules used in the array (volts)

The efficiency of the 'Final Design' can now be evaluated by back-calculating through the design process, using previously calculated design values and comparing component based pumped water volume and pump rate with what was initially input and/or calculated as user requirements. Equations (70) and (71) are use for this purpose.

$$Q_{\text{Dr\_design}} = \frac{P_{\text{Array}} \cdot \eta_{\text{Pump}} \cdot \overline{H}_{\text{t}} \cdot F_{\text{PVm}} \cdot 366{,}972}{TDH} \tag{70}$$

$$Q_{\text{P\_design}} = \frac{Q_{\text{Dr\_design}}}{\overline{H}_{\text{t}}} \tag{71}$$

where

Q_{Dr_design} = 'Final Design' water pumped (litres/day)

Q_{P_design} = 'Final Design' pump rate (litres/hour)

P_{Array} = PV array power (watts)

η_{Pump} = 'Wire to water' pump/motor combination efficiency factor

$\overline{H_t}$ = Mean monthly irradiation per day (kWh/m²/day), *i.e.* ESH or PSH (Equivalent or Peak) sun hours per day.

TDH = Total dynamic head (metres)

F_{PVm} = Total PV module adjustment factor

It is imperative that the water source (aquifer/borehole) is able to deliver the maximum Q_{Dr_design} volume. If it is unable to deliver the design volume, then the design must be down-sized until an equitable figure is achieved. The capacity of the water source should not be exceeded, as this would cause the pump to run dry and could result in serious equipment damage.

Iterative variation of module and/or pump selection allows manual component matching and system optimisation as far as available components allow, with the software providing a display of under- or over performance via percentage, graphical and tabular formats, on a monthly basis for a one year period. Alternatively a 'Best Fit' analysis can be performed by the software and applied to the design by the operator. The 'Best Fit' algorithm is based on efficiency and quantitative analysis using equations (67), (70) and (71).

The final design values presented by the application software are based on 'worst case' scenarios, although a full 'monthly data' based design is presented for each month of the year in the 'Detailed Results' applet. A structured software dump of all system parameters and calculation results is possible from the Detailed Results applet, which saves the data in a 'spreadsheet' compatible comma-separated-variable (.CSV) format.

3.2.3.7 PV array orientation module

This module is used to generate location specific yearly magnetic declination corrections for magnetic (compass) North to true (solar) North correction. No existing methodology for this requirement could be found, resulting in the development of an application specific solution that allows the user to correctly orientate the PV array to true North at installation, using a simple directional compass bearing.

The location specific magnetic declination correction is calculated using equation (72), using location data from the Energy & Location Module together with data sourced from the magnetic declination database and the date maintained by the computer operating system (system date is assumed as correct by the application). Magnetic declination correction values are generated for the current year and four consecutive years into the future, allowing for installation and periodic verification.

$$MDC = \left| MDC_b + \left(\left[Y_c - 2006 \right] \cdot Y_{offset} \right) \right| \tag{72}$$

where

MDC = Magnetic declination correction (degrees; from calculation)

MDC_b = Magnetic declination correction 'base value' (degrees; from database)

Y_c = Gregorian calendar century and year (ccyy), for which the MDC is required

Y_{offset} = Yearly offset correction (degrees; from database)

3.2.3.8 calculated results module

In this module, the user is provided with an on-screen overview of the results of the various design phases, based on user input, statistical/database input and appropriate calculations. If detailed results are required, the Detailed Results applet under PV module selection can be used, or a detailed report printed from the main application menu bar.

3.2.3.9 quick estimator module

This module is used to input a solar irradiation value and produce an estimate of either PV module power, vertical pumping 'head' (TDH), or pumped water delivery, making use of two known variables and calculating the third. Provision is made to tweak the calculation via sub-system efficiency and array mismatch factor adjustments. The formula used is based on an adapted version of the ITDG algorithm (Intermediate Technology Development Group 2002:8) and is given in equation (73). This equation is manipulated to produce the correct configuration for the calculation mode chosen.

The 'Quick Estimator' is useful for generating rough estimates if a full design process is not required.

$$P_{\text{Array}} = \frac{2{,}725 \times 10^{-3} \cdot Q_{\text{Dr}} \cdot TDH}{\overline{H}_{\text{t}} \cdot \eta_{\text{sub}} \cdot F_{\text{AM}}} \qquad (73)$$

where

P_{Array} = PV array power (watts)

Q_{Dr} = Daily water requirement/delivery (litres/day)

TDH = Total dynamic head (metres)

$\overline{H}_{\text{t}}$ = Mean monthly irradiation per day (kWh/m²/day), *i.e.* ESH or PSH (Equivalent or Peak) sun hours per day.

η_{sub} = Daily sub-system efficiency; Typical range is between 0,25 and 0,4

F_{AM} = PV array mismatch factor; typically set at 0,85

When solving for Q_{Dr}, the low range water calculation has a step-wise adaptation to more accurately represent water delivery ability at low irradiation values, as derived from test data given in Figure 39. The adaptation takes place as follows:

- If $\overline{H}_{\text{t}} < 0{,}49$ then $Q_{\text{Dr}} = 0$
- If $0{,}49 < \overline{H}_{\text{t}} < 0{,}75$ then $Q_{\text{Dr}} = Q_{\text{Dr}} \div 3$

- If $0{,}75 < \overline{H}_t < 1{,}0$ then $Q_{Dr} = Q_{Dr} \div 2$
- If $1{,}0 < \overline{H}_t < 1{,}5$ then $Q_{Dr} = Q_{Dr} \div 1{,}5$

The standard equation given in (73) is valid for $\overline{H}_t$ values greater than 1,5.

The PV array mismatch factor (F_{AM}) and Daily sub-system efficiency (η_{sub}) can be refined by the operator but is initialised to 0,85 and 0,235 respectively. This is based on result matching with the main application program at default settings. At a setting of $F_{AM} = 0{,}85$ and $\eta_{sub} = 0{,}276$ the equation generates results similar to that of the empirical GTZ equation given in (27). The F_{AM} value can also be equated to PV module efficiency at NOCT (η_r), as a function of module composition material as given in Table 5. This is provided as a drop-down list selection option in the application program.

3.2.4 application databases

In order to limit external program dependence for operation and licensing, a 'flat-file' database structure was developed. This was deemed adequate to serve the requirements of the application program as the size of the database is not anticipated to be extraordinarily large and the complexity does not warrant a relational database. To facilitate maintenance and backup operations, independent database files where created for each requirement category. The application uses five databases to feed the calculation engine.

3.2.4.1 map database

The application software uses an embedded 'ActiveX' application and a proprietary geographic information system (GIS) database to generate a map of Southern Africa. 'Point-and-click' selection of a geographic location on the map generates latitude and longitude coordinates for that location. This coordinate data is then used to generate database lookup vectors for the Surface Meteorology & Solar Energy Database, as well as the Magnetic Declination Database. Of the various location capturing methodologies tested, this strategy provided the most accurate and consistent results.

3.2.4.2 surface meteorology and solar energy database

Comprehensive, year-round, surface meteorology and solar irradiation for the Southern African region as a whole proved impossible to source, with few meteorological stations existing that are able to provide extended solar irradiation data. An alternative was sought in the form of satellite data, which research has shown would be satisfactory for photovoltaic water pumping system preliminary design (see section 2.1.3.4). Investigation into satellite data availability revealed that the NASA Langley Research Centre - Atmospheric Sciences Data Centre (NASA-ASDC), could provide the required data. With prerequisite registration and access authorisation, satellite and ground station data for Southern Africa was available via internet based interrogation of the NASA Surface Meteorology and Solar Energy (SSE) release 5.1 data set (NASA-ASDC 2005). The SSE data set, derivation methodology and accuracy are discussed in detail by Whitlock (2004). Data access was arranged and permission to use the SSE data was obtained (Carter 2006:1). The required data was sourced and processed and a local database compiled.

The database content is built up into monthly data for a period of one year, compiled from raw and processed data for each fixed-degree (whole number) latitude and longitude intersection coordinate (node) within the design specification (16 Degrees East, minus 22 Degrees South to 33 East, minus 35 Degrees South). In order to speed up time consuming numerical processing (also reported by Townsend (1989:13) and Moraes-Duzat (2000:130)), some data values have been pre-processed and the results given in the database, dramatically improving (shortening) processing time. Pre-processed database values include irradiance at tilt, calculated according to equations (2) to (18), direct normal radiation and PV array tilt. A bi-linear horizontal interpolation, vertical bisection interpolation algorithm is used to generate all data for the required geographic location from this one-degree-by-one-degree resolution, latitude/longitude grid database. This is calculated according to equations (74) to (85), with reference to Figure 30.

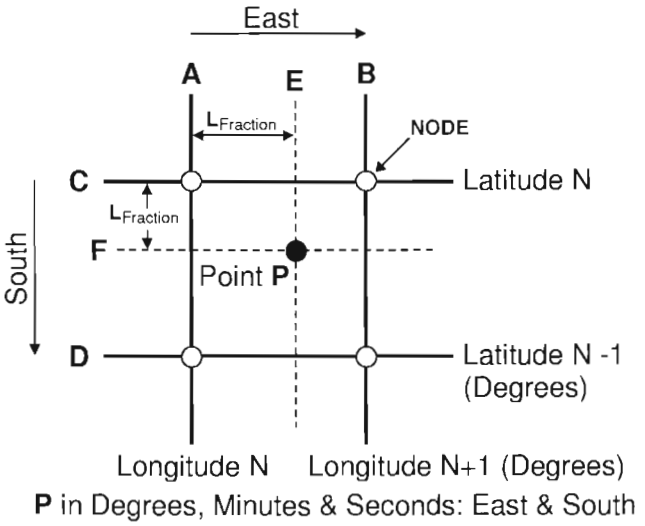

Figure 30 Coordinate data calculation grid

Data extraction from the database relies on lookup vectors created from the geographic latitude and longitude coordinates. These coordinates, given in degrees, minutes of arc and seconds of arc, are split into two components, an integer value and a fractional value. The integer value is the whole number degree value, used for the physical lookup vector, while the fractional part is the minutes and seconds of arc converted to a decimal fraction, done for both latitude and longitude using equation (74) and used in the data interpolation algorithm.

$$L_{\text{Fraction}} = \frac{|M|}{60} + \frac{|S|}{3600} \tag{74}$$

where

L_{Fraction} = Latitude or Longitude fraction value (CF or AE respectively, in Figure 30)

M = Latitude or Longitude: Minutes of arc (')

S = Latitude or Longitude: Seconds of arc (")

With reference to Figure 30, map or user input coordinates for point P would generate the first database lookup vector pair AC, using the methodology described above, with the fractional portions being represented by AE and CF. It can be seen however, that four vectors pairs (AC, AD, BC & BD) are required, and that data sets

must be acquired for all four bounding nodes in order to derive a data set for point P. The database lookup vectors are calculated according to equations (75) to (82).

$$\text{Latitude AC} = \text{Latitude P} - L_{\text{Fraction}}\text{CF} \tag{75}$$

$$\text{Longitude AC} = \text{Longitude P} - L_{\text{Fraction}}\text{AE} \tag{76}$$

$$\text{Latitude AD} = \text{Latitude AC} - 1 \tag{77}$$

$$\text{Longitude AD} = \text{Longitude AC} \tag{78}$$

$$\text{Latitude BC} = \text{Latitude AC} \tag{79}$$

$$\text{Longitude BC} = \text{Longitude AC} + 1 \tag{80}$$

$$\text{Latitude BD} = \text{Latitude AC} - 1 \tag{81}$$

$$\text{Longitude BD} = \text{Longitude AC} + 1 \tag{82}$$

These lookup vectors allow the four data sets bounding point P to be extracted from the database using base and offset pointers. The bi-linear horizontal interpolation, vertical bisection interpolation algorithm given in equations (83) to (85) below, is then used sequentially, on each of the data values in turn, in the four data sets (1008 iterations of the algorithm), to derive a data set for Point P.

If $D_{val}AC < D_{val}BC$ then Equation (83a); **or** If $D_{val}AC > D_{val}BC$ then Equation (83b).

$$D_{val}AE = D_{val}AC + (L_{Fraction}AE \cdot [D_{val}BC - D_{val}AC]) \tag{83a}$$

$$D_{val}AE = D_{val}AC - (L_{Fraction}AE \cdot [D_{val}AC - D_{val}BC]) \tag{83b}$$

If $D_{val}AD < D_{val}BD$ then Equation (84a); **or** If $D_{val}AD > D_{val}BD$ then Equation (84b).

$$D_{val}DE = D_{val}AD + (L_{Fraction}AE \cdot [D_{val}AD - D_{val}BD]) \tag{84a}$$

$$D_{val}DE = D_{val}AD - (L_{Fraction}AE \cdot [D_{val}AD - D_{val}BD]) \tag{84b}$$

If $D_{val}AE < D_{val}DE$ then Equation (85a); **or** If $D_{val}AE > D_{val}DE$ then Equation (85b).

$$D_{val}P = D_{val}AE + (L_{Fraction}CF \cdot [D_{val}DE - D_{val}AE]) \tag{85a}$$

$$D_{val}P = D_{val}AE - (L_{Fraction}CF \cdot [D_{val}AE - D_{val}DE]) \tag{85b}$$

where

D_{val}?? = Specific data value at specified coordinate point

$L_{Fraction}$?? = Fractional value for specified coordinate point as calculated from (74)

The monthly data set contents available per latitude/longitude node in the database is summarised in Table 11, with a location specific node example provided in Table 12. The full Southern African Surface Meteorology and Solar Energy Database content extends to 252 nodes multiplied by the number of components (21) multiplied by the number of months in a year (12). This equates to 63504 data points; or 129 pages of data tables, as provided in Annexure 5.

Table 11 Latitude/Longitude node data set contents

Number	Component Description	Units
base offset +1	**SSE (minimum)**: The monthly average amount of the total solar radiation incident on a horizontal surface at the surface of the earth for the year that has the least, or minimum, monthly averaged value in the 10 year period, July 1983 - June 1993.	kWh/m^2/day
base offset +2	**Clearness Index (K_t minimum)**: The monthly average amount of the total solar radiation incident on a horizontal surface at the surface of the earth for the year that has the least, or minimum, monthly averaged value in the 10 year period divided by the monthly average incoming top-of-atmosphere irradiation (insolation) for that month.	dimensionless 0,0 – 1,0
base offset +3	**Diffused Irradiation**: The monthly average amount of solar radiation for a given month incident on a horizontal surface at the surface of the earth under all-sky conditions with the direct radiation from the sun's beam blocked by a shadow band or tracking disk for the year that has the most, or maximum, monthly averaged value in the 10 year period (Page method).	kWh/m^2/day

base offset +4	**Direct Normal Radiation (DNR)**: The monthly average amount of solar radiation incident on a surface oriented normal to the solar radiation for a given month, averaged for that month over the 10 year period, July 1983 - June 1993. The direct normal radiation is evaluated using the Extended Page/Empirical Staylor Hourly Method described in SSE Methodology Section 5.3.2 (Whitlock 2004:7).	kWh/m^2/day
base offset +5	**ESH at Tilt 0 degrees**: The monthly average amount of the total solar radiation incident on a surface tilted relative to the horizontal and pointed toward the equator for the year that has the least, or minimum, monthly averaged value in the 10 year period. Note that the differences between the Tilt 0 values and the SSE MIN values are due to approximations in the inputs and time integration inaccuracies when processing the equations and integrating over the 'monthly average day' Refer to Table 2 and SSE Methodology, Section [see 5.1.1, footnote (Whitlock 2004:4)]. Total solar radiation for each tilt angle was determined using SSE MIN in the Perez Non-Isotropic/Extended Page Horizontal Diffuse Method discussed in SSE Methodology Section 6.1.2 (Whitlock 2004:8-9).	kWh/m^2/day
base offset +6	**ESH at Tilt = Latitude - 15 degrees**: Description as per Number "base offset +5"	kWh/m^2/day
base offset +7	**ESH at Tilt = Latitude degrees**: Description as per Number "base offset +5"	kWh/m^2/day
base offset +8	**ESH at Tilt = Latitude + 15 degrees**: Description as per Number "base offset +5"	kWh/m^2/day
base offset +9	**ESH at Tilt = 90 degrees**: Description as per Number "base offset +5"	kWh/m^2/day
base offset +10	**Optimum Equivalent Sun Hours (ESH)**: The monthly average amount of total solar radiation incident on a surface tilted at the optimum angle relative to the horizontal and pointed toward the equator (Perez/Page Method).	kWh/m^2/day

base offset +11	**ESH Optimum Tilt**: The angle relative to the horizontal for which the monthly averaged total solar radiation is at maximum.	degrees
base offset +12	**SSE (maximum)**: The monthly average amount of the total solar radiation incident on a horizontal surface at the surface of the earth for the year that has the most, or maximum, monthly averaged value in the 10 year period, July 1983 - June 1993.	$kWh/m^2/day$
base offset +13	**Clearness Index (K_t maximum)**: The monthly average amount of the total solar radiation incident on a horizontal surface at the surface of the earth for the year that has the most, or maximum, monthly averaged value in the 10 year period divided by the monthly average incoming top-of-atmosphere irradiation (insolation) for that month.	dimensionless 0,0 – 1,0
base offset +14	**Optimum Peak Sun Hours (PSH)**: The monthly average amount of total solar radiation incident on a surface tilted at the optimum angle relative to the horizontal and pointed toward the equator.	$kWh/m^2/day$
base offset +15	**PSH Optimum Tilt**: The angle relative to the horizontal for which the monthly averaged total solar radiation is a maximum.	degrees
base offset +16	**Number of No-sun Days**: The number of no-sun or 'black' days per month where no direct solar irradiance is incident on the specified location.	days/month
base offset +17	**Monthly Averaged Daylight Cloud Amount**: Percent of cloud amount during daylight for a given month, averaged for that month over the 10 year period July 1983 - June 1993. A value of zero indicates clear skies and a value of 100 indicates totally overcast skies.	percent

base offset +18	**Monthly Averaged Air Temperature**: The monthly average air temperature for a given month, averaged for that month over the 10 year period, July 1983 - June 1993. Temperature values are for 10 metres above the surface of the earth. Each monthly averaged value is evaluated as the numerical average of 3 hourly values for the given month. See SSE Methodology, Section 8.1 (Whitlock 2004:10-11). This value is assumed to be the ambient location temperature by the SAS-SWP application.	degrees Celsius
base offset +19	**Monthly Averaged Wind Speed**: The monthly average wind speed for a given month, averaged for that month over the 10 year period, July 1983 - June 1993, where the wind speed was evaluated at 10 metres above the surface of the earth assuming the underlying terrain is similar to that typical of airports, *e.g.* 'airport' flat rough grass category taken from Gipe (1999:10); See SSE Methodology, Section 7 (Whitlock 2004:10).	metres/second
base offset +20	**Monthly Averaged Top-of-atmosphere Irradiation**: The monthly average amount of the total solar irradiation (insolation) incident on the top-of-atmosphere for a given month, averaged for that month over the 10 year period, July 1983 - June 1993. Also referred to as extraterrestrial irradiation.	$kWh/m^2/day$
base offset +21	**Monthly Averaged Surface Albedo**: The monthly average ratio of the solar energy reflected by the surface of the earth to monthly average solar energy incident on the surface of the earth for a given month, averaged for that month over the 10 year period, July 1983 - June 1993, *i.e.* Fraction of irradiation (insolation) reflected by the surface of the earth.	dimensionless 0,0 – 1,0

Table 12 Latitude/Longitude node data set example

Southern African Surface Meteorology and Solar Energy Database

		Latitude: -22° South											
	Descriptor	January	February	March	April	May	June	July	August	September	October	November	December
Longitude: 16° East	1	6.39	5.84	5.34	4.47	4.23	3.67	3.91	4.57	5.43	6.08	6.73	6.52
	2	0.54	0.52	0.53	0.52	0.59	0.56	0.58	0.58	0.58	0.57	0.59	0.55
	3	2.28	2.2	1.97	1.69	1.34	1.24	1.27	1.47	1.74	2.01	2.13	2.29
	4	6.5	5.57	5.37	5.08	6.05	5.47	5.67	6.03	6.43	6.68	6.93	6.76
	5	6.36	5.72	5.26	4.43	4.2	3.56	3.78	4.53	5.37	5.97	6.7	6.49
	6	6.29	5.8	5.48	4.76	4.7	4.01	4.24	4.97	5.67	6.1	6.65	6.65
	7	5.89	5.72	5.72	5.27	5.56	4.81	5.04	5.68	6.08	6.14	6.28	6.72
	8	5.17	5.32	5.62	5.48	6.09	5.32	5.54	6.06	6.14	5.8	5.57	6.39
	9	1.6	1.95	2.93	3.76	5.01	4.52	4.61	4.55	3.62	2.31	1.64	2.65
	10	6.36	5.81	5.72	5.48	6.25	5.51	5.71	6.11	6.16	6.17	6.7	6.74
	11	0	11	25	39	51	53	52	45	32	16	0	17
	12	7.82	6.83	6.2	5.61	5.2	4.63	4.78	5.63	6.65	7.53	7.45	8.01
	13	0.67	0.61	0.62	0.66	0.72	0.71	0.71	0.72	0.72	0.71	0.65	0.68
	14	7.78	6.79	6.68	7.05	7.8	7.18	7.09	7.59	7.49	7.58	7.41	8.27
	15	0	11	25	40	51	54	52	45	31	14	0	17
	16	2.2	2.6	2.16	2.85	2.8	4.39	3.45	3.22	3.51	2.95	1.48	3.79
	17	54.5	57.3	48.1	40.8	14.4	5.45	7.69	8.3	21.9	37.1	43.7	40.6
	18	24.5	23.6	22.7	20.7	18.3	15.3	15.4	18.1	20.8	23.1	24.6	24.6
	19	2.92	2.68	2.84	3.31	3.63	3.93	4.09	4.05	4.09	3.71	3.47	3.02
	20	11.6	11	9.94	8.47	7.14	6.46	6.72	7.8	9.22	10.5	11.3	11.7
	21	0.22	0.21	0.22	0.21	0.22	0.21	0.22	0.23	0.23	0.21	0.22	0.22

Index #	Descriptor
1	SSE (min.) Daily Sun Hours
2	Clearness Index (Kmin.)
3	Diffused Radiation (Page method)
4	Direct Normal Radiation (DNR – Page method)
5	ESH @ Tilt = 0°
6	ESH @ Tilt = Latitude -15°
7	ESH @ Tilt = Latitude°
8	ESH @ Tilt = Latitude + 15°
9	ESH @ Tilt = 90°
10	Optimum Equivalent Sun Hours (ESH - Perez/Page method)
11	Optimum Tilt Angle ° for ESH
12	SSE (max.) Daily Sun Hours
13	Clearness Index (Kmax.)
14	Optimum Peak Sun Hours (PSH)
15	Optimum Tilt Angle ° for PSH
16	Number of NO-SUN or BLACK Days (days/month)
17	Monthly Averaged Daylight Cloud Amount (%)
18	Monthly Averaged Air Temperature at 10m above the surface of the Earth (°C)
19	Monthly Averaged Wind Speed at 10m above the surface of the Earth for terrain similar to Airports (m/s)
20	Monthly Averaged Top-of-atmosphere Insolation (kWh/m²/day)
21	Monthly Averaged Surface Albedo (0 to 1.0)

3.2.4.3 solar pump database

The Solar Pump Database is comprised of pump data suitable for directly coupled solar water pumping applications.

At first glance, pump performance modelling and rating data for the database would appear to be a simple process of transcribing manufacturer data – Unfortunately, in reality pumping systems are complex and multi-dimensional, eloquently described by Collins and Jones (2002:3). Pumping rate (flow) is dependant on water pressure (head), system efficiencies and applied power, while the power is dependent on the photovoltaic system composition, configuration and setup, as well as the available solar irradiation as dictated by the physical geographic location. Pump data cannot be characterised by a single set of values. It is equipment specific and generally provided by the manufacturer in the form of head versus pump rate graphs (or tables) at a specified drive power.

In order to facilitate simple data entry but maintain adequate pump data for design and component matching, multiple data entries per pump were added to the database. Systematic database entries were made for individual pumps at various head and power values, encapsulating manufacturer data in an incremental tabular format. A total of six manufacturers and 820 pump entries are provided in the default database, with new additions easily accommodated.

The pump database may be randomly browsed, or sorted by manufacturer, model, head, power, pump rate or efficiency, with the selected pump's data being transferred to the application program for inclusion in the design process.

All the manufacturer data sheets used in compiling the default pump-set database are provided on the companion CD, in portable document format (.PDF) under directory [../Data_Sheets/PV_Water_Pumps], with default database data listed in Annexure 6.

3.2.4.4 solar (PV) panel database

The Solar Panel Database is comprised of a multitude of solar panels currently available in the marketplace.

The panel database may be randomly browsed, or sorted by manufacturer, model, material, I_{SC}, V_{OC}, I_{MP}, V_{MP}, P_{MP}, *NOCT* or *dp%*, with the selected panel's data being transferred to the application program for inclusion in the design process.

A total of seventeen manufacturers and 156 full panel data entries are provided in the default database, with new additions easily accommodated.

All the manufacturer data sheets used in compiling the default PV module database are provided on the companion CD, in portable document format (.PDF) under directory [../Data_Sheets/PV_Panels], with the default database data listed in Annexure 7.

3.2.4.5 magnetic declination database

The earth's magnetic field is constantly changing. This factor makes it impossible to accurately predict what the field will be at any point in the far distant future. By constantly measuring the magnetic field, the change over a period of years can be observed. Using this information, it is possible to create a mathematical representation of the earth's main magnetic field and how it is changing. Since the field varies in the way it is changing, new observations must continually be made and models generated to accurately represent the magnetic field for the short to medium term. The International Geomagnetic Reference Field Model (IGRF) is the international research reference model for magnetic field prediction (National Geophysical Data Centre 2006) and was the model used to generate the Southern African reference data that was analysed.

Magnetic declination data for ten years into the future, starting in 2006, was sourced from the American National Geophysical Data Centre (NGDC), using the IGRF10 model as the generation source (National Geophysical Data Centre 2006). The data

set was analysed and a magnetic declination correction database was compiled and mapped to latitude and longitude references as given in Table 14 and graphically depicted in Figure 31. The database data is extracted, calculated according to equation (72) and interpolated to provide a location specific value as per the bounding four node methodology used in the Southern African Surface Meteorology and Solar Energy Database described earlier.

Comparison between the calculated declination correction values (year base 2008) for various major South African cities and values delivered by the NGDC (National Geophysical Data Centre 2006) show that this simplified methodology delivers results within a half degree (refer to Table 13) of the complex IGRF10 model predictions – well within acceptable orientation offset constraints for PV arrays. It should be noted that localised geo-magnetic anomalies are not catered for in the adopted strategy.

Table 13 Magnetic declination comparison

Location			Declination		
	South Latitude	East Longitude	SAS-SWP Calculated	NGDC (mid-year)	Difference
Johannesburg	- 26° 09' 06"	28° 02' 21"	17,98°	18,10°	- 0,12°
Bloemfontein	- 29° 08' 02"	26° 12' 50"	21,44°	21,55°	- 0,11°
Durban	- 26° 52' 12"	30° 54' 51"	24,28°	24,35°	- 0,07°
Cape Town	- 33° 56' 50"	18° 31' 44"	24,38°	24,48°	- 0,10°
Year base for comparison = 2008					

Base Magnetic Declination Correction Table for Year 2006 (MDCb in Degrees)

		East Longitude:																	
		16	17	18	19	20	21	22	23	24	25	26	27	28	29	30	31	32	33
South	-22	-13.178	-12.893	-12.644	-12.433	-12.262	-12.132	-12.044	-11.999	-11.997	-12.038	-12.120	-12.243	-12.405	-12.603	-12.836	-13.101	-13.395	-13.714
Latitude:	-23	-14.089	-13.830	-13.607	-13.422	-13.278	-13.175	-13.115	-13.098	-13.124	-13.192	-13.301	-13.449	-13.636	-13.858	-14.113	-14.399	-14.712	-15.048
	-24	-15.022	-14.791	-14.597	-14.442	-14.328	-14.256	-14.226	-14.238	-14.293	-14.390	-14.526	-14.701	-14.913	-15.159	-15.436	-15.742	-16.074	-16.427
	-25	-15.967	-15.769	-15.607	-15.485	-15.404	-15.364	-15.366	-15.411	-15.496	-15.622	-15.787	-15.989	-16.226	-16.496	-16.795	-17.121	-17.470	-17.839
	-26	-16.918	-16.755	-16.629	-16.543	-16.497	-16.491	-16.528	-16.605	-16.722	-16.878	-17.072	-17.301	-17.564	-17.857	-18.177	-18.522	-18.888	-19.272
	-27	-17.866	-17.741	-17.653	-17.604	-17.595	-17.626	-17.698	-17.809	-17.959	-18.146	-18.369	-18.625	-18.913	-19.228	-19.569	-19.932	-20.315	-20.713
	-28	-18.801	-18.717	-18.669	-18.660	-18.689	-18.758	-18.866	-19.011	-19.194	-19.412	-19.664	-19.947	-20.259	-20.597	-20.958	-21.339	-21.737	-22.148
	-29	-19.715	-19.673	-19.667	-19.698	-19.768	-19.875	-20.019	-20.200	-20.416	-20.665	-20.945	-21.255	-21.591	-21.950	-22.330	-22.728	-23.141	-23.565
	-30	-20.600	-20.601	-20.638	-20.711	-20.820	-20.966	-21.147	-21.363	-21.611	-21.891	-22.199	-22.535	-22.894	-23.274	-23.673	-24.088	-24.514	-24.950
	-31	-21.448	-21.493	-21.573	-21.688	-21.837	-22.021	-22.239	-22.489	-22.770	-23.079	-23.415	-23.776	-24.158	-24.558	-24.975	-25.405	-25.846	-26.294
	-32	-22.254	-22.343	-22.465	-22.621	-22.811	-23.033	-23.286	-23.570	-23.882	-24.220	-24.583	-24.968	-25.372	-25.792	-26.227	-26.672	-27.126	-27.585
	-33	-23.011	-23.144	-23.309	-23.506	-23.734	-23.993	-24.281	-24.598	-24.940	-25.307	-25.695	-26.103	-26.528	-26.968	-27.419	-27.880	-28.347	-28.818
	-34	-23.718	-23.894	-24.100	-24.336	-24.602	-24.897	-25.219	-25.567	-25.938	-26.332	-26.745	-27.176	-27.621	-28.079	-28.547	-29.022	-29.502	-29.985
	-35	-24.373	-24.589	-24.835	-25.110	-25.412	-25.741	-26.095	-26.473	-26.873	-27.292	-27.729	-28.181	-28.646	-29.122	-29.606	-30.096	-30.589	-31.083

Yearly Offset Table (Yoffset in Degrees)

		East Longitude:																	
		16	17	18	19	20	21	22	23	24	25	26	27	28	29	30	31	32	33
South	-22	0.1	0.1	0	0	0	0	0	0	0	0	0	0.1	0.1	0.1	0.1	0.1	0.1	0.1
Latitude:	-23	0.1	0	0	0	0	0	0	0	0	0.1	0.1	0.1	0.1	0.1	0.1	0.1	0.1	0.1
	-24	0	0	0	0	0	0	0	0	0.1	0.1	0.1	0.1	0.1	0.1	0.1	0.1	0.1	0.1
	-25	0	0	0	0	0	0	0	0.1	0.1	0.1	0.1	0.1	0.1	0.1	0.1	0.1	0.1	0.1
	-26	0	0	0	0	0	0	0.1	0.1	0.1	0.1	0.1	0.1	0.1	0.1	0.1	0.1	0.2	0.2
	-27	0	0	0	0	0	0.1	0.1	0.1	0.1	0.1	0.1	0.1	0.1	0.1	0.2	0.2	0.2	0.2
	-28	0	0	0	0	0.1	0.1	0.1	0.1	0.1	0.1	0.1	0.1	0.2	0.2	0.2	0.2	0.2	0.2
	-29	0	0	0	0.1	0.1	0.1	0.1	0.1	0.1	0.1	0.1	0.2	0.2	0.2	0.2	0.2	0.2	0.2
	-30	0	0	0.1	0.1	0.1	0.1	0.1	0.1	0.1	0.1	0.2	0.2	0.2	0.2	0.2	0.2	0.2	0.2
	-31	0	0.1	0.1	0.1	0.1	0.1	0.1	0.1	0.2	0.2	0.2	0.2	0.2	0.2	0.2	0.2	0.2	0.2
	-32	-0.1	0.1	0.1	0.1	0.1	0.1	0.1	0.2	0.2	0.2	0.2	0.2	0.2	0.2	0.2	0.2	0.2	0.2
	-33	-0.1	0.1	0.1	0.1	0.1	0.1	0.2	0.2	0.2	0.2	0.2	0.2	0.2	0.2	0.2	0.2	0.2	0.2
	-34	-0.1	0.1	0.1	0.1	0.1	0.2	0.2	0.2	0.2	0.2	0.2	0.2	0.2	0.2	0.2	0.2	0.2	0.2
	-35	-0.1	0.1	0.1	0.1	0.1	0.2	0.2	0.2	0.2	0.2	0.2	0.2	0.2	0.2	0.2	0.2	0.2	0.2

Magnetic Declination Calculation for True North

$$MDC = \left| MDC_b + \left([Y_c - 2006] \cdot Y_{offset} \right) \right|$$

where

MDC = Magnetic declination correction (degrees; from calculation, added to compass north bearing in an easterly [clockwise] direction to obtain True North)

MDC_b = Magnetic declination correction Base Value (degrees; from Table, for location)

Y_c = Gregorian calendar century and year (ccyy), for which the MDC is required (Yc ≥ 2006)

Y_{offset} = Yearly offset correction (degrees; from Table, for location)

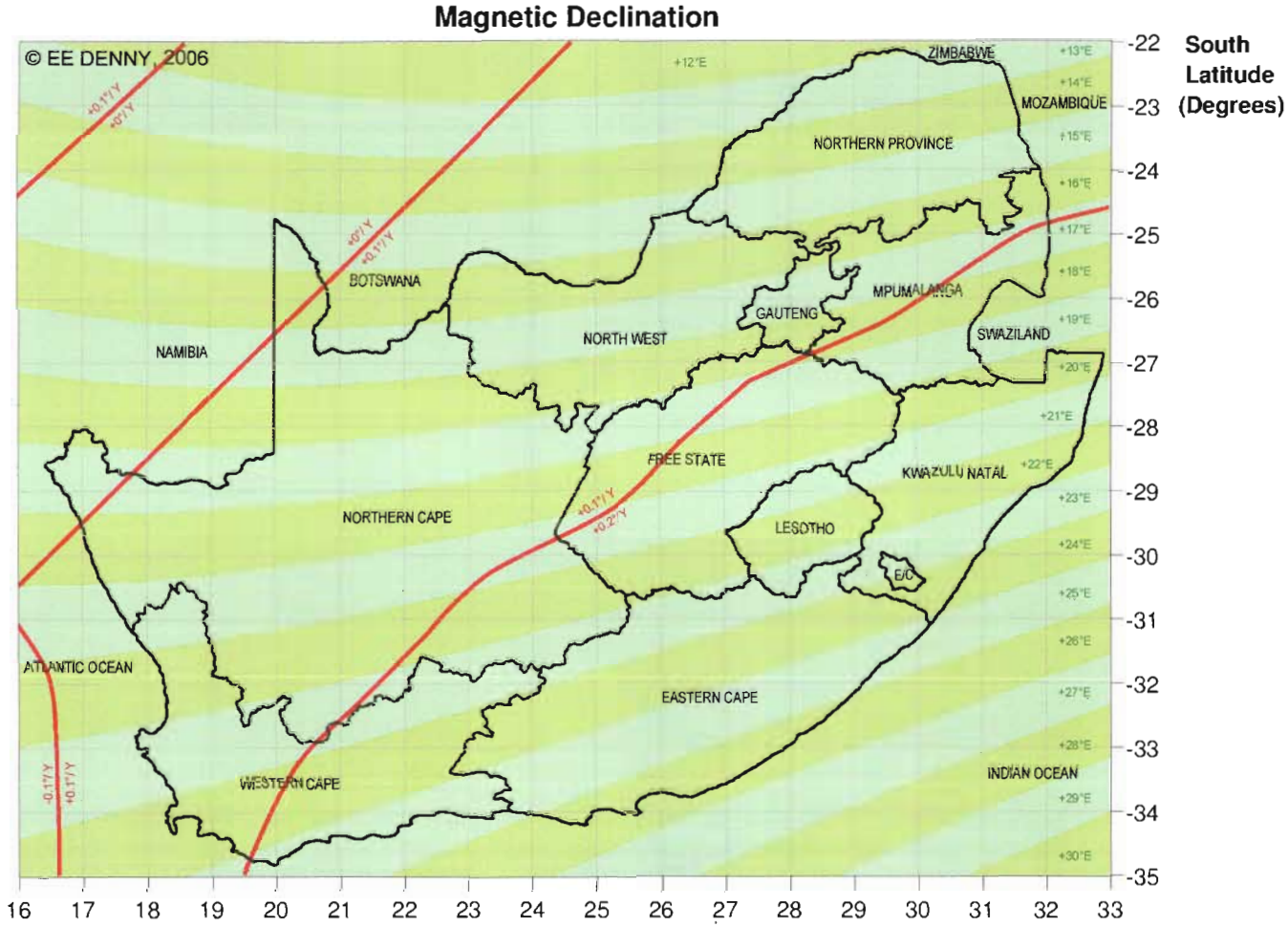

Figure 31 Magnetic declination zones surface plot – RSA

Magnetic Declination and Correction Zones (Compass Degrees - Year: 2006)

3.3 Application software description

The application software consists of an executable file developed in a custom test, measurement and data acquisition application development package. 'Run-time' applications created with this development package are license and royalty free. The program is fronted by a simple, intuitive, Graphical User Interface (GUI), that presents the operator with menu driven design steps, enabling non-technical personnel to easily operate the application. On-line, context sensitive help is available in all menu steps, with overall help being accessed via menu selection or use of the 'F1' function key.

3.4 Design synopsis

A graphical user interface, calculation engine, database interface and databases have been coded into an application program according to set design specifications. Program flow can be seen in the Program Model Bounce Diagram given in Annexure 1, while the Software Listing is given in Annexure 3 and Database Tables are given in Annexure 5 through 7.

Program module operations are characterised by event-triggered GUI operations, Input, Calculations, Database operations, Help system and Output, as seen in the Bounce Diagram and simplified Calculation Chain given in Figure 32 which, together with the Software Listing, should be used as a reference for all software functionality. Program operation is described in detail in the Application Program Help File (Software – File name: SAS-SWP.hlp), as well as in the Help File listing given in Annexure 2. The front-end GUI, together with all other menus, applets, windows, panels, data entry and operation are illustrated in this annexure. The help file information is available to the operator as 'On-line' help, either as a whole, or via context sensitive linking from within specific application modules.

A fully functional, installable version of the application software is provided on the companion CD, under directory [../SAS-SWP_Install/setup.exe].

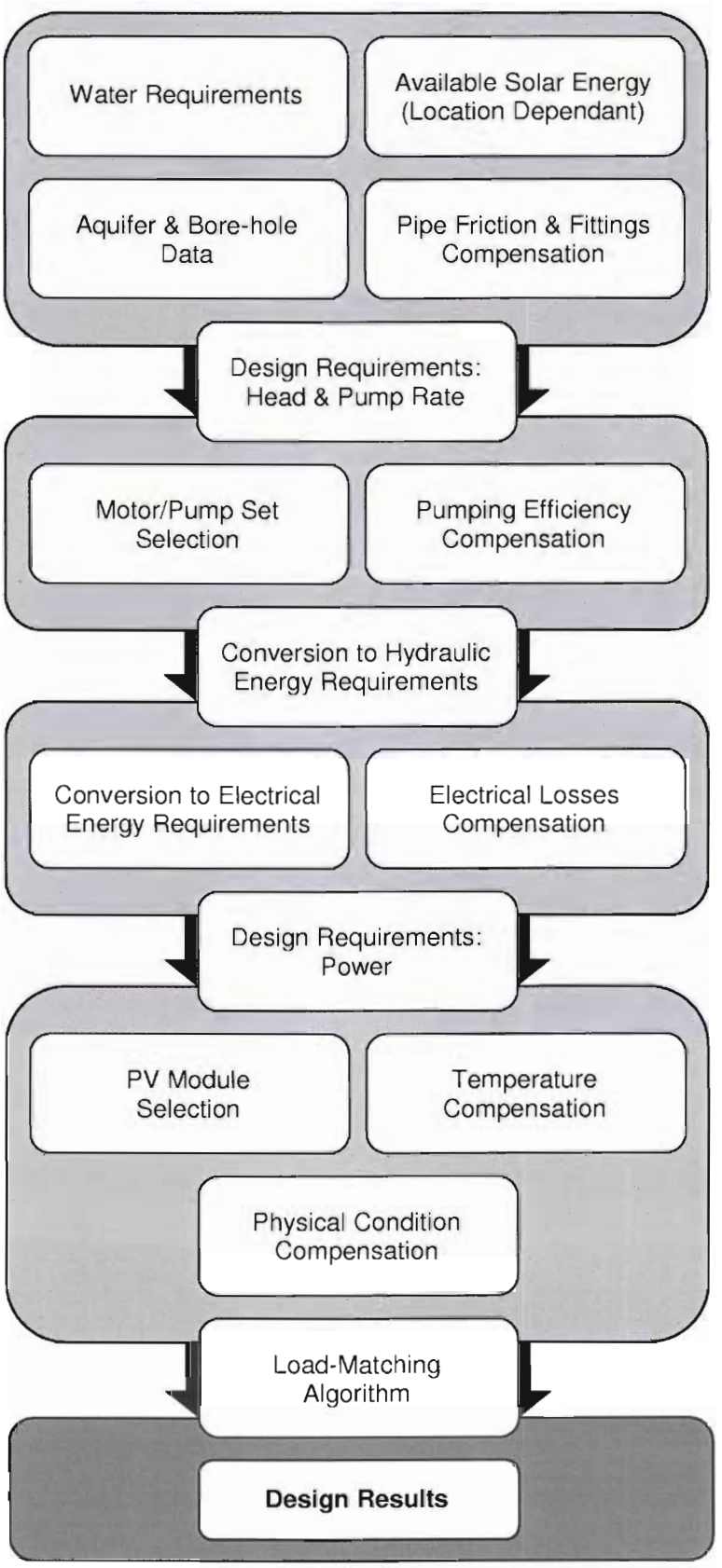

Figure 32 **Simplified SAS-SWP calculation chain**

CHAPTER 4 - Tests and Results

4.1 Software module tests

The results delivered by the various software databases and modules for the Application Software 'South African Stand-alone Solar (PV) Water Pumping Design Aid' (SAS-SWP), as coded, was checked and compared to external references or manual calculation for correctness, as detailed below.

4.1.1 location

The coordinates of major South African cities were obtained from the map module and 1:50000 scale topographical maps. Comparison of the coordinate data revealed that the map module and database delivered fractional differences in the seconds of arc in the latitude and longitude coordinate data, relative to the topographical maps. This can be attributed to minor measurement offset in the measurement and subsequent calculation of coordinates from the physical maps, as well as variation in the precise location selection on the GIS map screen. Comparison with Google Earth virtual 'on-line' maps (Google Earth 2007) delivered comparable results.

Variations of a few arc-seconds will have no significant impact on coordinate dependant calculations and the results delivered by this module are therefore deemed valid.

4.1.2 energy

Base solar irradiation and ancillary data as contained in the application program database was compared to source data from the NASA SSE 5.1 data set and found to be an accurate representation. One degree by one degree grid node data retrieval was found to be an accurate match, while interpolation algorithm data was verified as correct against manually calculated multi-point data.

An irradiation data comparison was done between various software packages able to deliver solar data, using a northerly site in the city of Pretoria as the test location (See Figure 33 for an aerial photograph).

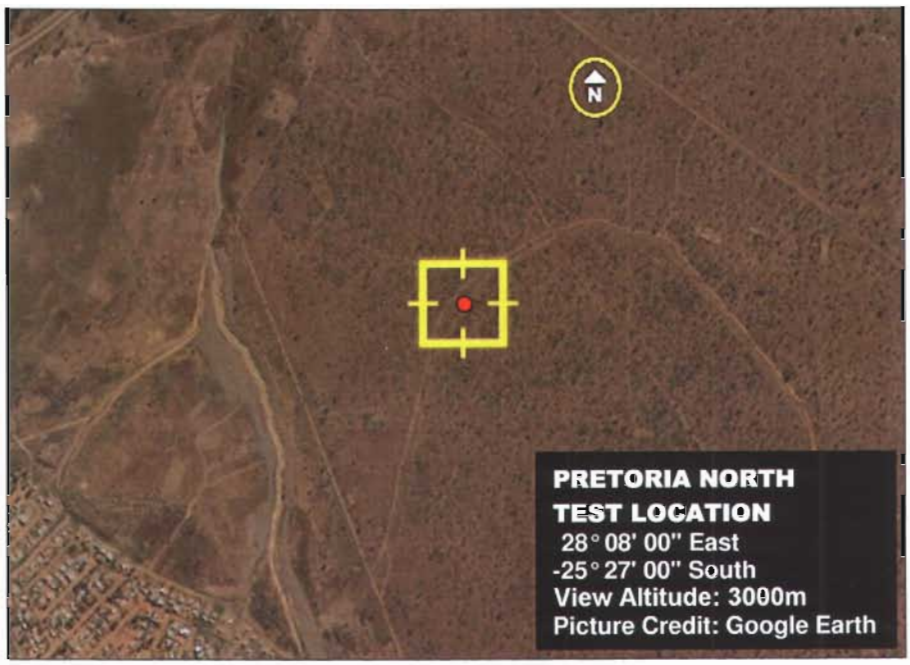

Figure 33 Solar irradiance test location – Pretoria area

Test Location Coordinates: Latitude -25° 27' 00" South
Longitude 28° 08' 00" East

The software applications that the SAS-SWP application was tested against did not have a monthly PV Array tilt setting facility, so a fixed tilt of twenty seven degrees was used as the reference tilt angle for all comparisons other than that given for the SAS-SWP Monthly Optimum reference trend. Data used for the SAS-SWP twenty seven degree and Monthly Optimum trends is based on monthly averaged daily ESH values, with SSE maximum and minimum values given as a reference. The comparison applications provide singular irradiation data sets as displayed and tabulated in Figure 34. All PV Array orientations are set to true North (Azimuth = 0).

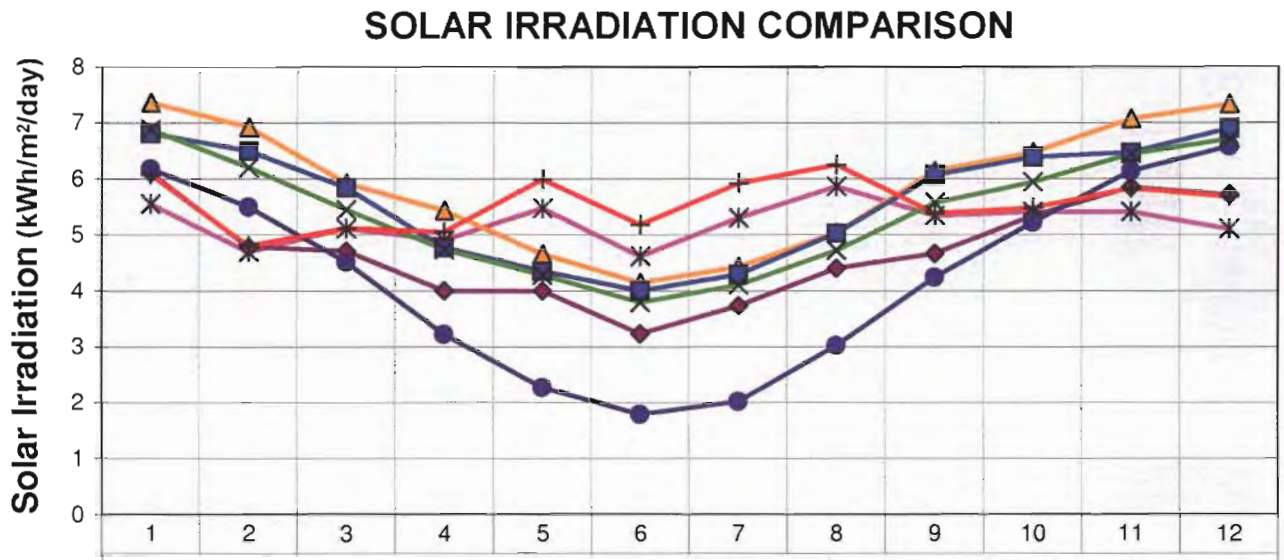

Figure 34 Solar irradiation comparison graph

Source Data (kWh/m²/d)												
SAS-SWP at 27° Tilt	5.55	4.69	5.11	4.9	5.47	4.61	5.3	5.86	5.34	5.41	5.41	5.1
SSE(maximum) at 27° Tilt	7.36	6.92	5.92	5.43	4.65	4.14	4.42	5.04	6.14	6.47	7.07	7.33
SSE(minimum) at 27° Tilt	6.11	4.78	4.71	4	4	3.23	3.73	4.4	4.66	5.34	5.85	5.71
RETScreen at 27° Tilt	6.18	5.5	4.51	3.22	2.27	1.79	2.02	3.02	4.24	5.22	6.14	6.58
Meteonorm at 27° Tilt	6.81	6.5	5.84	4.77	4.35	4	4.29	5.03	6.07	6.39	6.47	6.9
Homer at 27° Tilt	6.88	6.2	5.45	4.73	4.28	3.79	4.1	4.72	5.57	5.94	6.44	6.71
SAS-SWP at Optimum Tilt	6.08	4.8	5.12	5.05	5.99	5.18	5.92	6.25	5.38	5.48	5.83	5.68

The following solar irradiation data sources are compared in Figure 34:

- SAS-SWP Application Software at User Defined PV array tilt of 27 degrees
  - SAS-SWP uses the modelling methodology outlined in this text
- SAS-SWP SSE Database maximum at a PV array tilt of 27 degrees
- SAS-SWP SSE Database minimum at a PV array tilt of 27 degrees
- RETScreen Software at a PV array tilt of 27 degrees.
  - RETScreen uses a modelling methodology as described by Ross *et al.* (2004:PV18-PV21)
- METEONORM at a PV array tilt of 27 degrees
  - METEONORM uses a modelling methodology as described by Remund *et al.* (2003:53-56)
- PV-SYS Software at a PV array tilt of 27 degrees.
  - PV-SYS uses the METEONORM modelling methodology
- HOMER Software at a PV array tilt of 27 degrees
  - HOMER uses the Hay, Davies, Klucher, Reindl (HDKR) model described by Duffie *et al.* (1991:92)
- SAS-SWP Application Software at Optimum Monthly PV array tilt

The sources for the data sets used are as noted below:

- SAS-SWP data set is derived from the NASA Surface Meteorology and Solar Energy database (NASA-ASDC 2005).
- RETScreen data comes from the RETScreen International Clean Energy Project Analysis Software (RETSCREEN 2005).
- HOMER data comes from the National Renewable Energy Laboratory (NREL) Software Optimisation Model for Distributed Power (HOMER 2005).
- METEONORM data comes from the commercial METEONORM Global Radiation Database Software (METEONORM 2006).
- PV-SYS data comes from the PV-SYS Software for Photovoltaic Systems (PV-SYS 2007). This software was found to use the METEONORM data set and is therefore not listed on the comparison graph.

Ground measurement data from the South African Weather Service (SAWS) is not available for the Pretoria North area (MCBRIDE 2007:1) and could therefore not form part of the comparative study. SAWS Publications department referenced the South African Centre for Scientific and Industrial Research (CSIR) as a possible data source (MCBRIDE 2007:1). The CSIR were able to provide an annual Solar

Radiation Surface Plot for South Africa (CSIR 2007), given in Figure 35. For comparative purposes, this may be compared to the monthly surface plots prepared from the SAS-SWP solar radiation database, illustrated in Annexure 4, with observed ranges given in Figure 36. Take care to note that the SAS-SWP solar radiation database surface plots are given in Equivalent Sun Hours (ESH in kWh/m²/day) at optimal tilt and the CSIR surface plot is given in annual solar radiation (MJ/m²/year) for a horizontal surface. Conversion from annual radiation to the more conventional 'kWh/m²/day' can be achieved by dividing the yearly mega-joule per square metre value by a conversion factor of 1314.

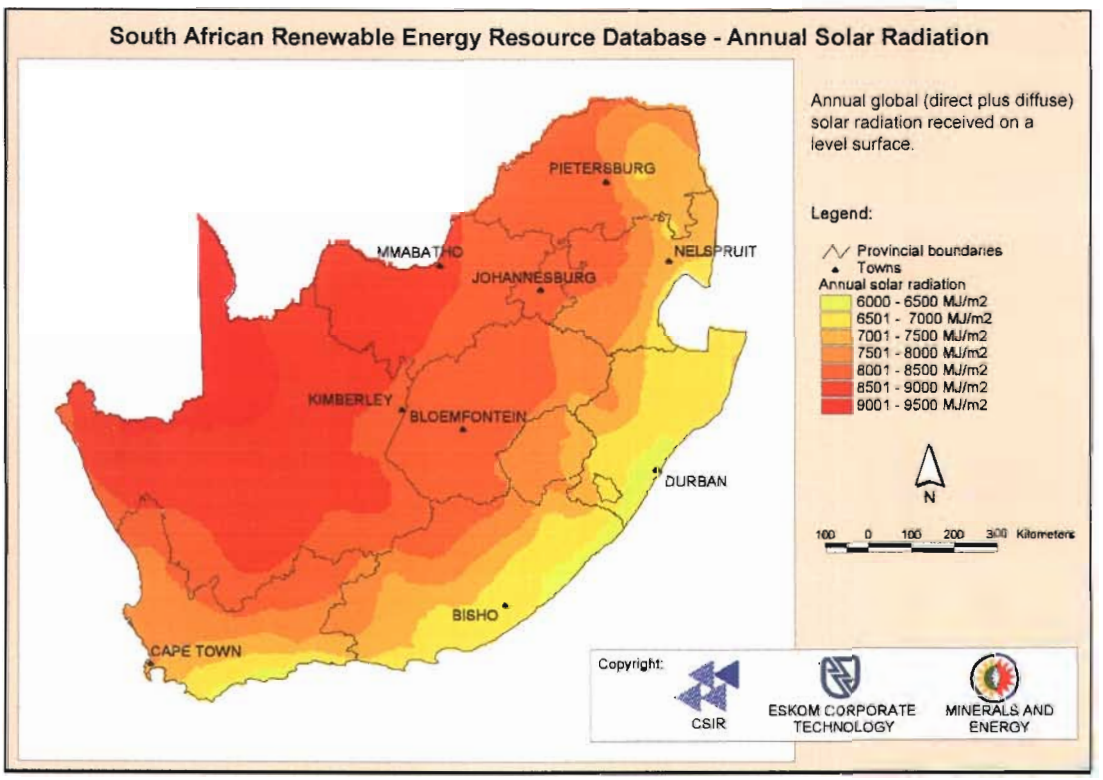

Figure 35 **Solar radiation surface plot for South Africa (CSIR 2007)**

Using the CSIR data for Pretoria (8001 to 8500 MJ/m²/year from Figure 35), this equates to a daily solar radiation range of 6,089 to 6,468 kWh/m²/day between winter and summer. This data, together with the graph data from Figure 34 and surface plot data from Kyocera Solar (Kyocera Solar 2002:16), is listed for ease of comparison in Table 15.

Table 15 Tabulated solar irradiation comparison

Solar Irradiation Comparison

Test Location Coordinates Longitude: 28° 08' 00" East Latitude: -25° 27' 00" South	January	Δ%	February	Δ%	March	Δ%	April	Δ%	May	Δ%	June	Δ%	July	Δ%	August	Δ%	September	Δ%	October	Δ%	November	Δ%	December	Δ%
SAS-SWP at Optimum Tilt	6.08	0.00	4.80	0.00	5.12	0.00	5.05	0.00	5.99	0.00	5.18	0.00	5.92	0.00	6.25	0.00	5.38	0.00	5.48	0.00	5.83	0.00	5.68	0.00
SAS-SWP at 27° Tilt	5.55	-8.72	4.69	-2.29	5.11	-0.20	4.90	-2.97	5.47	-8.68	4.61	-11.00	5.30	-10.47	5.86	-6.24	5.34	-0.74	5.41	-1.28	5.41	-7.20	5.10	-10.21
SSE(maximum) at 27° Tilt	7.36	21.05	6.92	44.17	5.92	15.63	5.43	7.52	4.65	-22.37	4.14	-20.08	4.42	-25.34	5.04	-19.36	6.14	14.13	6.47	18.07	7.07	21.27	7.33	29.05
SSE(minimum) at 27° Tilt	6.11	0.49	4.78	-0.42	4.71	-8.01	4.00	-20.79	4.00	-33.22	3.23	-37.64	3.73	-36.99	4.40	-29.60	4.66	-13.38	5.34	-2.55	5.85	0.34	5.71	0.53
RETScreen at 27° Tilt	6.18	1.64	5.50	14.58	4.51	-11.91	3.22	-36.24	2.27	-62.10	1.79	-65.44	2.02	-65.88	3.02	-51.68	4.24	-21.19	5.22	-4.74	6.14	5.32	6.58	15.85
Meteonorm at 27° Tilt	6.81	12.01	6.50	35.42	5.84	14.06	4.77	-5.54	4.35	-27.38	4.00	-22.78	4.29	-27.53	5.03	-19.52	6.07	12.83	6.39	16.61	6.47	10.98	6.90	21.48
Homer at 27° Tilt	6.88	13.16	6.20	29.17	5.45	6.45	4.73	-6.34	4.28	-28.55	3.79	-26.83	4.10	-30.74	4.72	-24.48	5.57	3.53	5.94	8.39	6.44	10.46	6.71	18.13
*CSIR at 0° Tilt	6.41	5.36	6.34	32.13	6.28	22.64	6.22	23.08	6.15	2.71	6.09	17.55	6.15	3.92	6.22	-0.55	6.28	16.71	6.34	15.74	6.41	9.87	6.47	13.89
*Kyocera 15°/40° Tilt (summer/winter)	5.67	-6.80	5.83	21.53	6.00	17.19	6.17	22.11	6.33	5.73	6.50	25.48	6.33	6.98	6.17	-1.33	6.00	11.52	5.83	6.45	5.67	-2.80	5.50	-3.17

* Linear distribution assumed

Irradiation in kWh/m²/day

Base for deviation (Δ%) is SAS-SWP at Optimum Tilt

Solar irradiation data for South Africa as derived from the SAS-SWP database and taken from surface plot data (Annexure 4), is given in Figure 36.

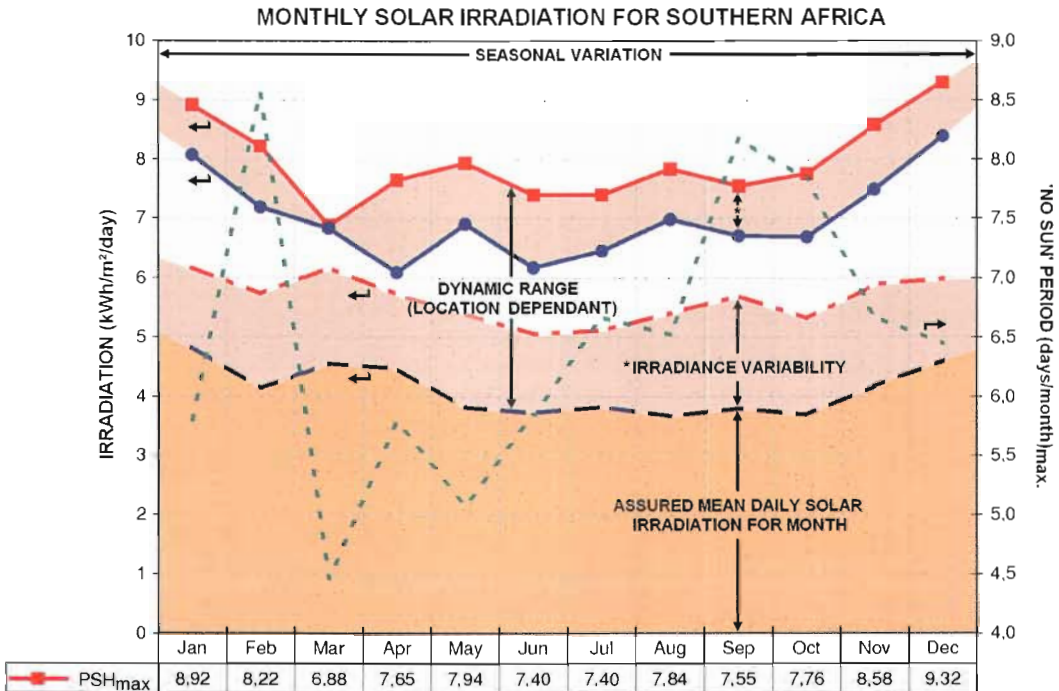

	Jan	Feb	Mar	Apr	May	Jun	Jul	Aug	Sep	Oct	Nov	Dec
PSH_{max}	8,92	8,22	6,88	7,65	7,94	7,40	7,40	7,84	7,55	7,76	8,58	9,32
PSH_{min}	6,17	5,73	6,18	5,73	5,40	5,06	5,12	5,41	5,70	5,32	5,89	5,98
ESH_{max}	8,07	7,19	6,84	6,10	6,91	6,18	6,46	6,99	6,71	6,69	7,49	8,39
ESH_{min}	4,83	4,14	4,56	4,48	3,82	3,73	3,83	3,67	3,80	3,69	4,18	4,61
'No Sun'	5,80	8,56	4,47	5,78	5,09	5,85	6,67	6,52	8,17	7,83	6,67	6,44

Figure 36 **Monthly solar irradiation ranges for Southern Africa**

The comparison of solar irradiation data in isolation should be done with caution when intended for photovoltaic use, as the power delivered by a PV panel is dependant on many additional local variables such as the ambient temperature, clearness index, wind strength and direction, panel ventilation, orientation, tilt, *etc.* As a general example, the efficiency of a PV panel increases at cooler ambient temperatures. This can result in the same or more power output at a lower solar irradiation value than a location with a higher solar irradiation and ambient temperature. This effect is illustrated in the PV array monthly efficiency versus ambient temperature analysis for the VUT trial design given in Figure 45.

Variances observed in the trend data in Figure 34 can be attributed to the use of different prediction models and/or differences in the source base horizontal solar irradiance data between the different software packages. A reasonable correlation (within $\approx$ 1 kWh/m^2) is evident between the various comparison packages and the SSE maximum data set during the summer months. This improves to better than half a kilowatt through the winter months, with the exception of RETScreen, which shows a negative variance in excess of two kilowatt at its maximum offset in June. Under-estimation of irradiation for tilted surfaces by the RETScreen package under Southern African conditions has also been observed by Bekker (2007:4), using the SunSim simulation package. The RETScreen variance can be attributed to its use of a generalised isotropic model for calculation of diffused irradiation on a tilted plane. SAS-SWP data is based on the NASA-ASDC SSE data set, which uses a more accurate anisotropic method (Bekker 2007:4) as recommended and used by, among others, Perez *et al.* (1990), Feuekmann *et al.* (1992), Cowan (1992) and Myers (2003). The accuracy and uncertainty levels of the NASA – ASDC SSE data set components are discussed by Whitlock (2004), with detailed results provided by NASA on their Surface Meteorology and Solar Energy internet web site (NASA-ASDC 2005).

Differences that can occur in predicted irradiation on a tilted surface using the same base horizontal solar irradiance data (Base data source: NASA – ASDC), but using three different modelling techniques, is illustrated in Figure 37.

The results delivered by the SAS-SWP application at user defined fixed tilt varies from the parabolic trend of the other applications because the SAS-SWP application uses the deviation from optimum monthly tilt angle to generate monthly irradiation predictions, based on data derived from the NASA SSE ESH data set for location specific PV arrays at optimum tilt (given in the 'SAS-SWP at Optimum Tilt' reference trend in Figure 34).

Surface plot data from the CSIR provided in Figure 35 was compiled from SAWS ground station data (CSIR 2007). This poses a problem when deriving data for a

location in excess of a twenty five kilometre radius from a ground station, as is shown by the Zelenka study (Zelenka *et al.* 1999:199-207). The study shows that satellite derived data has been shown to be the most accurate irradiance modelling option for this purpose when compared to low density ground measurement interpolation.

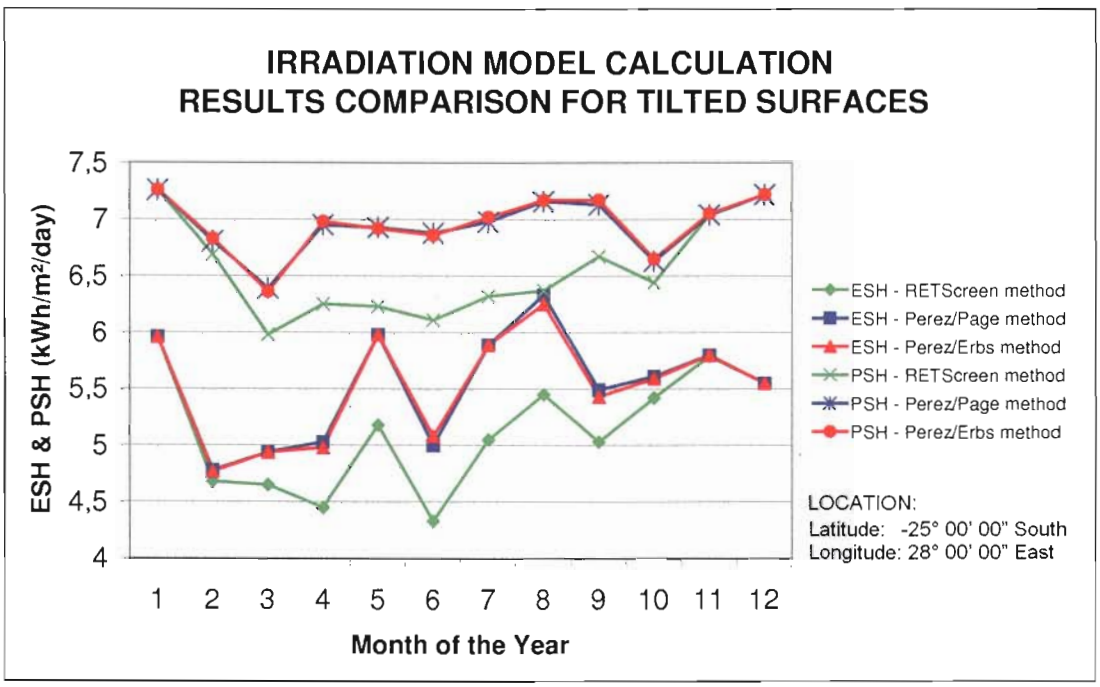

Figure 37 **Solar irradiation model output comparison graph**

4.1.3 friction losses

Friction head losses in piping, as calculated by the SAS-SWP Application have been verified by manual calculation using formulae as supplied. In addition, the friction losses for pipes in the 'thermoplastic' category have been verified against design assistance software from the Plastics Pipe Institute (PPI 2006), based on their TR-14 specification "Water Flow Characteristics of Thermoplastic Pipe" (Plastics Pipe Institute 2000:1-12).

4.1.4 electrical losses

Electrical losses as calculated by the SAS-SWP Application have been verified by manual calculation using formulae as supplied. In addition, the calculations have

been manually verified using formulae and data from Gieck (1985:S5 & Z21) and Hughes (1987:11).

Current (ampere) capacities for wiring recommendations generated by SAS-SWP have been checked against general electrical installation regulations and the South African Bureau of Standards (SABS) "Code of Practice for the Wiring of Premises" (SABS 0142-1987: 97, Table B). The SAS-SWP recommendations are well within the safe limits recommended by both the SABS and the US-NEC (Wiles 2001) due to the low tolerance for electrical losses (3 to 5 percent) implemented in the SAS-SWP design methodology.

4.1.5 photovoltaic temperature and efficiency compensation

PV array output has been temperature compensated according to an adaptation of the method proposed by Evans (1981:555-560). Compensation results have been verified by comparison to manual calculation using formulae as supplied.

4.1.6 quick estimator

The SAS-SWP 'Quick Estimator' was subjected to a performance trial using a validated data set extracted from report IEA PVPS T9-07: Sixteen Case Studies on the Deployment of Photovoltaic Technologies in Developing Countries (IEA 2003). The relevant data can be found in Section 2.3 "Drinking Water Supply with Photovoltaic Water Pumps (PVP)", prepared for the International Energy Agency (IEA) by Posorski of the GTZ (IEA 2003:22).

Because of the variability in Quick Estimator output made possible via adjustment of the 'Sub-system Efficiency' and 'Array De-rate Factor' calculation parameters (illustrated in Figure 38), the upper and lower dynamic range, together with a mid-range output have been given for the 'Quick Estimator', compared to output from two available sizing programs, namely DASTPVPS and Grundfos CASS software, as well as actual photovoltaic water pumping measurement data from the IEA/GTZ. This is best depicted graphically, as shown in Figure 39

.

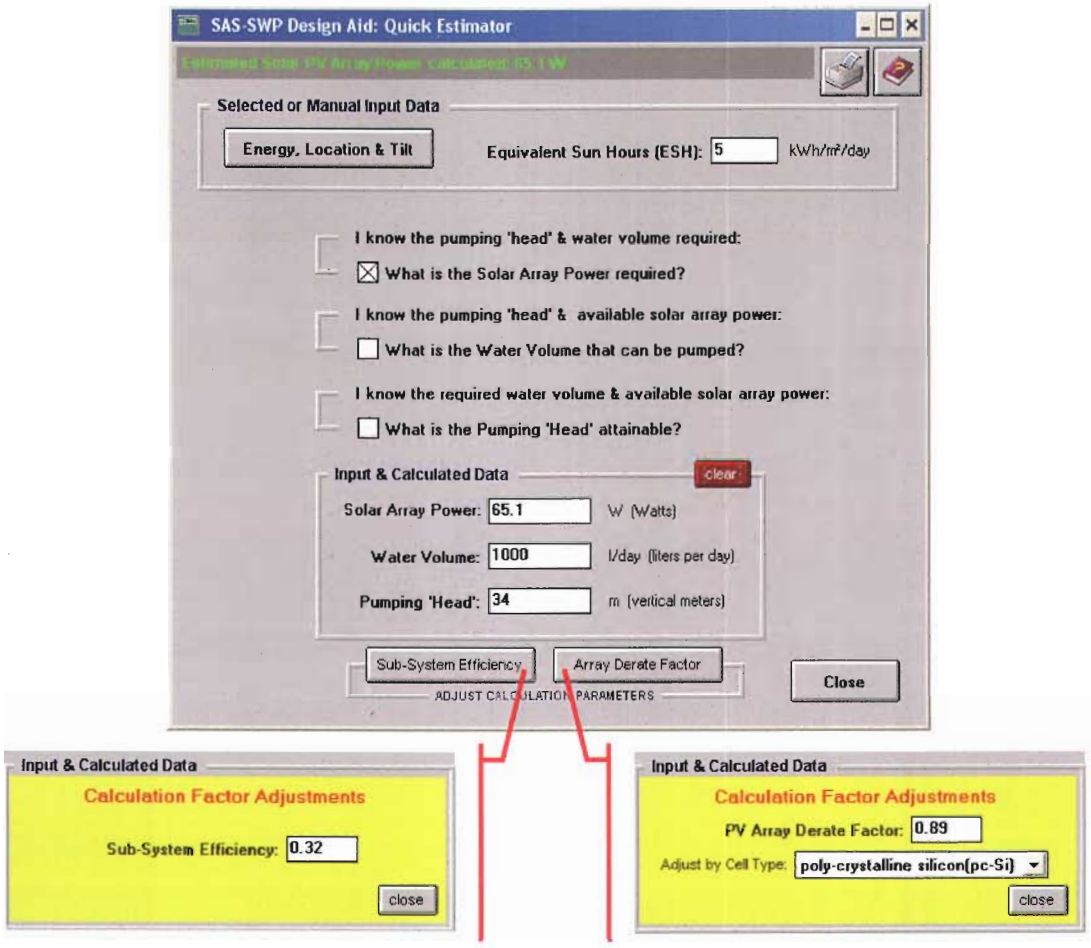

Figure 38 SAS-SWP 'Quick Estimator' showing parameter adjustments

Refinement of the SAS-SWP Quick Estimator calculation parameters based on expected installation site conditions enhances accuracy of the overall prediction ability. The graph in Figure 39 illustrates that selection of the correct PV panel material type and using a mean range de-rate factor was found to provide good general feasibility/quantification estimates.

4.1.7 ancillary calculations

All ancillary calculations performed within the SAS-SWP application have been verified by comparison to manual calculation using formulae as supplied.

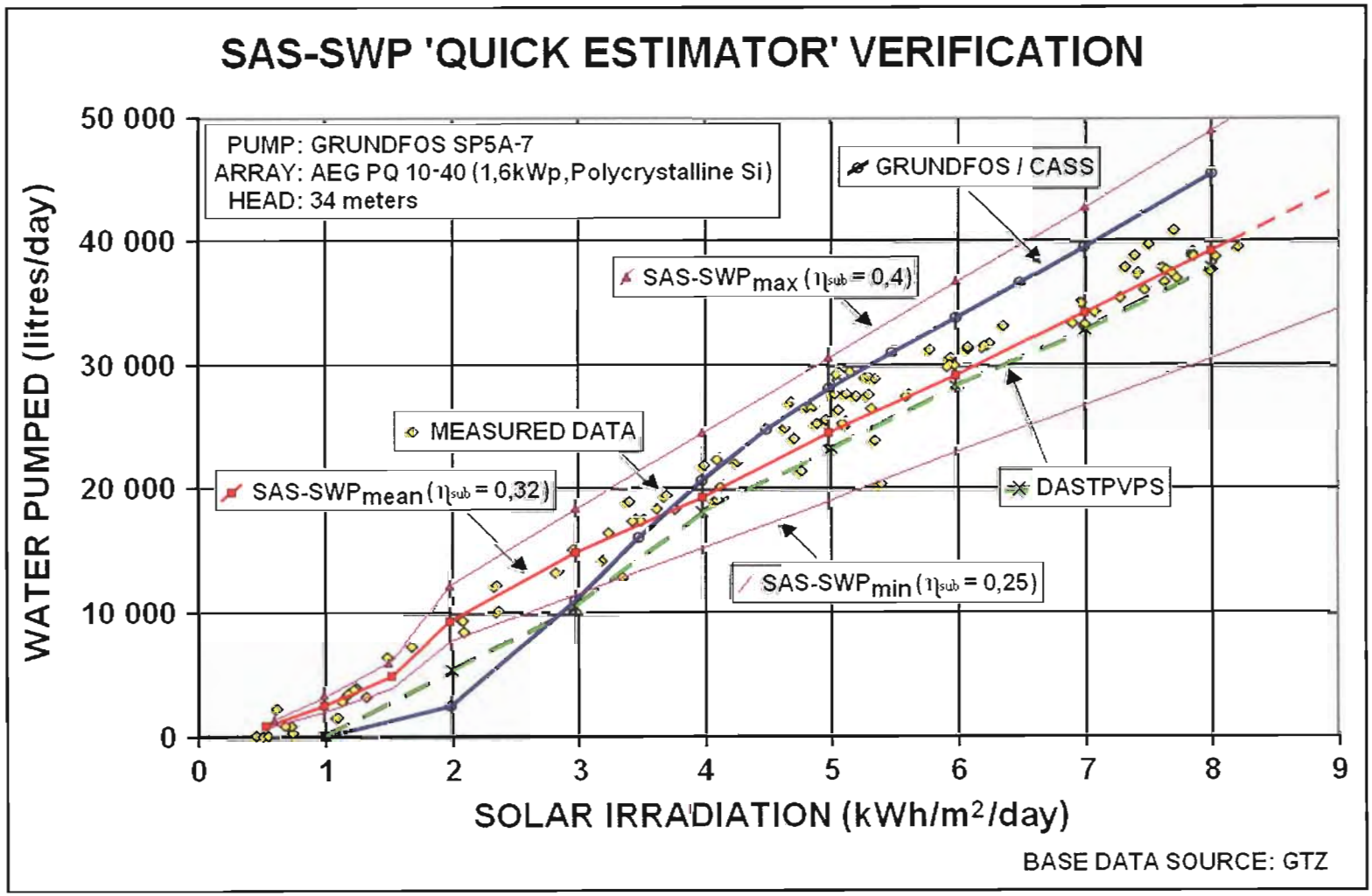

Figure 39 SAS-SWP 'Quick Estimator' validation graph

4.2 Software trials

An alpha version of the SAS-SWP application program was tested by the developer and an informal peer group and de-bugged and amended based on group feedback. A beta version of the program was then delivered to the Vaal University of Technology (VUT) for testing and comment. Minor additions were requested by the VUT solar laboratory team with respect to the visibility and accessibility of system data used internally within the application program. Based on this request, an extensive data file of system parameters and calculation results was compiled, which can be saved to an external file via a structured 'software dump' from the Detailed Results applet in the PV Module Selection phase. An example of the data file contents is presented in the example shown in Table 16. Data is saved to storage media in a 'spreadsheet' compatible comma-separated-variable (.CSV) format.

4.2.1 software verification

SAS-SWP design results were compared to actual data from an operational stand-alone, directly coupled PV water pumping system, as detailed below.

4.2.1.1 test system

A comprehensive research system that includes the required PVPS configuration for SAS-SWP verification exists at the VUT solar laboratory. The staff of the solar laboratory was approached with a request for data, which was subsequently provided by Mr. Martin Joubert. He provided a randomly selected numerical PV water pumping data set for 30 March 2006, together with the physical parameters for the pumping system as implemented at VUT.

The physical parameters for the VUT stand-alone, directly coupled PV water pumping system are as follows:

- Solar Panels: Two series connected 12 V; 75 W; BP375 PV Panels, giving an array configuration of 24 VDC, 150 W
- Array Tilt: 30 Degrees, fixed. Azimuth at zero degrees (true North orientation)
- Pumping Head: 13 m

- Piping Used: 12 mm inner diameter PVC pipe
- Wiring: 30 m of 4 mm² copper wire
- Motor/Pump Set: Shurflow model 9325-043-101, 24 VDC
- Flow Meter: Omega FTB2003 Turbine flow sensor

The performance of any PV pumping system is a factor of the physical design, hardware used and installation location. The design and hardware determine the system performance characteristic boundaries, while the location determines energy availability and transfer characteristics via site specific solar irradiance and local micro-climatic conditions on a seasonal time continuum. An analysis of the PVPS as used by VUT is therefore required.

The location coordinates for the site are as indicated on the aerial photograph provided in Figure 40.

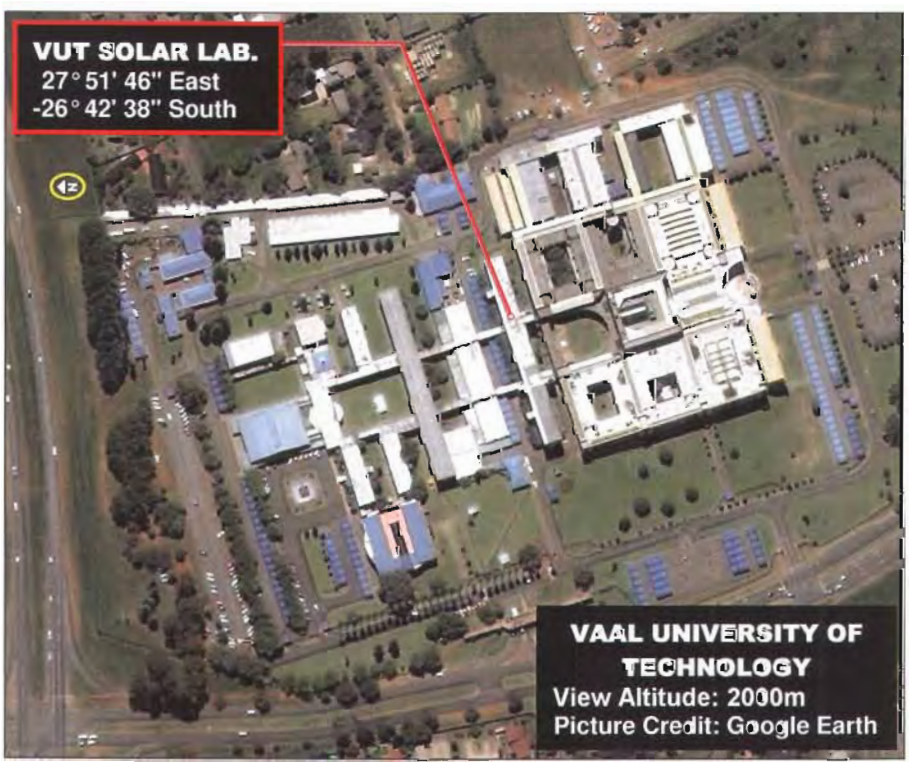

Figure 40 **VUT solar laboratory location - Vanderbijlpark**

Table 16 SAS-SWP detailed data dump

South African Stand-alone Solar (PV) Water Pumping Design Aid (SAS-SWP)

LOCATION:
Longitude: 27° 51' 46" East
Latitude: -26° 42' 38" South

DESIGN DATA:
Water Required (liters/day): 1751
Total Dynamic Head (m): 16
Pump Used: Manufacturer: Shurflow, Model: 9325-043-101
PV Module Used: Manufacturer: BP Solar; Model: BP375

	January	February	March	April	May	June	July	August	September	October	November	December
SSE(minimum)	5.88	4.31	4.53	3.98	3.82	3.15	3.7	4.28	4.44	5.25	5.88	5.84
SSE(maximum)	7.27	6.88	5.98	5.22	4.58	4	4.25	4.89	6.06	6.5	7.01	7.35
Clearness Index (Kmin.)	0.49	0.39	0.46	0.5	0.58	0.55	0.61	0.59	0.5	0.5	0.51	0.48
Clearness Index (Kmax.)	0.61	0.62	0.61	0.65	0.7	0.69	0.7	0.67	0.68	0.62	0.61	0.61
Diffused Radiation	2.35	2.26	1.96	1.58	1.12	1.08	0.99	1.23	1.75	2.06	2.26	2.41
Direct Normal Radiation	5.76	3.77	4.64	4.99	6.2	5.35	6.32	6.18	5.41	5.38	5.81	5.66
Monthly Averaged Top-of-atmosphere Insolation (kWh/m²/day)	11.77	11	9.63	7.94	6.47	5.75	6.03	7.21	8.81	10.3	11.4	11.9
Monthly Averaged Surface Albedo	0.18	0.18	0.2	0.18	0.19	0.19	0.2	0.21	0.19	0.18	0.18	0.18
ESH @ Tilt = 0°	5.85	4.21	4.46	3.95	3.7	3.08	3.61	4.26	4.39	5.14	5.85	5.81
ESH @ Tilt = Latitude - 15°	5.8	4.31	4.78	4.49	4.51	3.83	4.47	5.04	4.82	5.36	5.85	5.71
ESH @ Tilt = Latitude°	5.44	4.25	4.96	4.94	5.29	4.59	5.33	5.77	5.11	5.36	5.55	5.3
ESH @ Tilt = Latitude + 15°	4.79	3.96	4.85	5.11	5.75	5.06	5.86	6.16	5.12	5.06	4.94	4.6
ESH @ Tilt = 90°	1.68	1.82	2.82	3.69	4.8	4.47	5.08	4.87	3.25	2.37	1.77	1.6
Optimum Equivalent Sun Hours (ESH)	5.86	4.32	4.96	5.11	5.86	5.24	6.03	6.21	5.15	5.4	5.88	5.81
Optimum Tilt Angle for ESH	3	15	29	43	54	57	56	50	35	20	6	0
Optimum Peak Sun Hours (PSH)	7.24	6.92	6.66	6.94	7.02	6.88	6.95	7.08	7.13	6.7	6.99	7.33
Optimum Tilt Angle for PSH	1	15	30	44	53	58	56	49	35	20	4	0
Selected PV Array Tilt Angle (degrees)	30	30	30	30	30	30	30	30	30	30	30	30
Energy Available at Selected Tilt Angle (kWh/m²/day)	5.27	4.17	4.93	4.99	5.41	4.72	5.47	5.87	5.11	5.28	5.39	5.11
Number of NO-SUN or BLACK Days (days/month)	3.78	7.76	4.18	3.94	2.62	4.44	2.46	2.41	5.56	3.09	2.45	3.61
Monthly Averaged Daylight Cloud Amount (%)	64.19	61.34	55.79	41.4	22.45	24.09	19.2	28.53	45.13	61.75	63.64	67.79
Monthly Averaged Air Temperature at 10m above the surface of the Earth (°C)	20.71	20.26	19.28	16.38	13.28	9.61	10	12.95	16.69	18.36	19.18	19.92
Monthly Averaged Wind Speed at 10m above the surface of the Earth (m/s)	2.8	2.69	2.66	2.79	3.02	3.31	3.42	3.76	3.97	3.73	3.32	2.93
Estimated Project Current Requirements (A)	2.57	3.25	2.75	2.72	2.51	2.87	2.48	2.31	2.65	2.57	2.51	2.65
Array Power (W)	150.5	150.5	150.5	150.5	150.5	150.5	150.5	150.5	150.5	150.5	150.5	150.5
Parallel Modules Required	1	1	1	1	1	1	1	1	1	1	1	1
Series Modules Required	2	2	2	2	2	2	2	2	2	2	2	2
Total Modules Required	2	2	2	2	2	2	2	2	2	2	2	2
Estimated Module Temperature (°C)	43.3	44.6	43.9	41.7	38.6	34.2	35	38.1	43.2	43	42.2	42
Estimated Array Efficiency (%)	10.2	10.1	10.2	10.3	10.4	10.6	10.6	10.4	10.2	10.2	10.2	10.3
Estimated Module Temperature Derate (%)	7.3	8.2	7.3	6.4	5.5	3.6	3.6	5.5	7.3	7.3	7.3	6.4
Required Pump Rate (liters/hour)	420	420	420	420	420	420	420	420	420	420	420	420
Estimated Pump Rate (liters/hour)	679.8	679.8	679.8	679.8	679.8	679.8	679.8	679.8	679.8	679.8	679.8	679.8
Required Pumped Water (liters/day)	1751	1751	1751	1751	1751	1751	1751	1751	1751	1751	1751	1751
Estimated Water Pumped (liters/day)	3582.7	2834.9	3351.5	3392.3	3677.8	3208.8	3718.6	3990.6	3473.9	3589.5	3664.2	3473.9
Maximum Estimated Water Pumped (liters/day)	4921.9	4704.4	4527.6	4718	4772.4	4677.2	4724.8	4813.1	4847.1	4554.8	4752	4983.1

RESULTS SUMMARY:

Peak Sun Hours (PSH): 7.33 kWh/m²/day (maximum)
Equivalent Sun Hours (ESH): 4.822 kWh/m²/day (yearly average)

Water Requirements: 1751 liters/day
Total Dynamic Head (TDH): 16 meters
Hydraulic Energy Required: 76.34 Wh/day

Current Required: 3.25 Amperes
System Voltage (nominal): 24 DC Volts
Estimated Wire Loss: 3.82 % for 30 m of 4 mm² cable
(= a volt-drop of 0.918 Volts)

PV Array: 2 modules consisting of 1 parallel strings of 2 series connected modules per string
PV Array Current: 4.35 Amps (Design)
PV Array Voltage: 34.6 Volts (Design)
Estimated PV Array Power: 150.51 Watts
Maximum Power Point Voltage: 34.44 Volts
Estimated PV Module Efficiency: 10.25 %
Estimated PV Cell Operating Temperature: 42.01 °C with a NOCT rating of 47 °C
Estimated PV Cell Temperature De-rate: 6.82 %

Projected Pump Rate: 679.82 liters/hour vs a required rate of 420 liters/hour
The design is under(-)/over rated by 61.86 % of required pump rate
Estimated Amount of Water that can be Pumped:
4983.1 liters/day at PSH=maximum
3278.1 liters/day at ESH=yearly average
3496.56 liters/day at ESH=Selected Data Set
2834.86 liters/day at ESH=minimum
NB.
Ensure that the bore-hole/well is able to deliver the 'PSH=maximum' volume
DO NOT EXCEED THE CAPACITY OF THE WATER SOURCE!
Autonomy Recommendations: 0 days (= 0 liters)
Recommended Reserve Water Tank Size: 1751 liters (minimum)

Solar & Meteorology Data based on NASA 'Surface Meteorology and Solar Energy (SSE) Data Set' Release 5.1
ESH = Monthly averaged Equivalent Sun Hours radiation incident on an true North-pointed tilted surface: Perez/Page Method (kWh/m²/day)
PSH = Monthly averaged Peak Sun Hours radiation incident on an true North-pointed tilted surface: Perez/Page Method (kWh/m²/day)

Note: Data is provided on a "best effort" basis - Use thereof is entirely at own risk
See SAS-SWP Help File for more information

A schematic layout of the VUT PV pumping system is given in Figure 41 below:

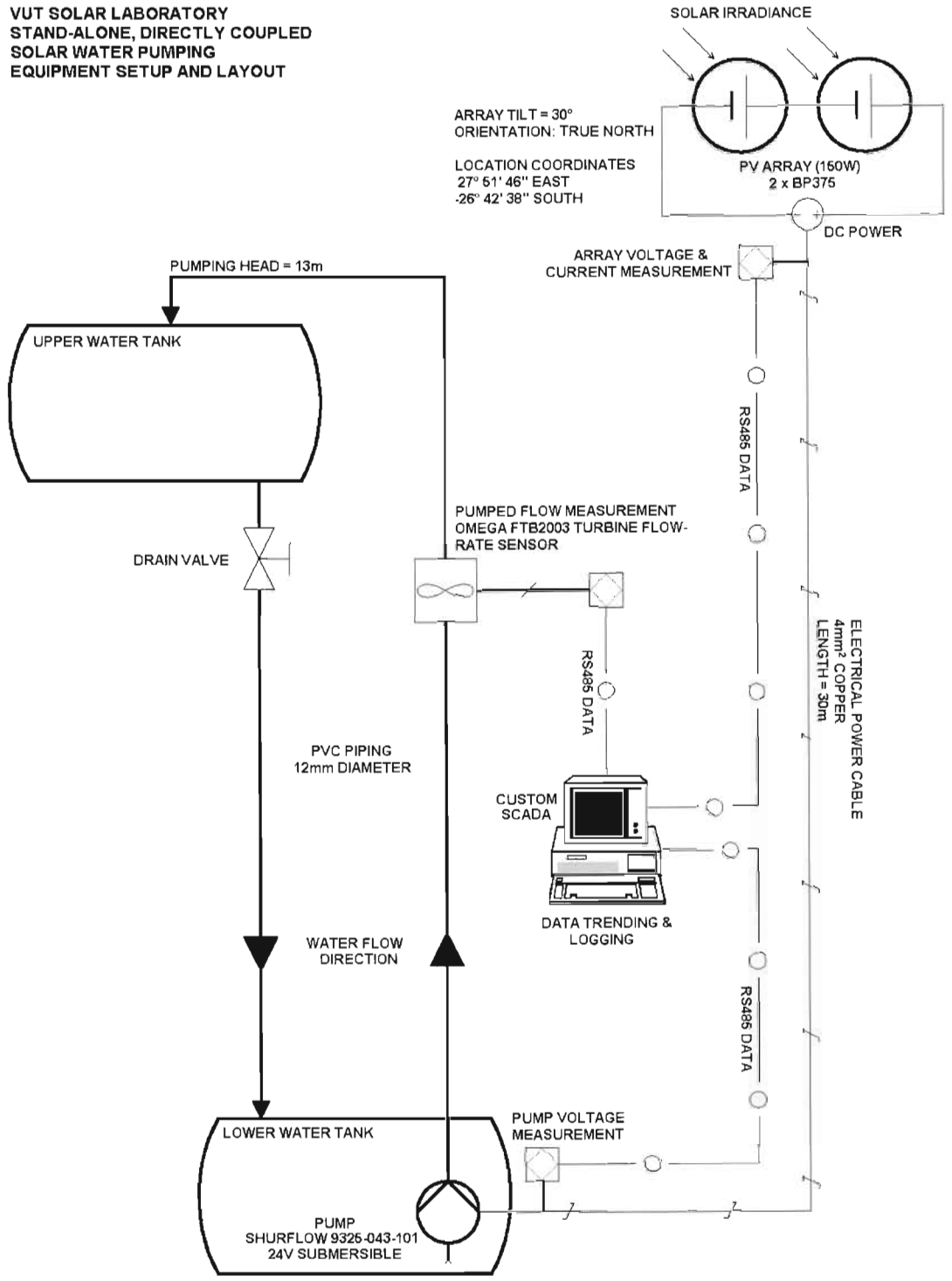

Figure 41 VUT PV pumping system – Schematic layout

Scrutiny of the PVPS layout in Figure 41 shows the use of a flow meter to measure flow rate, used to determine the amount of water pumped by the system. The pressure drop across the flow meter introduces an additional loss factor in the piping system that requires compensation when input into the SAS-SWP application. Pressure drop across the meter is relative to the flow through the meter, as can be seen from graphical manufacturer data given in Figure 42. The expected maximum flow of the PVPS is therefore required to estimate this parameter.

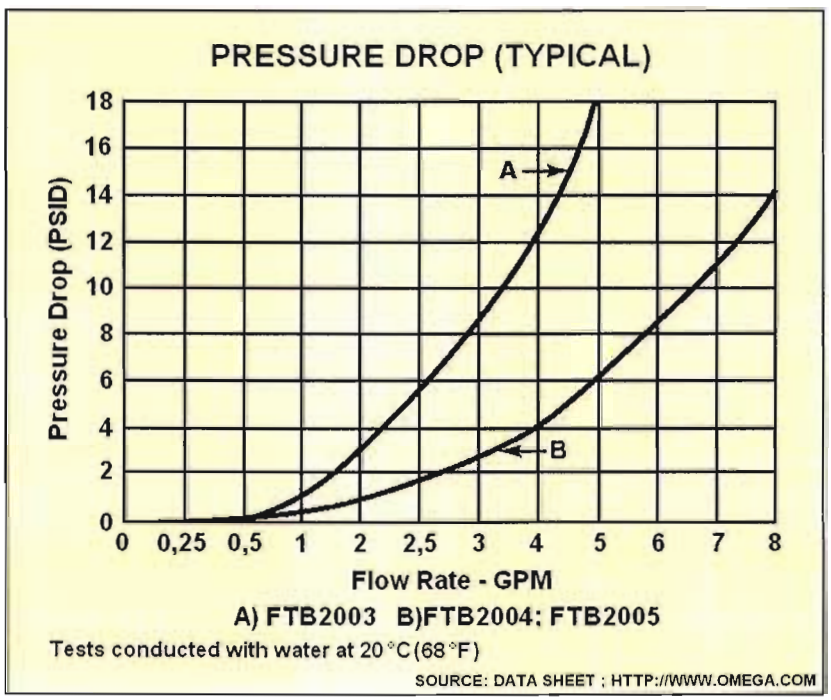

Figure 42 **Flow meter pressure drop graph**

Maximum flow can be determined from data given in the pump manufacturer data sheet provided in Annexure 8, using the given system pumping head of thirteen metres plus an additional one metre of head equivalent for pipe friction losses (from SAS-SWP calculation). The data sheet flow rate for the installed pump at a pumping head of fourteen metres is 428 litres per hour (7,13 litres per minute or 1,884 US-GPM). Referencing the pressure drop graph, this equates to a pressure drop of approximately 20 kPa (approximately 3 PSI). Using the conversion formula given in Equation (46), this equates to an addition head equivalent loss of two metres. Total dynamic head for the VUT pumping system is therefore 16 metres. Using this data

and pump manufacturer data sheet information partially graphed in Figure 43, pump information can now be entered into the SAS-SWP pump database.

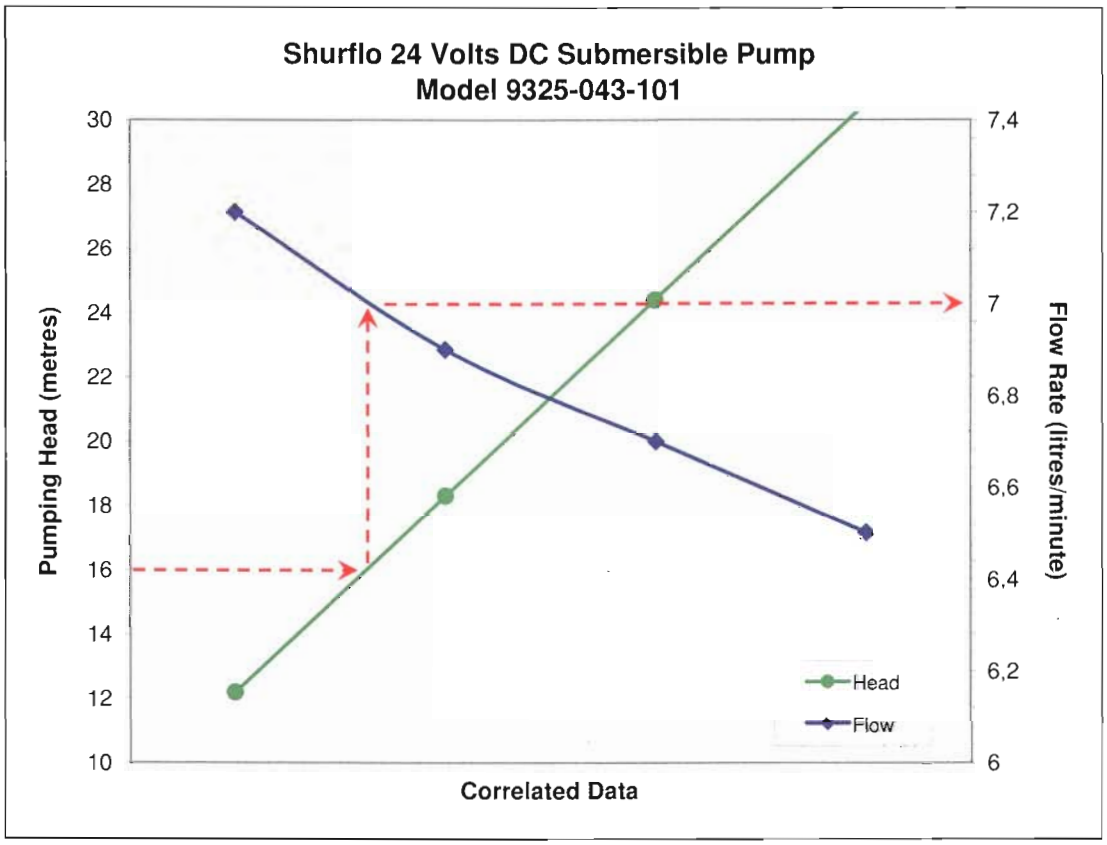

Figure 43 **Pump flow rate vs. Pumping head graph**

Pump Data for SAS-SWP database:

- Pump: Shurflo model 9325-043-1001
- Head: 16 m
- Flow: 7 litres per minute
- Power: 75 W
- Voltage: 24 VDC
- Efficiency: 24,4 percent (from SAS-SWP calculation)

Similarly, the PV panel data could be entered into the SAS-SWP database, if it did not already exist.

PV Panel Data for SAS-SWP database:

- Panel: BP375
- Material: Poly-Crystalline Silicon (pc-Si)
- I_{SC}: 4,75 A
- V_{OC}: 21,8 V
- I_{MP}: 4,35 A
- V_{MP}: 17,3 V
- P_{MP}: 75,3 W (V_{MP} x I_{MP}, from SAS-SWP calculation)
- *NOCT*: 47 °C
- *dP%*: 6 percent (from SAS-SWP calculation)

SAS-SWP is an integrated design aid that is generally used to produce a PVPS design. In order to generate a comparison design, which is in effect a reverse engineering approach, a few factors need to be taken into consideration: The SAS-SWP application uses a 'worst case' design approach that provides a full-year (all seasons) design. The implication of this factor when comparing an existing design and related performance data is that the operator needs to know what data to input into SAS-SWP in order to generate a valid comparison. Most of the required data (detailed previously), is logically evident and self explanatory. This is not the case for the 'water requirements' input. For comparative purposes, the water requirement value is obtained from two parameters, namely: worst case monthly ESH for the year (at applicable tilt) and the maximum pump rate of the pump used (at applicable TDH). The ESH value can be obtained by running at 'dummy' design for the relevant location and PV array tilt on SAS-SWP and noting the value from the detailed results applet of the PV module selection. This ESH value is then multiplied by the hourly maximum pump rate (or litres/minute × 60) to give a comparative daily water requirement. This value is made available to the SAS-SWP application via the data field labelled 'other' in the Water Requirements module. Using this

methodology, the water requirement value for the VUT PVPS comparison exercise would be 1751,4 litres per day. This is obtained from:

- Worst case ESH for the selected location at thirty degree array tilt, which is 4,17 kWh/m²/day and occurs in February (The full data set is detailed in Table 16)
- A maximum pump rate of seven litres per minute (420 litres per hour) at a 16 metre pumping head, taken from manufacturer data detailed in Figure 43

Calculated water requirement data is confirmed by checking the SAS-SWP calculation result for required hourly water pump rate, which should be equal to the maximum hourly pump rate for the pump, as provided by the manufacturer.

No 'Safety Factor' or 'Autonomy' selections should be entered for the test, as this would bias the water requirements in an upward direction.

4.2.1.2 data comparison

Using the preceding data, the SAS-SWP application has been configured to generate a design based on VUT PV Pumping System location and hardware specifications. Detailed design results are provided in Table 16. The SAS-SWP design recommends a PV panel configuration for the month of March that coincides with that implemented at VUT, *i.e.* two by 12 volt 75 watt panels in series. Coincidentally it can be noted that the optimum tilt angle for March recommended by SAS-SWP is thirty degrees – precisely the angle at which the VUT system was set at as a yearly operational average. This should result in an optimum energy transfer comparison.

Data provided in the VUT solar laboratory "30 March 2006" data set included time stamped water flow rate, PV array current and motor/pump-set voltage, all provided at a time resolution of one minute, for a period of nine hours and thirty six minutes (08h31 – 18h07), details of which are tabulated in Annexure 8, with a graphical overview given in Figure 44.

The VUT data shows that actual pumping started at 09h01 and stopped at 17h44. This is a pumping period of 524 minutes; of which 153 minutes was operated below the rated pump voltage of twenty-four volts, including a zero pumping period of thirty-two minutes (total). In the directly coupled mode applied in this PVPS, the pump overcame its rotational starting torque threshold at approximately one volt (at $\approx$ 1,32 A). From Figure 44 it can be seen that the pump starts to develop head soon after, with flow beginning as soon as the frictional and dynamic head conditions are overcome. The pump-set operated to a maximum pump motor voltage of 36,23 volts and current of 2,18 ampere (79 watts). By way of clarification, it should be noted that the applied DC voltage controls the motor shaft speed, while the motor torque dictates electrical current requirements. The flow rate at these levels peaked at 8,68 litres per minute. During the trial pumping period the pump operated above the twenty four volt nominal design specification for 371 minutes (75,4 percent of the time). This provides excellent motivation in selecting a direct coupled mode of operation, as a MPPT would have clamped this to the system battery voltage, while providing a marginal boost benefit for only 23 percent of the time.

Comparison of SAS-SWP design data as provided in Table 16 and Table 17 to actual figures achieved by VUT, show that the SAS-SWP application predicts a daily pumped water volume of 3351,5 litres per day for the month of March, while the actual volume achieved by the VUT PVPS was 3241 litres per day. This equates to an over-prediction of 3,28 percent by the SAS-SWP application.

Pumped water volume is highly dependant on applied available solar irradiation, so a normalised data set was generated based on the VUT data, but removing the irradiance outages (dips) due to cloud. Summation of the discrete product function of the pumped water for this data set shows the maximum possible pumped water to be 3722 litres for the day. In this scenario, the SAS-SWP application under-predicted the water volume by 11 percent. A full SAS-SWP design would cater for this via tweaking of water volume with the 'Safety Factor' and 'Autonomy' settings.

A comparison of select design output data is provided for perusal in Table 17.

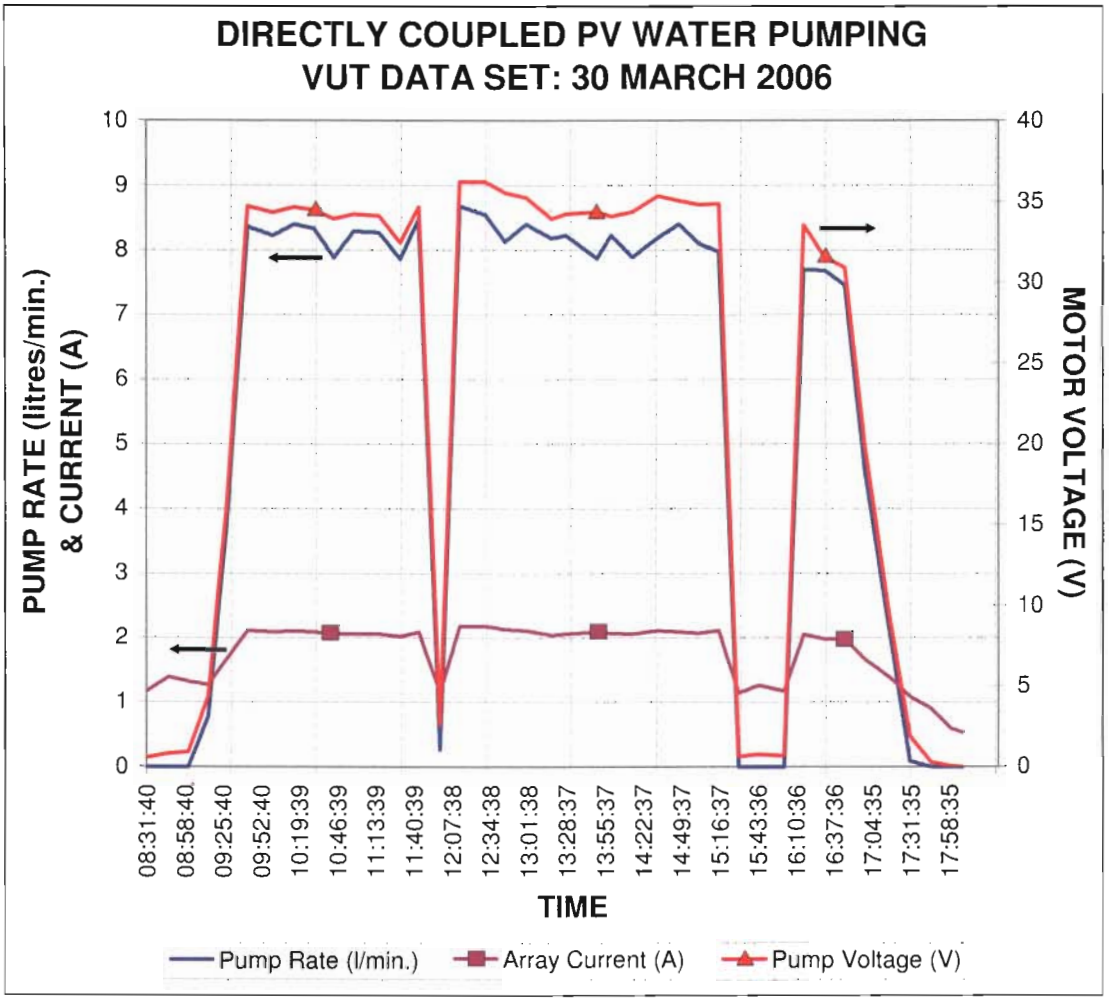

Figure 44 **VUT directly coupled PV water pumping data graph**

Comparison of 'VUT actual' and 'VUT predicted' data set maximum water pumped values shows a possible result variation of 14,8 percent. This gives an indication as to how sensitive the physical PVPS is to variations in irradiance and emphasises the importance of an accurate solar irradiation database for modelling purposes.

These results support the findings of Dunlop (1988:1187), who showed that optimally designed direct-coupled systems generally operate at a pump-motor voltage lower than V_{MP} for lower solar irradiance levels and higher than V_{MP} for higher irradiance levels.

The SAS-SWP application sets the maximum possible water pumped for the month of March at 4527,6 litres per day. This is based on all available factors being at

optimum, *i.e.* peak irradiation, optimum array tilt and clearness index, *etc.* This value can be regarded as the theoretical upper pumped volume limit for that month and is provided as an indication of a prudent value to use as a delivery capacity check limit for the well or borehole for that month.

Table 17 Design output comparison table

Design Output Comparisons

Source	litres/day	Δ%
VUT Actual (30 March 2006)	3241,04	base
VUT maximum predicted	3721,74	14,83
SAS-SWP at 30° Tilt	3351,50	3,41
SAS-SWP maximum predicted	4527,60	39,70
SAS-SWP Quick Estimator (**1**) at default settings	2628,28	-18,91
SAS-SWP Quick Estimator (**1**) de-rated for poly-crystalline Si.	3799,03	17,22
SAS-SWP Quick Estimator (**2**) at default settings	4621,83	42,60
SAS-SWP Quick Estimator (**2**) de-rated for poly-crystalline Si.	4839,32	49,31
SAS-SWP Quick Estimator (**3**) at default settings	4415,76	36,25
SAS-SWP Quick Estimator (**3**) de-rated for poly-crystalline Si.	4623,56	42,66
GTZ Formula (**1**)	4267,00	31,66
GTZ Formula (**2**)	5435,40	67,71
GTZ Formula (**3**)	5193,00	60,23

Δ% = Percentage Differential

(**1**) Used March Solar Irradiation from SAS-SWP at 30° Tilt = 4,93 kWh/m²/day

(**2**) Used March Solar Irradiation from CSIR = 6,28 kWh/m²/day

(**3**) Used March Solar Irradiation from Kyocera Solar = 6 kWh/m²/day

GTZ Formula as given in Equation (27)

Note: While it is accepted that the CSIR and Kyocera solar irradiation values are not at the correct comparative array tilt, they are given as illustrative values, knowing that the correct array tilt would increase the effective irradiation and therefore the calculated deviation, to an even greater extent than that shown.

In addition to the detailed design data presented by the SAS-SWP application, various aspects of the design are presented in graphical format, of which the PV array and pumping performance for the VUT design as calculated by SAS-SWP is given in the example shown in Figure 45.

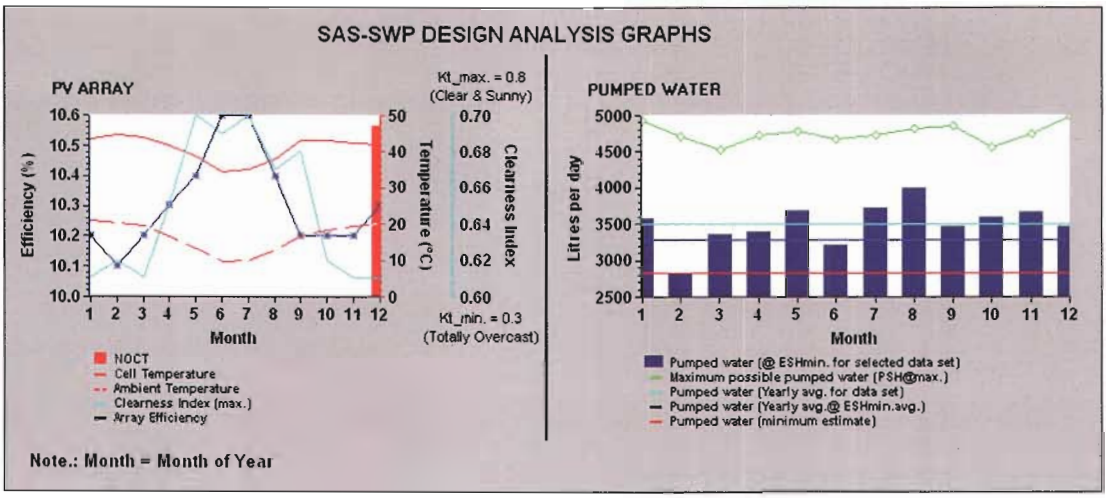

Figure 45 SAS-SWP design analysis graphs

A base-line pumping comparison including the PV-SYS 4.1 (PV-SYS 2007) and RETScreen (RETScreen 2005) applications was attempted but failed due to the difficulty of exact data and equipment matching required for comparison with the VUT data.

4.2.2 peer review

The official release of version 1.0 of the SAS-SWP application program, together with a paper on the development, functionality and operation (Denny & Case 2007:7-13) was subjected to peer-review when submitted, presented and demonstrated at the sixteenth annual South African Universities Power Engineering Conference (SAUPEC) at the University of Cape Town in January 2007.

The SAS-SWP Design Aid received a positive response at the conference with no negative issues with respect to the presented paper or application program being raised.

CHAPTER 5 – Conclusion and Recommendations

The objectives and goals of this research have been successfully attained, substantiated as follows:

The research started by presenting a motivation as to the necessity for the research output. This was followed by investigation, analysis and presentation of the components and aspects related to solar/photovoltaic water pumping that were considered important as pre-emptive knowledge, in order to understand program model requirements for the design of a PVPS software application. A specification then ensued, developed from applicable technical input and stakeholder consultation.

Resultant from the research, a PVPS design strategy and calculation methodology was devised. This was followed by a detailed software design, incorporating specification requirements and presented in modular format. The design was coded into a computer software program to aid in the design of non-tracking, directly-coupled, stand alone photovoltaic (solar) powered water pumping systems. Salient features of the program include the following:

- User-friendly graphical user interface - 'Point-and-Click' type operation.
- Embedded context sensitive help system.
- Fast computational times ('fast' being defined as a few seconds, at most).
- Integrated twenty-one point solar irradiation and ancillary component data set for any location within the defined Southern African region (full Southern African Solar Radiation Database developed and included with the application – Refer to Table 11 for full database content details).
- Comprehensive array tilt strategy recommendations, including energy analyses.
- Vendor independent equipment selection and integrated, expandable, equipment databases (wide range of pumps and PV panels included in the hardware databases provided).
- Various temperature and efficiency compensation algorithms.

- Component matching and optimisation analysis.
- Geo-magnetic database for correct compass orientation of PV arrays.
- Full design for each month of the year.

5.1 Comments and observations

- It should be noted that the initial water requirement input is a starting point for any design. Once bore-hole/well parameters have been entered and hardware and balance-of-system (BOS) selections made in the SAS-SWP application, these, together with the local meteorological environment form the boundary conditions for the PVPS delivery capability. The SAS-SWP application enforces a minimum design clamp based on initial water requirements and worst case meteorological conditions, but does not impose an upper boundary. This stresses the importance of choosing correctly sized hardware (pump-set/PV array) for the design at hand, minimising over-design and thereby providing a cost-effective engineering solution.
- System optimisation is achieved via a combination of analytical and iterative means, with physical hardware efficiencies and BOS equipment loss factors dynamically calculated throughout the design process. Photovoltaic powered directly-coupled pump motors perform optimally at specific array series-parallel configurations (Dunlop 1988:1187). This is achieved in the SAS-SWP application via a comprehensive PV array database 'Best Fit' analysis, providing both efficiency and quantitative feedback. This allows informed design and implementation decisions from both an engineering and cost perspective.
- Validation of the SAS-SWP software program and its various components has been carried out via comparison to a diverse variety of modelled results from specialist software packages and manual calculations, as well as with practical test data as described in the previous chapter. Results within three and a half percent of actual 'pumped water' measurement data was achieved in the VUT trial, with acceptable or explicable results being achieved in all other cases.

- Evaluation of the pumping trial data and physical design shows that a correctly designed and implemented, non-tracking, directly-coupled PVPS, is the least complex design able to meet output requirements. It is a robust solution, suitable for implementation in rural and other 'low technology' or remote areas. Analysis of the trial data suggests that in predominantly sunny areas of the country, this design configuration would be able to out-perform non-tracking MPPT assisted systems. This deduction is made due to the fact that all available power is utilised in the pumping process and not clamped or diverted for battery charging. Similarly, the benefit of including a linear current booster (LCB) in the circuit to assist in start-up/shutdown conditions is negated by its own power consumption throughout the remainder of the daily pumping period. This argument is not valid for areas where the applied solar irradiance is subject to frequent interruption due to factors such as cloud, in which case the electronically assisted designs would provide benefit due to their power management ability.

5.2 Improvements

- The SAS-SWP application program has been designed for directly-coupled, stand alone operation. More design versatility could be achieved if the software was expanded to include other modes of operation.
- The SAS-SWP model uses a single derived total dynamic head value. In reality this value can vary relative to the drawdown characteristics of the bore-hole or well, as the dynamic water level and water flow rate are strongly interrelated. The software could benefit from a more comprehensive hydrological model. Aspects to consider are the well/bore-hole, the aquifer and the drawdown characteristics of a dynamically pumped well, as described in research by Tegethoff (1995).
- A hydrogeological GIS map of South Africa, encompassing data from the National Groundwater Data Bank (NGDB) was completed in 2002 (Jonck & Meyer 2003). The GIS depicts aquifer type, together with the expected borehole yield. This information would be ideal for incorporation into the SAS-SWP application as a location based water yield and depth estimate database and could be accessed in conjunction with the Solar Irradiation data 'point-and-click' map

interface. An overview of the hydrogeological map series available from the South African Department of Water Affairs and Forestry (DWAF) is shown in Figure 46. DWAF also provide data in the form of a 'Groundwater Harvest Potential' map (RSA 2007c), as illustrated in Figure 47 (Holtzhausen 2005:16).

- Similarly, borehole location and distribution (also available from DWAF) can be added to the application database as a reference.
- While it is a relatively simple task to deduce basic equipment cost for a design using retail pricing, the intricacies of Life Cycle Costing (LCC) is assumed beyond the average capability of the intended target market for this program. This functionality could be added to the base software as an additional module.
- The operative language used in the SAS-SWP application GUI is English. Future developments in the SAS-SWP application should make provision for various language modules, enabling use of the program in a local language of choice.
- The SAS-SWP application currently relies on manual database backup procedures (as described in the software Help File). System functionality would be enhanced by the inclusion of an automated database backup procedure.

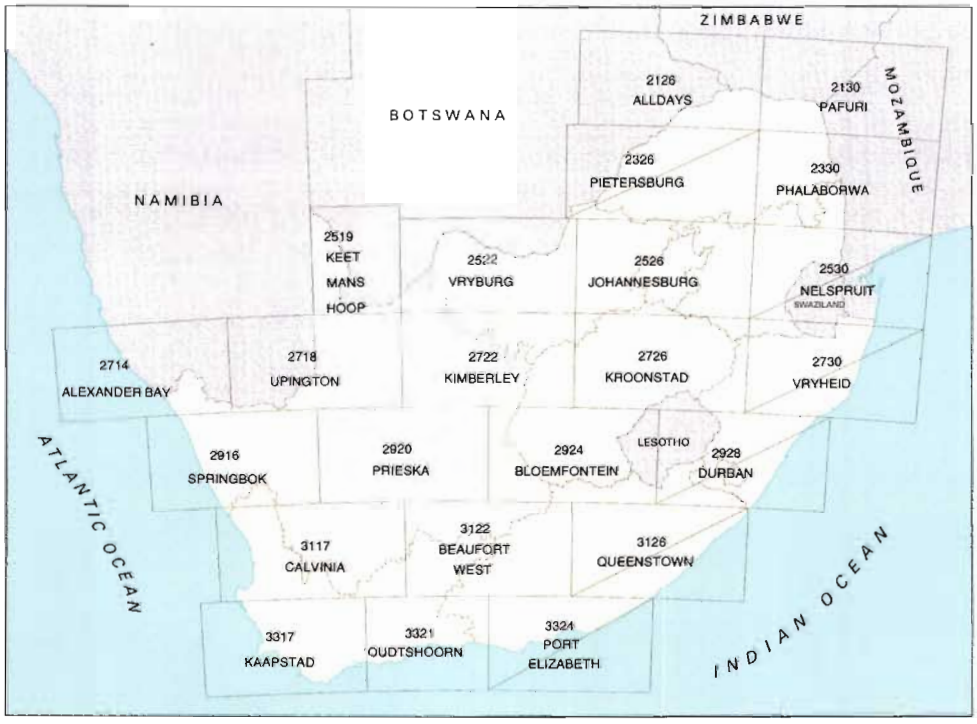

Figure 46 **Hydrogeological map series for the RSA (Jonck & Meyer 2003)**

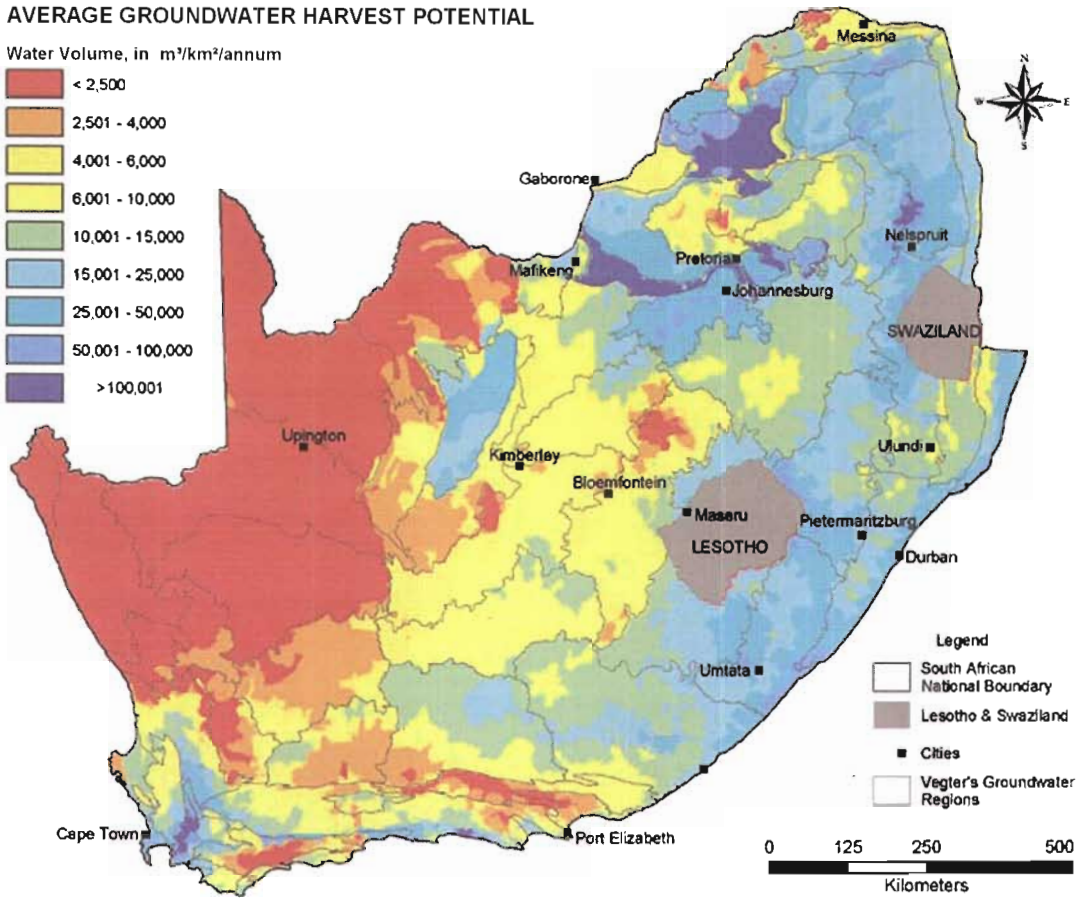

Figure 47 **Average groundwater harvest potential map – RSA (Holtzhausen 2005:16)**

5.3 Recommendations

- The SAS-SWP program has only been subject to short-term trials. It would be beneficial to tweak the application using validated long term data.
- The SAS-SWP application produces a design based on worst-case ESH irradiation data (see descriptions in Table 11). Solar radiation can generally increase to the PSH irradiation value, or even exceed it when certain atmospheric conditions are present, *e.g.* 'edge-of-cloud' irradiance enhancement effects. Many manufacturers build in as much as a 60 percent safety factor to cater for over-range conditions. The VUT pumping trial, for example, reached a maximum current of 2,18 ampere and a voltage of 36,23 volts (at the motor) – This is 12,23 volts (50,96 percent) over nominal design voltage, although in this case, at 79

watts, still well within the rated power of the motor (120 W; 4 A maximum). The designer should ensure that the nominal and peak ratings of equipment used (*e.g.* the pump motor) are appropriately sized for the application and conditions of use.

- A possible topic of future research is identified from the above point, *i.e.* an adjustable, minimal loss, passive (or active) protection circuit for directly-coupled PV systems.
- Technical competence is assumed for the user of the application software – A qualified professional should be consulted for installation and connection of any electrical apparatus.

5.4 Late update

This document and the SAS-SWP software provided are based on and developed from NASA-ASDC Surface Meteorology and Solar Energy (SSE) release 5.1 data. This Data Set was made available in 2005 and contained 10 years of data (July 1983 - June 1993).

In 2008 NASA made the SSE release 6.0 Data Set available to researchers via their internet web site. Meteorology and solar radiation data for release 6.0 has been generated from the NASA Science Mission Directorate's satellite and re-analysis research programs and extends the temporal coverage of the solar and meteorological data from 10 years to more than 22 years (July 1983 - June 2005).

The relevant release 6.0 data for South Africa was obtained from NASA and reworked for the SAS-SWP application. The new solar radiation database file ("RSAsolarData.dat") is provided on the companion CD, under directory [../Updates]. The user may choose to update the SAS-SWP application by manually replacing the existing "RSAsolarData.dat" file in the SAS-SWP application software root directory with the updated version of the same name. A back-up of the old file should be made if a software 'roll-back' is anticipated.

The only perceived difference between the data sets other than updated solar radiation data, is that "Earth Surface Temperature" is now available instead of "Air Temperature at an altitude of 10 m above the earth surface" (see Table 11), as was previously used – this shall result in more accurate temperature compensation calculations in the software.

BIBLIOGRAPHY

AL-IBRAHIM, A.M. 1996. Optimum Selection of Direct-Coupled Photovoltaic Pumping System in Solar Domestic Hot Water Systems. PhD. Thesis. University of Wisconsin – Madison, USA.

ANIS, R., MERTES, R.P. & VAN OVERSTAETEN, R.J. 1985. Coupling of a Volumetric Pump to a Photovoltaic Array. *Solar Cells*, 14:27-42.

APPELBAUM, J. & BANY, J. 1979a. Analysis of a Direct Coupled DC Motor and a Photovoltaic Converter. *In: Proceedings of 1st Commission of European Community Conference on Photovoltaic Solar Energy*, Luxembourg, September 1979.

APPELBAUM, J. & BANY, J. 1979b. Performance Analysis of DC-Motor-Photovoltaic Converter System. *Solar Energy*, 22(5):439-445.

ARENT, D. 1998. *Rural Electrification in South Africa*. Golden, CO: National Renewable Energy Laboratory (NREL). (NREL/FS-52024633).

ARGAW, N. 2004. *Renewable Energy Water Pumping Systems Handbook*. Golden, CO: National Renewable Energy Laboratory (NREL). (NREL/SR-500-30481).

ARGAW, N., FOSTER, R. & ELLIS, A. 2003. *Renewable Energy for Water Pumping Applications in Rural Villages*. Golden, CO: National Renewable Energy Laboratory (NREL). (NREL/SR-500-30361).

AUER, F. & VIEL, L. 1996. The Optimal Rated Power and Storage Capacity of Photovoltaic Drinking Water Pumps. *In: Proceeding of the 1st European Solar Energy Congress, EUROSUN '96*, Freiburg, Germany, September 1996, 1436-1440.

BEKKER, B. 2007. South African Irradiation and PV Array Energy Output Estimation. *In: Proceeding of 16th South African Universities Power Engineering Conference*, Cape Town, January 2007, 2-6.

BETKA, A. 2005. Perspectives for the Sake of Photovoltaic Pumping Development in the South. DSc. Thesis. University of Batna, Algeria.

BRANDT, O. 2001. The Potential for Solar Water Pumping for Community Water Supply in Zululand, South Africa. Research Paper, Department of Geography and Geoinformatics, University of Pretoria.

BUCHER, W. 1996. Aspects of Solar Water Pumping in Remote Regions. *Energy for Sustainable Development*, 3(4):8-27.

BUSCHERMOHLE, M.J. & BURNS, R.T. 2000. *Solar-Powered Livestock Watering Systems*. Knoxville, TN: University of Tennessee, Agricultural Extension Service. (PB 1640).

CABRAAL, A., SEISS, A., SLOMINSKI, L., BURESCH, M. & KENNA, J. 1887. *A Comparative Assessment of Photovoltaic's, Hand-pumps and Diesels for Rural Water Supply*. Albuquerque, NM: Sandia National Laboratories. (SAND87-7015).

CALIFORNIA ENERGY COMMISSION. 2001. *A Guide to Photovoltaic (PV) System Design and Installation*. Sacramento, CA: Endecon Engineering, for the California Energy Commission. (Publication Number 500-01-020).

CARNICERO DOMÍNGUEZ, B.A. 2001. Characterization of Pyranometer Thermal Offset and Correction of Historical Data. MSc. Thesis. Virginia Polytechnic Institute and State University, USA.

CARTER, P. 2006. October 23. Subject: Use of Surface Meteorology and Solar Energy (SSE) Data. [Online]. Personal E-mail from Mr. Paul Carter, ASDC User Services, NASA.
<larc@eos.nasa.gov>

CASE, M.J., JOUBERT, M.J. & HARRISON, T.A. 2002. A Novel Photovoltaic Array Maximum Power Point Tracker. *In: Proceedings of 2002 EPE-PEMC Conference*, Dubrovnik, Croatia, September 2002, T5-005.

CHAPMAN, R.N. 1989. Development of Sizing Nomograms for Stand-Alone Photovoltaic Storage Systems. *Solar Energy*, 43:71.

COLLARES-PEREIRA, M. & RABL, A. 1979. The Average Distribution of Solar Radiation Correlations between Diffuse and Hemispherical and between Daily and Hourly Insolation Values. *Solar Energy*, 22(1):155-164.

COLLINS, R.F. & JONES, A.R. 2002. *A New Method for Optimal Selection of Solar Pumping Systems*. Scottsdale, AZ: Kyocera Solar Inc.

COWAN, W.D. (ed.). 1992. *RAPS Design Manual*. Cape Town: Energy & Development Research Centre, University of Cape Town.

COX, R., GYS, L., KLUNNE, W., PURCELL, C. & LOUINEAU, J. 2002. Learning a Lesson – Assessing PV Programmes in Rural South Africa. *Renewable Energy World*, March/April 2002:83-97.

CROS, S., MAYER, D. & WALD, L. 2004. *The Availability of Irradiation Data*. Paris: Centre d'Energétique, Ecole des Mines de Paris/Armines, France. International Energy Agency – Photovoltaic Power Systems Programme. (IEA-PVPS T2-04:2004).

CSIR. 2007. South African Renewable Energy Resource Database – Annual Solar Radiation Surface Plot. [Online]. Available at: <http://www.csir.co.za/plsql/ptl0002/ptl0002_pge100_loose_content?loose_page_no=7034781> Accessed: 06/03/2007.

DASTPVPS. 2006. Design and Simulation Tool for Photovoltaic Pumping Systems. [Online]. Available at: < http://www.ibom.de/dastpvps.htm> Accessed: 25/05/2006.

DE VILLIERS, I. 2003. Fundamental Design Requirements for Solar-Electric Powered Water Pumping Systems. [Online].
Available at: <http://www.divwatt.co.za/fundamental.htm> Accessed: 10/06/2003.

DENNY, E.E. & CASE, M.J. 2007. Development of a Computer Based Aid for General Use in the Design of Directly Coupled Stand-Alone Solar Powered Water Pumping Systems. *In: Proceeding of 16th South African Universities Power Engineering Conference*, Cape Town, January 2007, 7-13.

DENNY, E.E. 2006. Stand Alone Solar (PV) Water Pumping Design Aid: SAS-SWP Application Software Help File. Vanderbijlpark: Vaal University of Technology.

DOGNIAUX, R., GRUETER, J.W., KASTEN, F., PAGE, J.K.,
PERRIN DE BRICHAMBAUT, C., TREBLE, F.C. & PALZ, W. 1984. Solar Meteorology (Units and Symbols). *International Journal of Solar Energy*, 2:249-255.

DUFFIE, J.A. & BECKMAN, W.A. 1991. *Solar Engineering of Thermal Processes.* 2nd ed. New York: John Wiley & Sons Inc.

DUNLOP, J.P. 1988. Analysis and Design Optimisation of Photovoltaic Water Pumping Systems. *In: Proceeding of the 20th IEEE Photovoltaic's Systems Conference*, Las Vegas, NV, September 1988, 1182-1185.

DUTTON, E.G., STOEFFEL, T. & MICHALSKY, J. 2001. Thermal Offset Errors in Solar Diffuse Measurements with some Commercial Pyranometers. *Journal of Atmospheric Oceanic Technology*, 18:297-314.

EBERHARD, A.A. 1990. *A Solar Radiation Data Handbook for Southern Africa.* Cape Town: Elan Press.

ECKSTEIN, J.H. 1990. Detailed Modelling of Photovoltaic System Components. MSc. Thesis. University of Wisconsin – Madison, USA.

EMCON CONSULTING GROUP. 2006. *Feasibility Assessment for the Replacement of Diesel Water Pumps with Solar Water Pumps.* Windhoek: EMCON Consulting Group. (Final Report to the Namibian Ministry of Mines and Energy, September 2006).

EVANS, D.L. 1981. Simplified Method for Predicting Photovoltaic Array Output. *Solar Energy*, 27(6):555-560.

FEUEKMANN, D. & ZEMEL, A. 1992. Validation of Models for Global Irradiance on Inclined Planes. *Solar Energy*, 48(1):59-66.

GIECK, K., translation by WALTERS, J. 1985. *A Collection of Technical Formulae.* 6th ed. Heilbronn, Germany: Gieck-Verlag.

GIPE, P. 1999. *Wind Energy Basics: A Guide to Small and Micro Wind Systems.* White River Junction, VT: Chelsea Green Publishing.

GOLDBLATT, M. 1996. Making the Cup Run Over - The Challenge of Urban Water Supply for South Africa's Reconstruction and Development Programme. *GeoJournal*, 39(1):21-26.

GOOGLE EARTH. 2007. Google Earth Virtual Globe Map Software. [Online]. Available at: <http://earth.google.com/download-earth.html> Accessed: 04/04/2007.

GREEN, M.A., EMERY, K., KING, D.L., IGARI, S. & WARTA, W. 2003. Solar Cell Efficiency Tables (Version 22). *Progress in Photovoltaic's: Research and Applications*, 11:347–352.

GREIF, J. & SCHARMER, K. (eds.). 2000. *European Solar Radiation Atlas*. Paris: Presses de l'Ecole, Ecole des Mines de Paris, France.

GRUNDFOS. 2006. WinCAPS. [Online].
Available at: <http://www.grundfos.com/web/homeza.nsf>
Accessed: 21/08/2006.

GTZ. 2002. *Drinking Water Supply with Photovoltaic Water Pumps (PVP)*.
Eschborn: Deutsche Gesellschaft für Technische Zusammenarbeit (GTZ) GmbH.

GULBRANDSEN, A. 1978. On the use of Pyranometers in the Study of the Spectral Solar Radiation and Atmospheric Aerosols. *Journal of Applied Meteorology*, 17:899-904.

HADI, H. 2003. Photovoltaic Water Pump System. PhD. Dissertation. Kochi University of Technology, Japan.

HAEFFELIN, M., KATO, S., SMITH, A., RUTLEDGE, K., CHARLOCK, T. & MAHAN, R. 2001. Determination of the Thermal Offset of the Eppley Precision Spectral Pyranometer. *Applied Optics*, 40(9):472-484.

HAEFFELIN, M.P., DOMÍNGUEZ, B.A.C., RUTLEDGE, K. & KATO, S. 2001. Improved Measurements of the Diffuse and Global Solar Irradiances at the Surface of the Earth. *In: Proceedings of the 11th Atmospheric Radiation Measurement Science Team Meeting*, Atlanta, Georgia, March 2001.

HAHN, A. 2000. *Photovoltaic Water Pumps*. Eschborn: gate Information Service /GTZ. May 2000. (Technical Information E4e).

HELIOSAT Project. 1992. Heliosat Project - Example. [Online]. Available at: <http://www.helioclim.net/heliosat/index.html>. Accessed: 18/11/2006.

HOLTZHAUSEN, L. 2005. Groundwater Assessment. *The Water Wheel*, November/December 2005:14-17

HOMER. 2005. National Renewable Energy Laboratory (NREL) Optimisation Model for Distributed Power - Software, version 2.19. [Online]. Available at: <http://www.nrel.gov/homer/> Accessed: 18/08/2005.

HSIAO, Y.R. & BLEVINS, B.A. 1984. Direct Coupling of Photovoltaic Power Source to Water Pumping System. *Solar Energy*, 32(4):489-498.

HUGHES, E., revised by MCKENZIE SMITH, I. 1987. *Hughes: Electrical Technology*. 6th ed. New York: Longman Scientific & Technical.

IEA. 2003. *Report IEA PVPS T9-07: 16 Case Studies on the Deployment of Photovoltaic Technologies in Developing Countries*. Paris: International Energy Agency - Photovoltaic Power Systems Programme. 18-26.

INEICHEN, P., PEREZ, R. & SEALS, R. 1987. The Importance of Correct Albedo Determination for Adequately Modelling Energy Received by Tilted Surfaces. *Solar Energy*, 39(4):301-305.

INTERMEDIATE TECHNOLOGY DEVELOPMENT GROUP. 2002. *Solar (Photovoltaic) Water Pumping*. Rugby, Warwickshire: Knowledge & Information Services, The Schumacher Centre for Technology & Development.

JÄGER-WALDAU, A. 2002. *Status of PV Research, Solar Cell Production and Market Implementation in Japan, USA and the European Union*. Ispra, Italy: European Commission - Joint Research Centre, Renewable Energies Unit.

JONCK, F. & MEYER, S. 2003. Hydrogeological Map Series of the Republic of South Africa. *In: Proceedings of 21st International Cartographic Conference*, Durban, South Africa, August 2003.

KAREKEZI, S. 2002. Renewables in Africa - Meeting the Energy Needs of the Poor. *Energy Policy*, 30(11-12):1059-1069.

KATO, S., ACKERMAN, T.P., CLOTHIAUX, E.E., MATHER, J.H., MACE, G.G., WESELY, M.L., MURCRAY, F. & MICHALSKY, J. 1997. Uncertainties in Modelled and Measured Clear-Sky Surface Shortwave Irradiances. *Journal of Geophysical Research*, 102(D22):25881-25898.

KING, D.L., BOYSON, W.E. & KRATOCHVIL, J.A. 2004. *Photovoltaic Array Performance Model*. Albuquerque, NM: Sandia National Laboratories, Photovoltaic Systems R&D Department. (SAND2004-3535).

KING, D.L., HUND, T.D., BOYSON, W.E. & KRATOCHVIL, J.A. 2002. Experimental Optimization of the Performance and Reliability of Stand-Alone Photovoltaic Systems. *In: Proceedings of the 29th IEEE PV Specialists Conference*, New Orleans, LA. 1428-1431.

KLEIN, S.A. & BECKMAN, W.A. 1984. Review of Solar Radiation Utilizability. *Journal of Solar Energy Engineering*, 106:393-402.

KLEIN, S.A. 1977. Calculation of Monthly Average Insolation on Tilted Surfaces. *Solar Energy*, 19:325-329.

KOLHE, M., JOSHI, J.C. & KOTHARI, D.P. 2004. Performance Analysis of a Directly Coupled Photovoltaic Water-Pumping System. *IEEE Transactions on Energy Conversion*, 19(3):613-618.

KONER, P.K., JOSHI, J.C. & CHOPRA, K.L. 1992. Matching Analysis of Photovoltaic Powered DC Series Motors and Centrifugal Pumps by Varying Motor Constants. *International Journal of Energy Research*, 16(4):301-313.

KOU, Q., KLEIN, S.A. & BECKMAN, W.A. 1998. A Method for Estimating the Long-Term Performance of Direct-Coupled PV Pumping Systems. *Solar Energy*, 64(1-3):33-40.

KYOCERA SOLAR. 2002. *Solar Water Pumping Applications Guide*. Scottsdale, AZ: Kyocera Solar Inc.

LENG, G., MELOCHE, N., MONARQUE, A., PAINCHAUD, G., THEVENARD, D., ROSS, M. & HOSETTE, P. 2004. *Clean Energy Project Analysis: RETScreen Engineering & Cases Textbook - Photovoltaic Project Analysis*. Varennes: CANMET Energy Technology Centre, Canada.

LESTER, A. & MYERS, D.R. 2006. A Method for Improving Global Pyranometer Measurements by Modelling Responsivity Functions. *Solar Energy*, 80(3):322-331.

LIPTON, M., LITCHFIELD, J., BLACKMAN, R., DE ZOYSA, D., QURESHY, L. & WADDINGTON, H. 2003. *Preliminary Review of the Impact of Irrigation on Poverty, with Special Emphasis on Asia*. Rome: Food and Agriculture Organisation of the United Nations (FAO). (AGL/MISC/34/2003).

LIU, B.Y.H. & JORDAN, R.C. 1960. The Interrelationship and Characteristic Distribution of Direct, Diffuse, and Total Solar Radiation. *Solar Energy*, 4:1-19.

LMNO ENGINEERING, RESEARCH, AND SOFTWARE, Ltd. 1998. [Online]. Available at: <http://www.lmnoeng.com/hazenwilliams.htm> Accessed: 28/06/2006.

LONG, C.N., ACKERMAN, T.P., DE LUISI, J.J. & AUGUSTINE, J. 1999. Estimation of Fractional Sky Cover from Broadband SW Radiometer Measurements. *In: Proceedings of the 10th Conference on Atmospheric Radiation*, Madison, Wisconsin, June/July 1999.

LOXSOM, F. & DURONGKAVEROJ, P. 1994. Estimating the Performance of a Photovoltaic Pumping System. *Solar Energy*, 52(2):215-219.

MASTERS, G.M. 2004. *Renewable and Efficient Electric Power Systems*. New York: John Wiley & Sons Inc.

MAUI SOLAR ENERGY SOFTWARE CORPORATION. 2006. Solar Design Studio. [Online]. Available at: <http://www.mauisolarsoftware.com> Accessed: 16/05/2006.

MCBRIDE, C. 2007. March 5. Subject: Request Data for Project. [Online]. Personal E-mail from Ms. Charlotte McBride, Assistant Manager - Publications, South African Weather Service (SAWS). <charlotte.mcbride@weathersa.co.za>

MCNUTT, P., KROPOSKI, B., HANSEN, R., DEBLASIO, R., THOMAS, M., DURAND, S., ROSENTHAL, A. & HUTCHINSON, P. 1999. *Procedures for Determining the Performance of Stand-Alone Photovoltaic Systems*. Golden, CO: National Renewable Energy Laboratory (NREL). September 1999. (NREL/TP-520-27031).

METEONORM. 2006. METEONORM Global Radiation Database Software, version 5.1. [Online].
Available at: <http://www.meteotest.ch/en/mn_dl?w=ber> Accessed: 08/10/2006.

MOINE, G., MARCEL, J. & CHAROY, A. 2003. *Common Practices for Protection Against the Effects of Lighting on Stand-Alone Photovoltaic Systems*. Paris: International Energy Agency. (IEA PVPS T3-14:2003).

MORAES-DUZAT, R.M. DE SIQUEIRA. 2000. Analytical and Experimental Investigation of Photovoltaic Pumping Systems. PhD. Thesis. University of Oldenberg, Germany.

MYERS, D.R. 2003. *Solar Radiation Modelling and Measurements for Renewable Energy Applications: Data and Model Quality*. Golden, CO: National Renewable Energy Laboratory (NREL). March 2003 (NREL/CP-560-33620).

NASA CERES. 2000. NASA Image Catalogue. [Online]. Available at: <http://visibleearth.nasa.gov/view_detail.php?id=187> Accessed: 26/07/2006.

NASA-ASDC. 2005. SSE Data Set, Release 5.1. [Online].
Available at: <http://eosweb.larc.nasa.gov/cgi-bin/sse/sse.cgi?>
Accessed: February 2006 – November 2006.

NATIONAL GEOPHYSICAL DATA CENTRE. 2006. [Online].
Available at: < http://www.ngdc.noaa.gov/geomagmodels/IGRFWMM.jsp>
Accessed: 23/08/2006.

NELSON, J. 2003. *The Physics of Solar Cells*. London: Imperial College Press.

NIEUWENHOUT, F.D.J., MARTENS, J.W., LASSCHUIT, P.E., LAFLEUR, M.C.C. & CLOIN, J. 2001. *Life-Cycle Analysis and Optimisation of Solar Home Systems*. Petten, The Netherlands: Energy Research Centre of the Netherlands (ECN). (ECN-C--01-057).

NIEUWLAAR, E. & ALSEMA, E. 1997. Environmental Aspects of PV Power Systems. *In: Proceedings of IEA PVPS Task 1 Workshop*, Utrecht University, The Netherlands, June 1997. (Report Number 97072).

NOVA INDEPENDENT RESOURCES LTD. 2002. *Solar-Electric Design Guide*. Kelowna, British Columbia: NOVA Canada.

OHMURA, A., DUTTON, E.G., FORGAN, B., FRÖHLICH, C., GILGEN, H., HEGNER, H., HEIMO, A., KÖNIG-LANGLO, G., MCARTHUR, B., MÜLLER, G., PHILLIPONA, R., PINKER, R.T., WHITLOCK, C.H., DEHNE, K. & WILD, M. 1998. Baseline Surface Radiation Network (BSRN/WCRP): New Precision Radiometry for Climate Research. *Bulletin of the American Meteorological Society*, 79(10):2115-2136.

OI, A. 2005. Design and Simulation of Photovoltaic Water Pumping System. MSc. Thesis. California Polytechnic State University, San Luis Obispo, CA, USA.

OLSEN, D.R., Jr. 1998. *Developing User Interfaces*. San Francisco, CA: Morgan Kaufmann Publishers Inc.

PAGE, J.K. 1964. The Estimation of Monthly Mean Values of Daily Total Shortwave Radiation on Vertical and Inclined Surfaces From Sunshine Records for Latitudes 40°N - 40°S. *In*: *Proceedings of the United Nations Conference on New Sources of Energy*, 4:378.

PEREZ, R., INEICHEN, P., MOORE, K., KMIECIK, M., CHAIN, C., GEORGE, R. & VIGNOLA, F. 2002. A New Operational Satellite-to-Irradiance Model – Description and Validation. *Solar Energy*, 73(5):307-317.

PEREZ, R., INEICHEN, P., SEALS, R., MICHALSKY, J. & STEWART, R. 1990. Modelling Daylight Availability and Irradiance Components from Direct and Global Irradiance. *Solar Energy*, 44(5):271-289.

PEREZ, R., STEWART, R., SEALS, R. & GUERTIN, T. 1988. *The Development and Verification of the Perez Diffuse Radiation Model.* Albuquerque, NM: Sandia National Laboratory PV Systems Design Assistance Centre. (SAND88-7030).

PINKER, R.T. & LASZLO, I. 1992. Modelling Surface Solar Irradiance for Satellite Application on a Global Scale. *Journal of Applied Meteorology*, 31:194-211.

PLASTICS PIPE INSTITUTE. 2000. *Water Flow Characteristics of Thermoplastic Pipe*. Washington, DC: Plastics Pipe Institute. (Technical report: TR-14, April 2000).

POLAK, P., ADHIKARI, D., NANES, B., SALTER, D. & SURYWANSHI, S. 2003. Transforming Rural Water Access into Profitable Business Opportunities. *In: Proceedings of the International Symposium on Water, Poverty and Productive Uses of Water at the Household Level*, Muldersdrift, South Africa, January 2003, 184-195.

POSORSKI, R. 1993. PV - Trinkwasserpumpen - Struktur und Ergbnisse des PVP-Programms. *Sonnenenergie*, 3:11-16.

PPI. 2006. Plastics Pipe Institute: Water Flow Characteristics of Thermoplastic Pipe – Design Assistance Software. [Online].
Available at: <http://www.plasticpipe.org/pdf/pubs/reports/TR14Software.ZIP>
Accessed: 21/02/2006.

PV-SYS. 2007. PV-SYS Software for Photovoltaic Systems, version 4.1. [Online]. Available at: <http://www.pvsyst.com/> Accessed: 15/01/2007.

QUASCHNING, V. 2003. The Sun as an Energy Resource. *Renewable Energy World*, 5:90-93.

QUASCHNING, V. 2004. Photovoltaic Systems. *Renewable Energy World*, 1:81-84.

REMUND, J. & KUNZ, S. 2003. *METEONORM: Solar Engineering Handbook*, (Version 5, Part II: Theory Part 1). Bern: METEOTEST, Bern, Switzerland.

RENEWABLE RESOURCE DATA CENTRE. 2001. PVWATTS Version 2 - A Performance Calculator for Grid-Connected PV Systems: Changing System Parameters. [Online].
Available at: <http://rredc.nrel.gov/solar/codes_algs/PVWATTS/system.html> Accessed: 31/05/2006.

REPUBLIC OF SOUTH AFRICA. 2001. Department of Water Affairs and Forestry. Government Notice R509, Water Services Act (108/1997); Regulations: Compulsory National Standards and Measures to Conserve Water. *Government Gazette* 22355, 8 June. (Regulation Gazette No. 7079).

REPUBLIC OF SOUTH AFRICA. 2004. Department of Minerals and Energy. White Paper on the Renewable Energy Policy of the Republic of South Africa. *Government Gazette* 26169, 14 May.

REPUBLIC OF SOUTH AFRICA. 2006a. *Stats SA - General Household Survey, July 2005*. Pretoria: Statistics South Africa. (Statistical Release P0318).

REPUBLIC OF SOUTH AFRICA. 2006b. Department of Minerals and Energy (DME). [Online]. Available at: <http://www.dme.gov.za/energy/renew_solar.stm> Accessed: 26/07/2006.

REPUBLIC OF SOUTH AFRICA. 2007a. Department of Water Affairs and Forestry (DWAF) - Water Services: National Information System. [Online]. Available at: <http://www.dwaf.gov.za/dir_ws/WSNIS/> Accessed: 01/05/2007.

REPUBLIC OF SOUTH AFRICA. 2007b. South Africa Yearbook 2006/07. Pretoria: Government Communication and Information System (GCIS).

REPUBLIC OF SOUTH AFRICA. 2007c. Department of Water Affairs and Forestry (DWAF): Groundwater Harvest Potential Map. [Online]. Available at: <http://www.dwaf.gov.za/Geohydrology/Maps/harvpot.asp> Accessed: 30/04/2007.

RETSCREEN. 2005. RETScreen International Clean Energy Project Analysis Software, version 3.2. [Online]. Available at: <http://www.retscreen.net/ang/d_o_view.php> Accessed: 26/08/2005.

RISSER, V. & POST, H. 1991. *Stand-Alone Photovoltaic Systems: A Handbook of Recommended Design Practices*. Albuquerque, NM: Sandia National Laboratory PV Systems Design Assistance Centre. (SAND87-7023).

ROGER, J.A. 1979. Theory of the Direct Coupling between DC Motors and Photovoltaic Solar Arrays. *Solar Energy*, 23(3):193-198.

RS. 1999. *Data Sheet Number 298-4578*. Corby, Northants: RS Components UK.

RSA *see* REPUBLIC OF SOUTH AFRICA.

SABS 0142-1987. 1991. *Code of Practice for the Wiring of Premises*. 2nd revision, as amended. Pretoria: South African Bureau of Standards.

SAIED, M.M. & JABOORI, M.G. 1989. Optimal Solar Array Configuration and DC Motor Field Parameters for Maximum Annual Output Mechanical Energy. *IEEE Transactions on Energy Conversion*, 4(3):459-465.

SALAMEH, Z. & TAYLOR, D. 1990. Set-Up Maximum Power Point Tracker for Photovoltaic Arrays. *Solar Energy*, 44(1):57-61.

SANDIA. 1991. *Maintenance and Operation of Stand Alone Photovoltaic Systems*. Albuquerque, NM: Architectural Energy Corporation in conjunction with Sandia National Laboratory PV Systems Design Assistance Centre. [Online]. Available at: <http://www.sandia.gov/pv/docs/PDF/98TLREF13.pdf> Accessed: 19/03/2007.

SARKAR, M.A.R., OBAIDULLAH, M., MAHMUD, Z. & MARTINAC, I. 2002. Solar PV Submersible Water Pumping for Small Scale Use in Bangladesh. *In: Proceedings of the 8th International Symposium for Renewable Energy Education*, University of Florida, Orlando, August 2002.

SAUNDERS, R.J. & WARFORD, J.J. 1976. *Village Water Supply: Economics and Policy in the Developing World*. Baltimore, MD: The John Hopkins University Press.

SINGER, S. & APPELBAUM, J. 1993. Starting Characteristics of Direct Current Motors Powered by Solar Cells. *IEEE Transactions on Energy Conversion*, 8(1):47-53.

SOLARBUZZ. 2007. *MarketBuzz 2007: Annual World Solar Photovoltaic Industry Report.* San Francisco, CA: Solarbuzz LLC.

SOUTH, D.W., CAMP, R., SIEGEL, J.S. & MEADE, T.B. 1999. *Handbook of Climate Change Mitigation Options for Developing Country Utilities and Regulatory Agencies.* Washington, DC: Energy Resources International, Inc., for the United States Energy Association (USEA).

SPALDING-FECHER, R. 2002. *Energy Sustainability Indicators for South Africa.* Cape Town: Energy and Development Research Centre, University of Cape Town.

STASSEN, G. 1996. Towards a Renewable Energy Strategy for South Africa. PhD Thesis. University of Pretoria.

SUNWIZE TECHNOLOGIES. 2006. *SunWize Solar System Design Guide.* Kingston, NY: SunWize Technologies Inc. [Online]. Available at: <http://www.sunwize.com/catalog/images/design_sunwize_guide.pdf> Accessed: 09/05/2006.

TEGETHOFF, W. 1995. Experimentelle und Theoretische Analyse eines Photovoltaisch Betriebenen Pumpsystems Unter Besonderer Berücksichtigung der Aquiferdynamik. Diploma Thesis. Philipps-Universität Marburg, Germany.

TESTPOINT. 2005. TestPoint version 6.1. [Online]. Available at: <http://www.test-point.com> Accessed: 08/12/2005.

THE ENGINEERING TOOLBOX. 2005. Hazen-Williams Equation - Calculating Friction Head Loss in Water Pipes. . [Online]. Available at: <http://www.engineeringtoolbox.com/hazen-williams-water-d_797.html> Accessed: 22/02/2006.

THOMAS, M.G. 1996. *Water Pumping: The Solar Alternative*. 11th Printing. Albuquerque, NM: Sandia National Laboratory PV Systems Design Assistance Centre. (SAND87-0804).

TOWNSEND, T.U. 1989. A Method for Estimating the Long Term Effects of Direct-Coupled Photovoltaic Systems. MSc. Thesis. University of Wisconsin – Madison, USA.

TRNSYS. 2006. A Transient Systems Simulation Program. [Online]. Available at: <http://sel.me.wisc.edu/trnsys/> Accessed: 25/05/2006.

VAN CAMPEN, B., GUIDI, D. & BEST, G. 2000. *Solar Photovoltaic's for Sustainable Agriculture and Rural Development*. Rome: Food and Agriculture Organisation of the United Nations (FAO).

VAN DYK, E.E., MEYER, E.L., SCOTT, B.J., O'CONNOR, D.A. & WESSELS, J.B. 1997. Analysis of Photovoltaic Energy Output Under Operating Conditions in South Africa. *In: Proceeding of 26th Photovoltaic Specialists Conference*, Anaheim, CA, October 1997, 1197-1200.

VAN TONDER, G.J., BOTHA, J.F. & VAN BOSCH, J. 2001. A Generalised Solution for Step-Drawdown Tests Including Flow Dimension and Elasticity. *Water SA*, 27(3):345-354.

WHITLOCK, C.H. 2004. *NASA Surface Meteorology and Solar Energy: Methodology*. Hampton, VA: NASA Langley Research Centre, Atmospheric Sciences Data Centre.

WILES, J. 2001. *Photovoltaic Power Systems and the National Electrical Code: Suggested Practices*. Albuquerque, NM: Sandia National Laboratory PV Systems Design Assistance Centre. (SAND2001-0674).

WOLETE, J.N. 1998. An Interactive Menu Driven Design Tool for Stand-Alone Photovoltaic Systems. MSc. Thesis. Virginia Polytechnic Institute and State University, USA.

ZELENKA, A., PEREZ, R., SEALS, R. & RENNÉ, D. 1999. Effective Accuracy of Satellite-Derived Irradiance. *Theoretical and Applied Climatology*, 62:199-207.

ZWEIBEL, K. 1990. *Harnessing Solar Power: The Photovoltaics Challenge*. New York: Plenum Publishing Corporation.

ANNEXURE 1

SAS-SWP Program Model Bounce Diagram

Location

As appended. This Annexure is also provided in Portable Document Format (.PDF) and can be found on the enclosed companion CD under the following directory and file name:

../Annexure/Annexure_1_Bounce_Diagram.pdf

Program Model Bounce Diagram

The simplified SAS-SWP program model Bounce Diagram provides a diagrammatic illustration of program flow and module interaction

Application Program

SAS-SWP version 1.0

Creation Date

10 February 2006

Pages

2 pages, excluding this cover page

Annexure to:

DEVELOPMENT OF A COMPUTER PROGRAM FOR GENERAL USE IN THE DESIGN OF SOLAR POWERED WATER PUMPING SYSTEMS

Part (i)

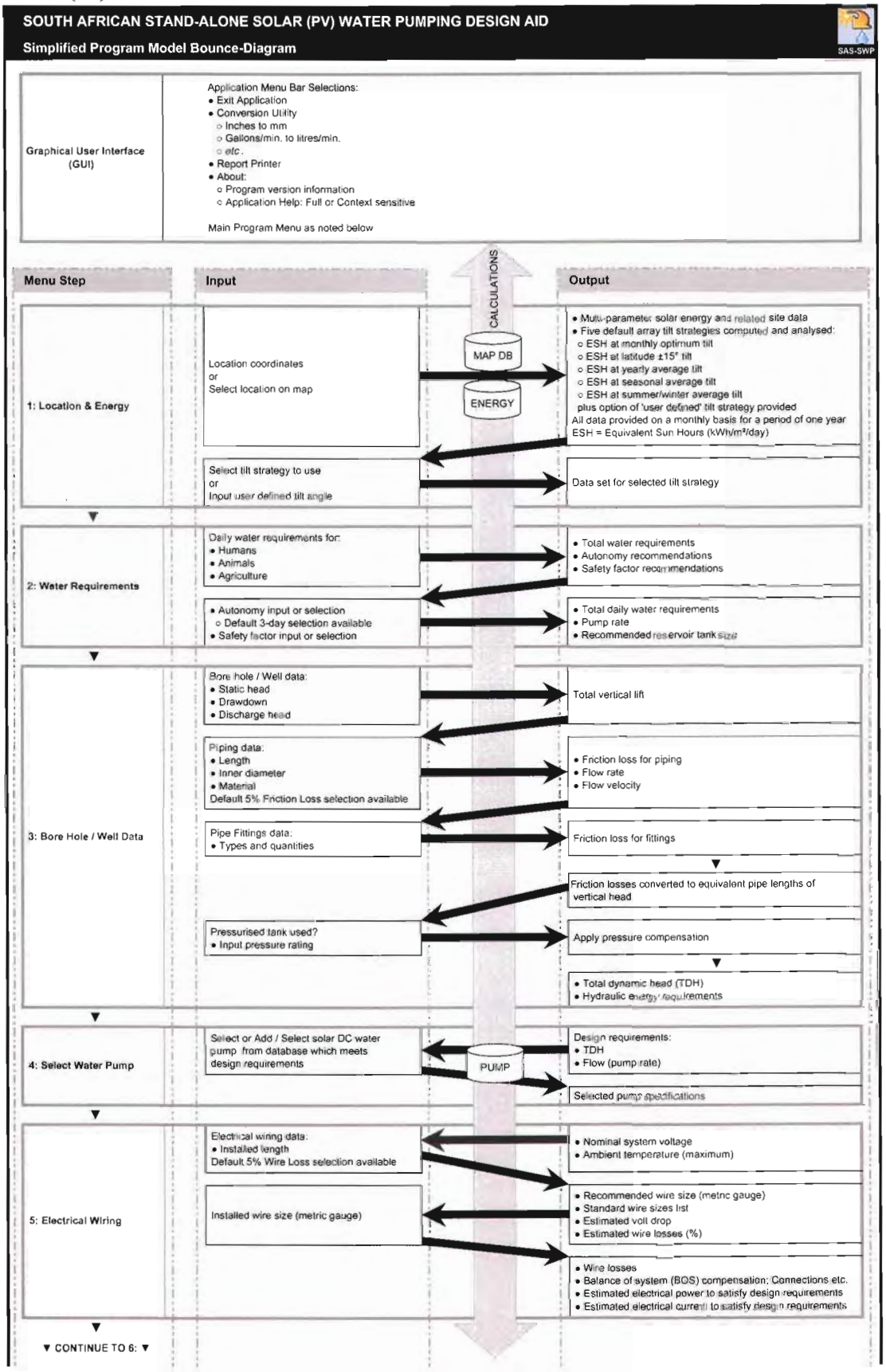
SOUTH AFRICAN STAND-ALONE SOLAR (PV) WATER PUMPING DESIGN AID
Simplified Program Model Bounce-Diagram
SAS-SWP
Graphical User Interface (GUI)
Application Menu Bar Selections:
• Exit Application
• Conversion Utility
○ Inches to mm
○ Gallons/min. to litres/min.
○ etc.
• Report Printer
• About:
○ Program version information
○ Application Help: Full or Context sensitive
Main Program Menu as noted below
Menu Step
Input
Output
CALCULATIONS
MAP DB
ENERGY
1: Location & Energy
Location coordinates or Select location on map
• Multi-parameter solar energy and related site data
• Five default array tilt strategies computed and analysed:
○ ESH at monthly optimum tilt
○ ESH at latitude ±15° tilt
○ ESH at yearly average tilt
○ ESH at seasonal average tilt
○ ESH at summer/winter average tilt
plus option of 'user defined' tilt strategy provided
All data provided on a monthly basis for a period of one year
ESH = Equivalent Sun Hours (kWh/m²/day)
Select tilt strategy to use or Input user defined tilt angle
Data set for selected tilt strategy
2: Water Requirements
Daily water requirements for:
• Humans
• Animals
• Agriculture
• Total water requirements
• Autonomy recommendations
• Safety factor recommendations
• Autonomy input or selection
○ Default 3-day selection available
• Safety factor input or selection
• Total daily water requirements
• Pump rate
• Recommended reservoir tank size
3: Bore Hole / Well Data
Bore hole / Well data:
• Static head
• Drawdown
• Discharge head
Total vertical lift
Piping data:
• Length
• Inner diameter
• Material
Default 5% Friction Loss selection available
• Friction loss for piping
• Flow rate
• Flow velocity
Pipe Fittings data:
• Types and quantities
Friction loss for fittings
Friction losses converted to equivalent pipe lengths of vertical head
Pressurised tank used?
• Input pressure rating
Apply pressure compensation
• Total dynamic head (TDH)
• Hydraulic energy requirements
4: Select Water Pump
Select or Add / Select solar DC water pump from database which meets design requirements
PUMP
Design requirements:
• TDH
• Flow (pump rate)
Selected pump specifications
5: Electrical Wiring
Electrical wiring data:
• Installed length
Default 5% Wire Loss selection available
• Nominal system voltage
• Ambient temperature (maximum)
Installed wire size (metric gauge)
• Recommended wire size (metric gauge)
• Standard wire sizes list
• Estimated volt drop
• Estimated wire losses (%)
• Wire losses
• Balance of system (BOS) compensation; Connections etc.
• Estimated electrical power to satisfy design requirements
• Estimated electrical current to satisfy design requirements
▼ CONTINUE TO 6: ▼

Part (ii)

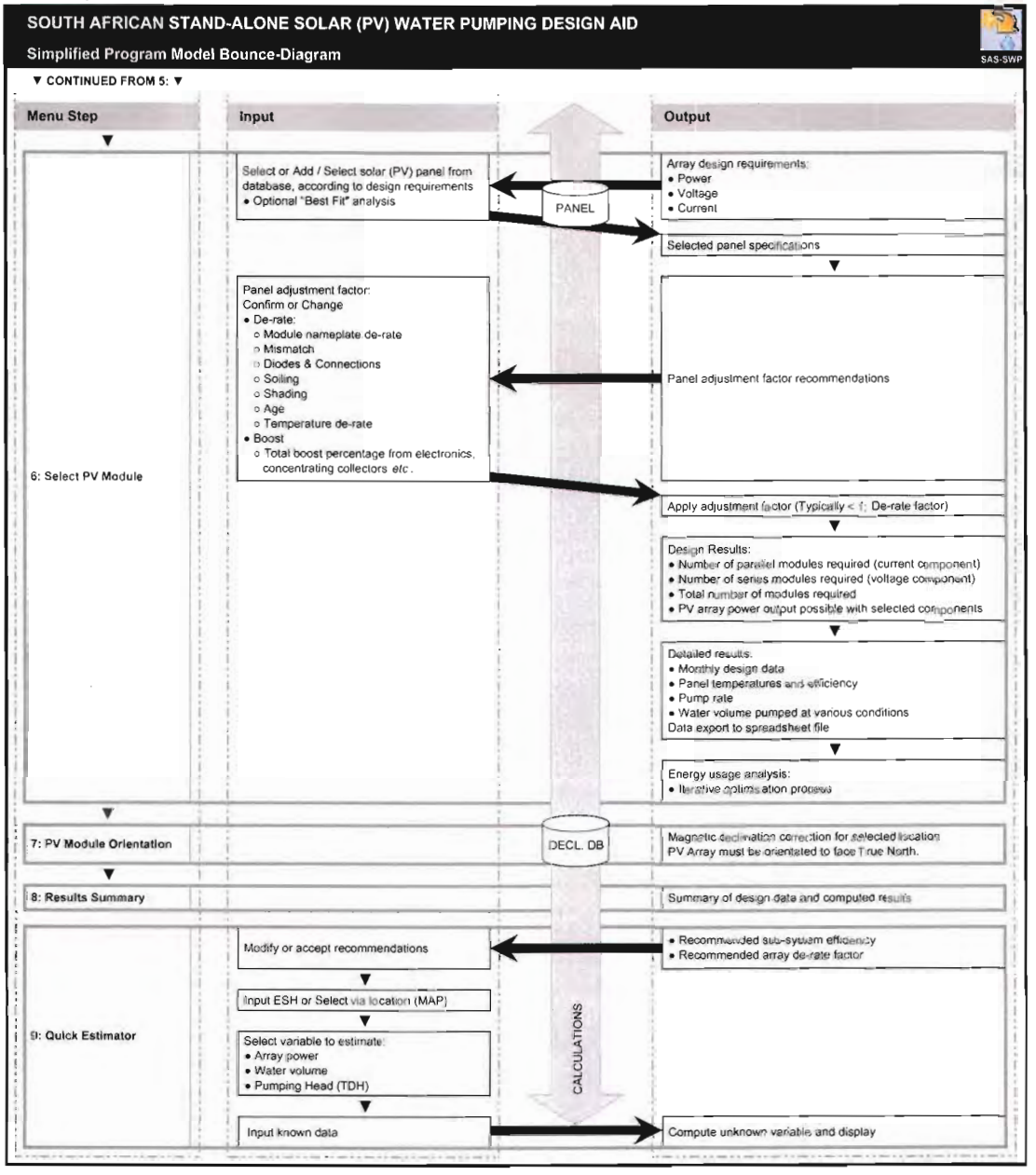
SOUTH AFRICAN STAND-ALONE SOLAR (PV) WATER PUMPING DESIGN AID
Simplified Program Model Bounce-Diagram
SAS-SWP
▼ CONTINUED FROM 5: ▼
Menu Step
Input
Output
Select or Add / Select solar (PV) panel from database, according to design requirements
• Optional "Best Fit" analysis
PANEL
Array design requirements:
• Power
• Voltage
• Current
Selected panel specifications
Panel adjustment factor:
Confirm or Change
• De-rate:
○ Module nameplate de-rate
○ Mismatch
○ Diodes & Connections
○ Soiling
○ Shading
○ Age
○ Temperature de-rate
• Boost
○ Total boost percentage from electronics, concentrating collectors etc.
Panel adjustment factor recommendations
6: Select PV Module
Apply adjustment factor (Typically < 1: De-rate factor)
Design Results:
• Number of parallel modules required (current component)
• Number of series modules required (voltage component)
• Total number of modules required
• PV array power output possible with selected components
Detailed results:
• Monthly design data
• Panel temperatures and efficiency
• Pump rate
• Water volume pumped at various conditions
Data export to spreadsheet file
Energy usage analysis:
• Iterative optimisation process
7: PV Module Orientation
DECL. DB
Magnetic declination correction for selected location
PV Array must be orientated to face True North.
8: Results Summary
Summary of design data and computed results
Modify or accept recommendations
• Recommended sub-system efficiency
• Recommended array de-rate factor
Input ESH or Select via location (MAP)
9: Quick Estimator
Select variable to estimate:
• Array power
• Water volume
• Pumping Head (TDH)
CALCULATIONS
Input known data
Compute unknown variable and display

ANNEXURE 2

SAS-SWP Help File Listing

Location

The Help File listing is provided in Portable Document Format (.PDF) and can be found on the enclosed companion CD under the following directory and file name:

../Annexure/Annexure_2_Help-File_Listing.pdf

The software listing has been reworked to create a printable SAS-SWP manual and can be found on the enclosed companion CD under the following directory and file name:

../Help_Files/SAS-SWP_manual.pdf

Programming Software

Microsoft Help Workshop version 4.03.0002

Application Program

SAS-SWP Help File version 1.04

Listing Generator

MS-Word Rich Text File (RTF) Document Printer

Listing Creation Date

15 February 2007

Pages

This introduction: 2 pages, excluding the cover page

Help File listing: 58 pages & SAS-SWP manual: 31 pages

Annexure to:

DEVELOPMENT OF A COMPUTER PROGRAM FOR GENERAL USE IN THE DESIGN OF SOLAR POWERED WATER PUMPING SYSTEMS

Accessing the SAS-SWP Help File

An indexed Help File is available from within the SAS-SWP application program by selecting the [About] option on the Main Application Menu and then selecting the [SAS-SWP Help File] option. This help file is also available via the operating system menu system by selecting [Start],[All Programs], [SAS_SWP Design Aid],[SAS-SWP Help File], as shown below:

Accessing the Help File via the 'Start' menu

Module context sensitive help is available by selecting the 'Help' icon  (as shown) on any of the applicable SAS-SWP module panels.

Help File Menu

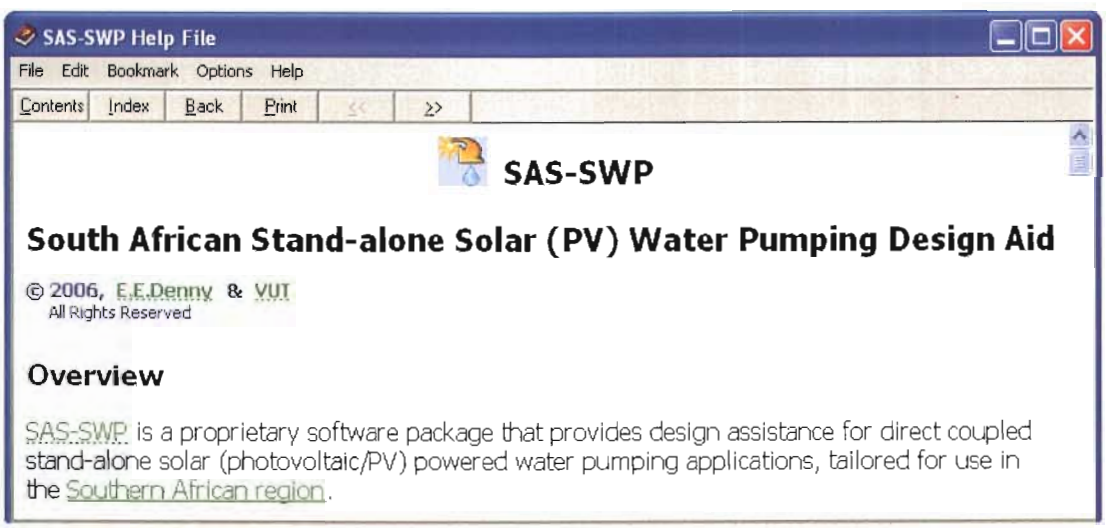

Help File Applet Menu System

The SAS-SWP Help File applet has the standard 'Windows' operating system controls and functionality, as shown above. This includes menus, search and browse functions, as well as 'pop-up' information, accessed via the green text with a dashed underline, or indexed jumps, accessed via green text with a solid underline.

SAS-SWP Help File Index

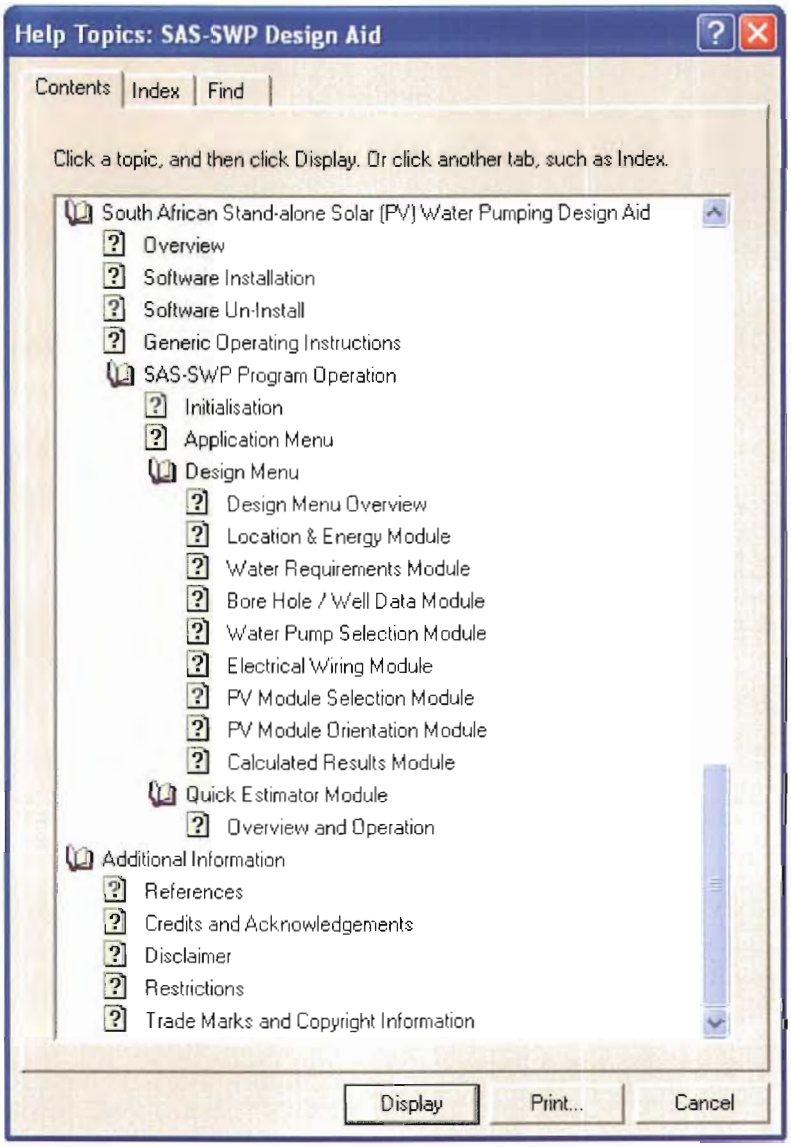

Help File Topics Index

Note: The full benefit of the Help File is best gained via use of the software version. The software listing has been reworked as noted, in order to create a printable SAS-SWP manual in Portable Document Format (.PDF).

ANNEXURE 3

SAS-SWP Application Software File Listing

Location

This Annexure is provided in Portable Document Format (.PDF) and can be found on the enclosed companion CD under the following directory and file name:

../Annexure/Annexure_3_Program_Listing.pdf

SAS-SWP Application Software File Listing

Software code program listing in TestPoint 6.1 format

Programming Software

TestPoint version 6.1

Application Program

SAS-SWP version 1.0

Listing Generator

Internal TestPoint program listing printer

Listing Creation Date

16 February 2007

Pages

672 pages, excluding this cover page

Annexure to:

DEVELOPMENT OF A COMPUTER PROGRAM FOR GENERAL USE IN THE DESIGN OF SOLAR POWERED WATER PUMPING SYSTEMS

ANNEXURE 4

SAS-SWP Solar Irradiation Surface Plots

Location

As Appended. This Annexure is also provided in Portable Document Format (.PDF) and can be found on the enclosed companion CD under the following directory and file name:

../Annexure/Annexure_4_Surface_Plots.pdf

Solar Irradiation Surface Plots

Monthly solar irradiation surface plots over a period of one year for Southern Africa, based on equivalent sun hours (ESH) at optimal PV array tilt angle

Data Source

SAS-SWP version 1.0

Application Program

SAS-SWP version 1.0

Database File

RSAsolarData.dat

Creation Date

7 November 2006

Pages

6 pages, excluding this cover page

Annexure to:

DEVELOPMENT OF A COMPUTER PROGRAM FOR GENERAL USE IN THE DESIGN OF SOLAR POWERED WATER PUMPING SYSTEMS

Surface Plot - January

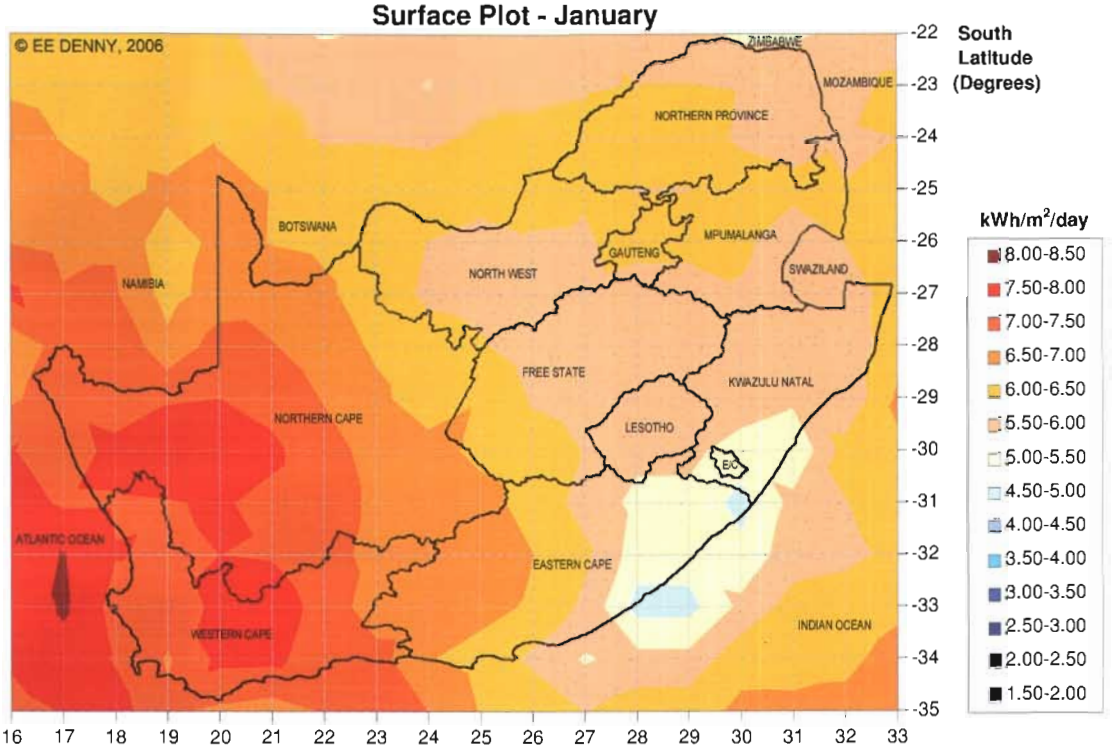

Monthly Averaged Equivalent Sun Hours Radiation Incident On An North-pointed Tilted Surface - Perez/Page Method

Surface Plot - February

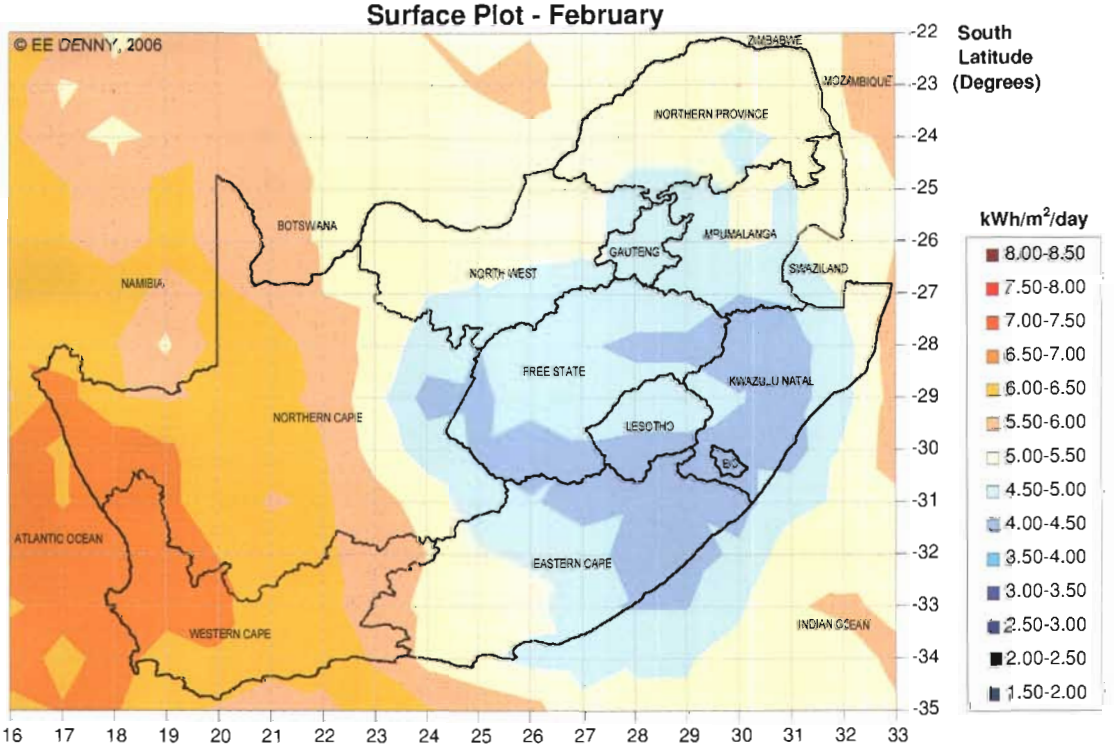

Monthly Averaged Equivalent Sun Hours Radiation Incident On An North-pointed Tilted Surface - Perez/Page Method

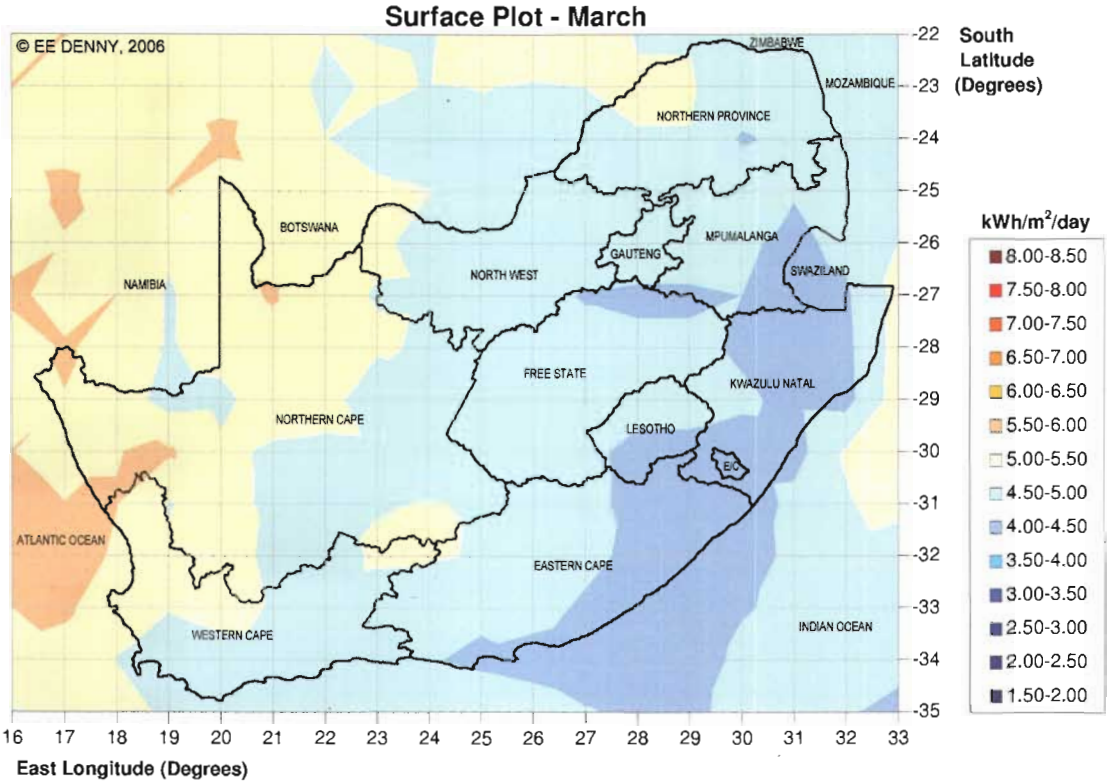

Monthly Averaged Equivalent Sun Hours Radiation Incident On An North-pointed Tilted Surface - Perez/Page Method

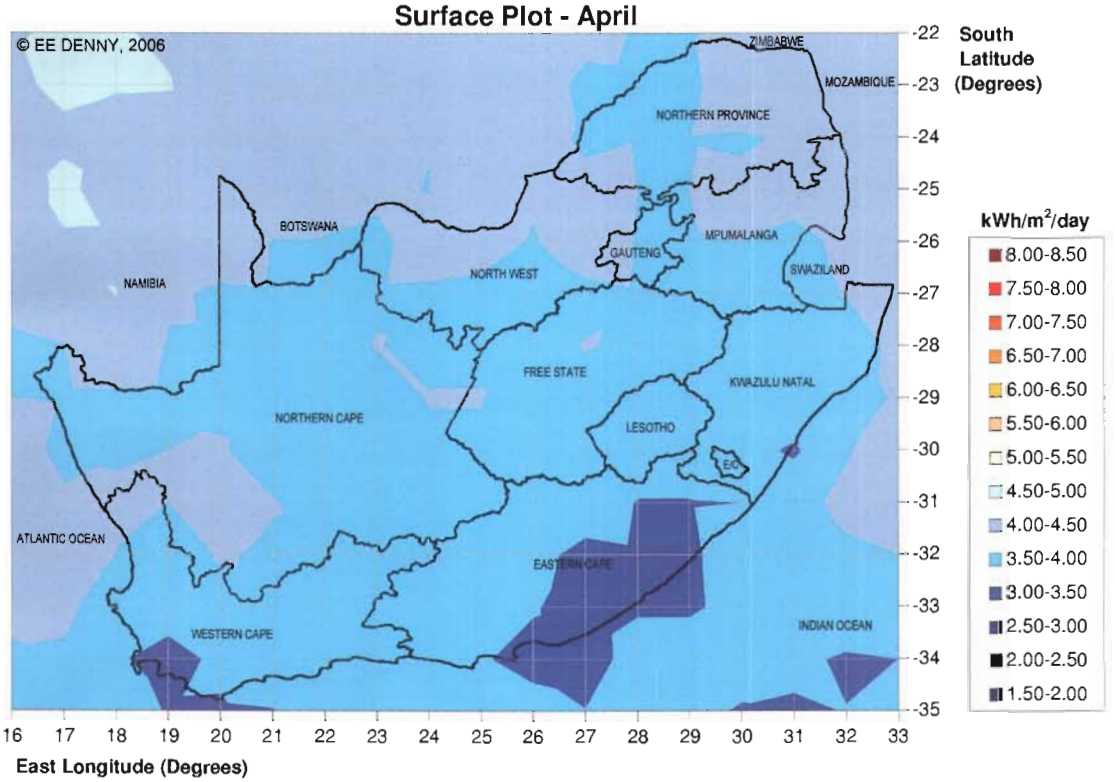

Monthly Averaged Equivalent Sun Hours Radiation Incident On An North-pointed Tilted Surface - Perez/Page Method

Surface Plot - May

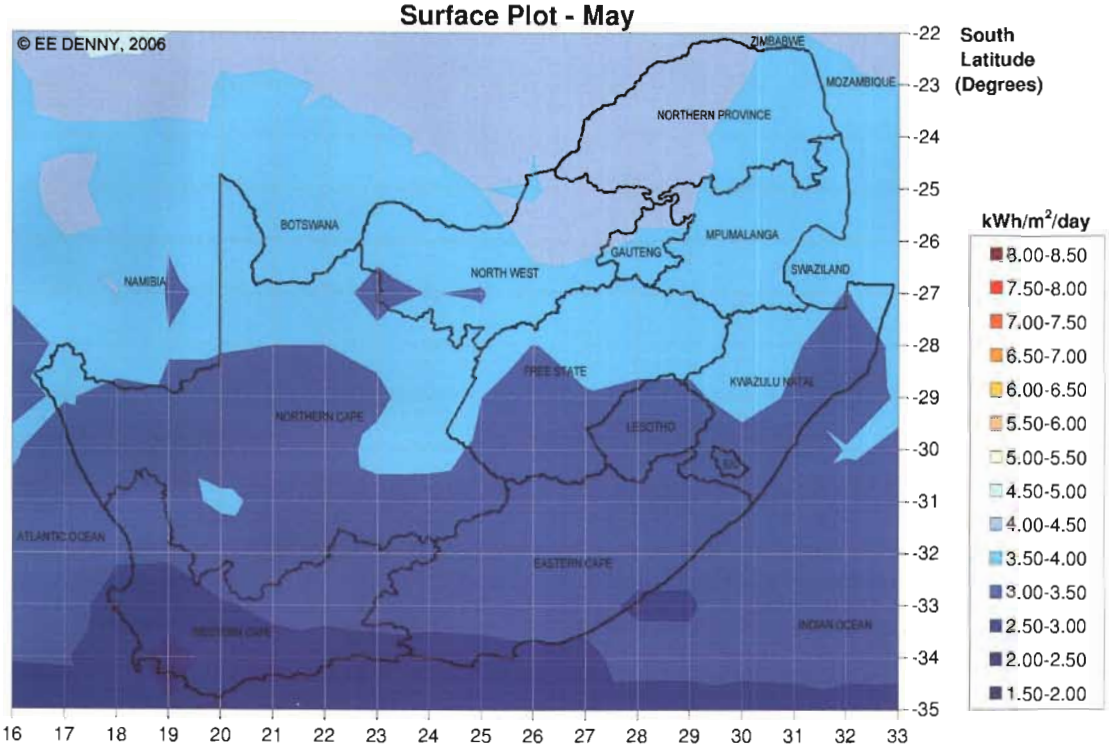

Monthly Averaged Equivalent Sun Hours Radiation Incident On An North-pointed Tilted Surface - Perez/Page Method

Surface Plot - June

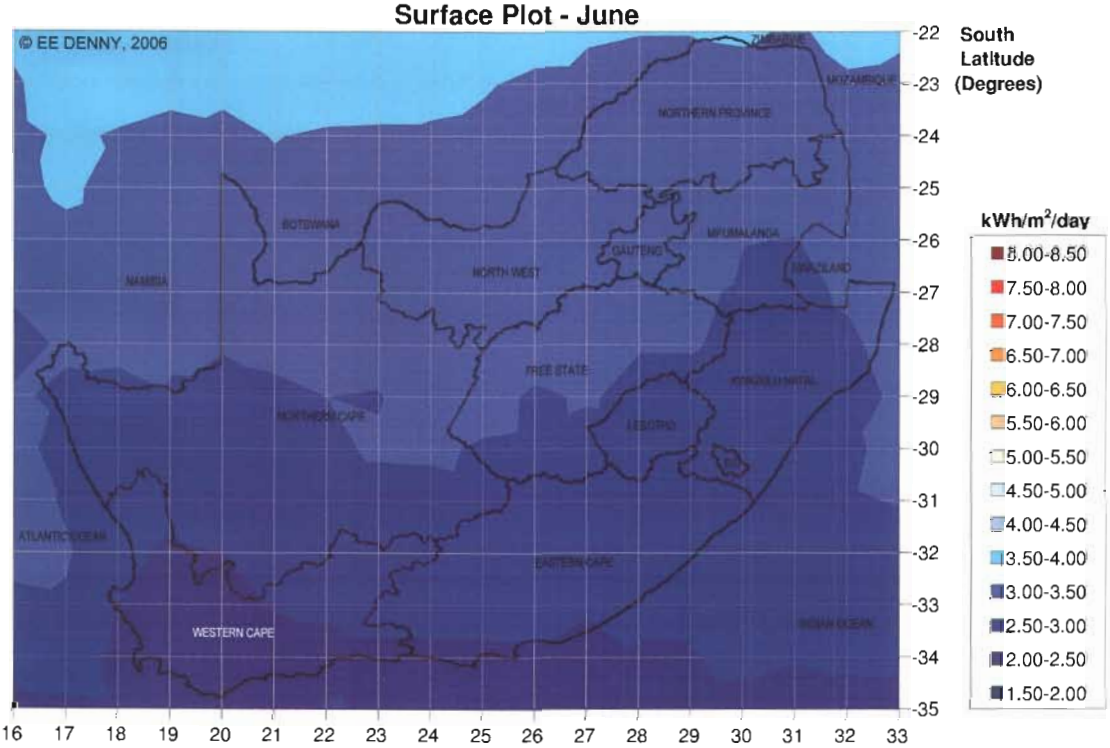

Monthly Averaged Equivalent Sun Hours Radiation Incident On An North-pointed Tilted Surface - Perez/Page Method

Surface Plot - July

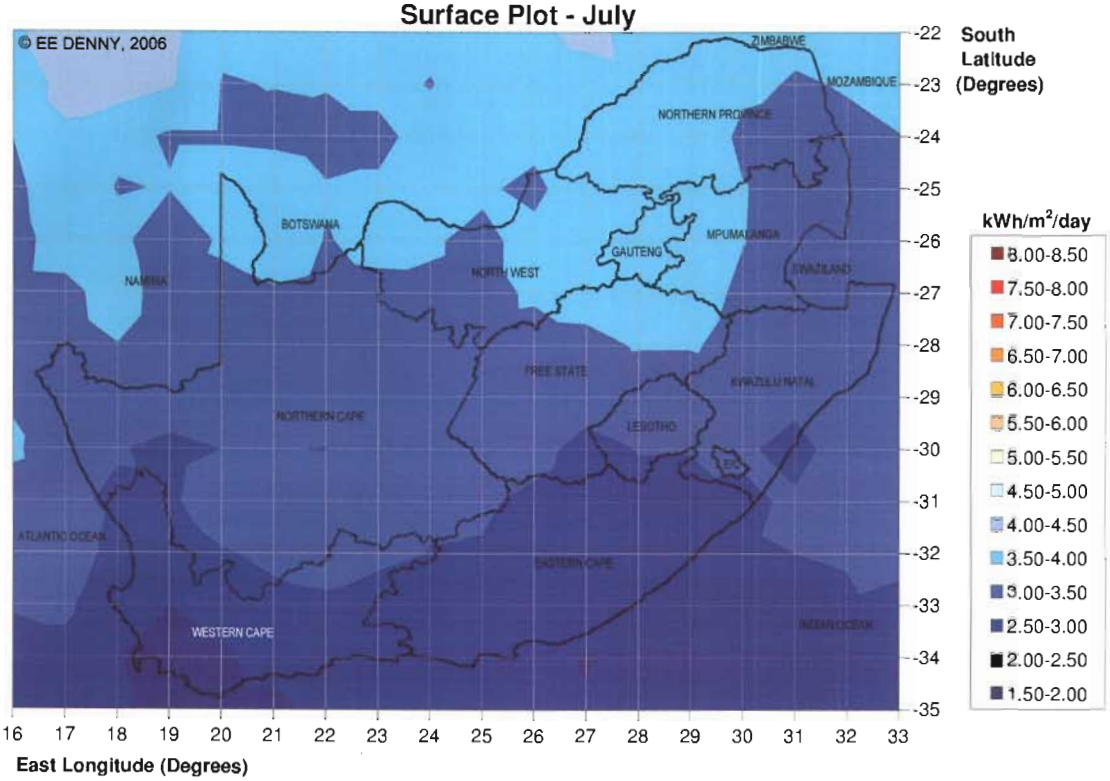

Monthly Averaged Equivalent Sun Hours Radiation Incident On An North-pointed Tilted Surface - Perez/Page Method

Surface Plot - August

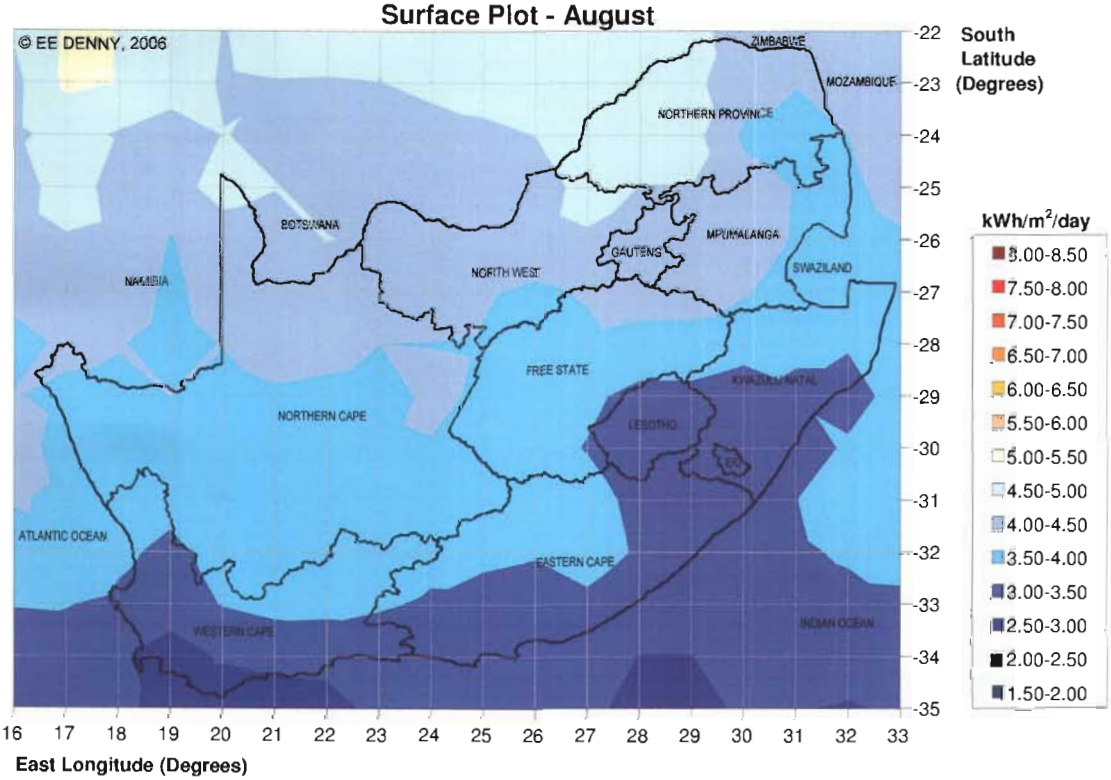

Monthly Averaged Equivalent Sun Hours Radiation Incident On An North-pointed Tilted Surface - Perez/Page Method

Surface Plot - September

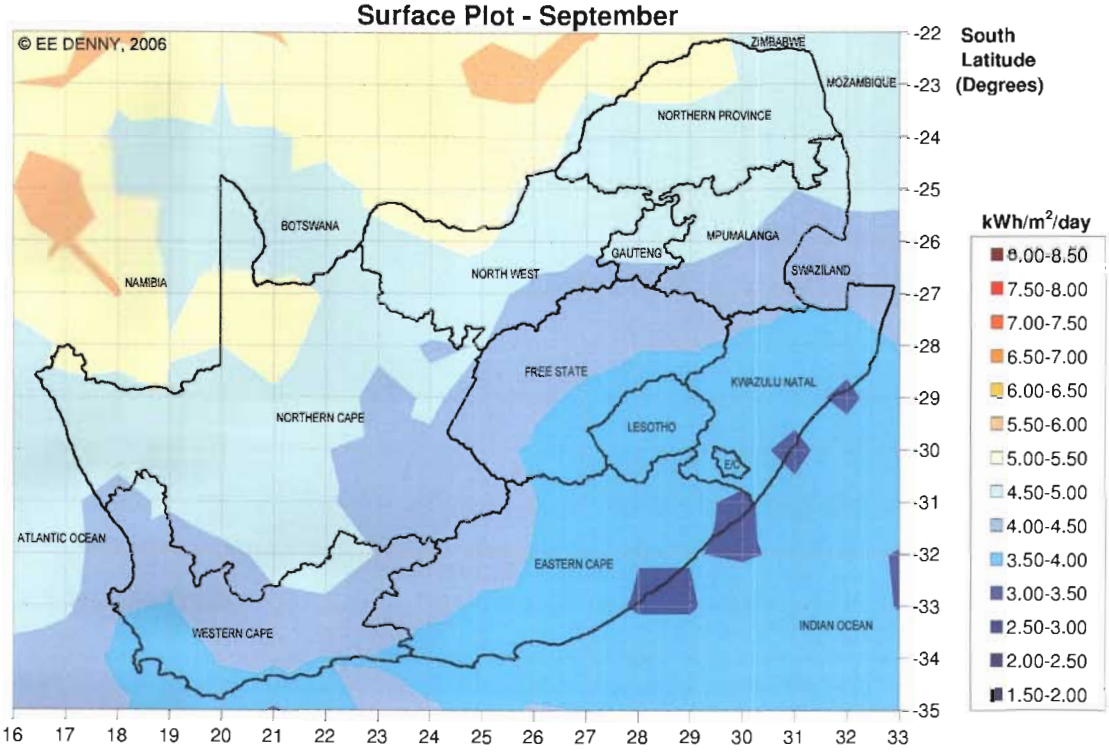

Monthly Averaged Equivalent Sun Hours Radiation Incident On An North-pointed Tilted Surface - Perez/Page Method

Surface Plot - October

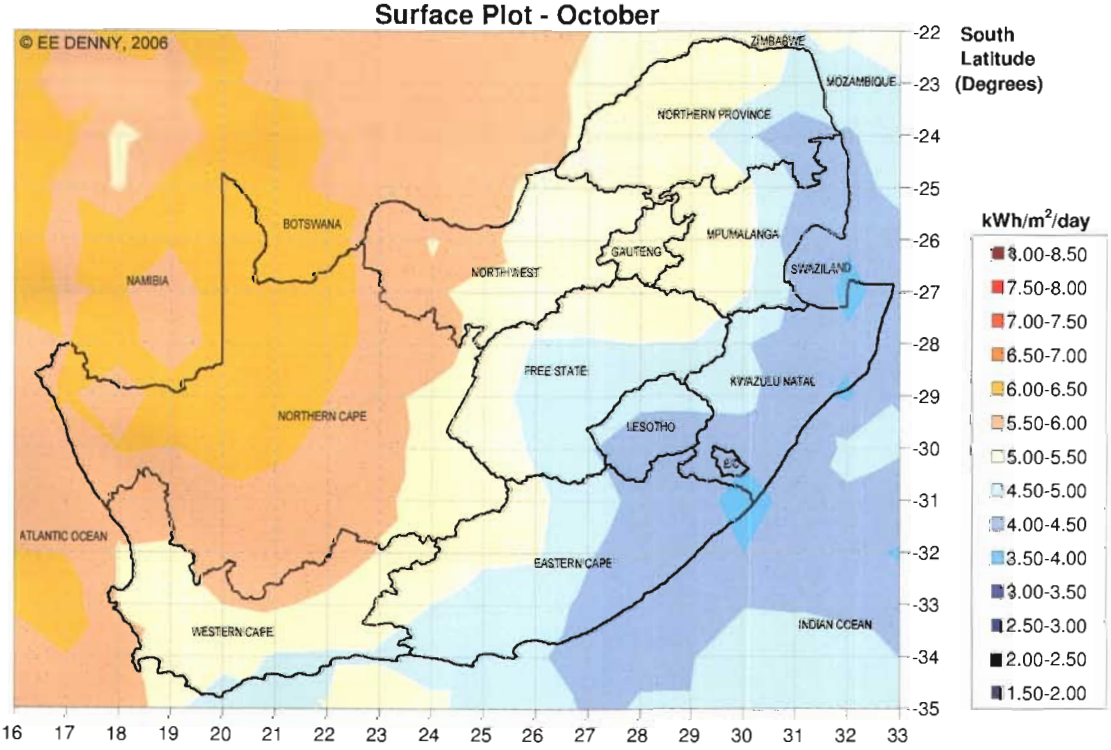

Monthly Averaged Equivalent Sun Hours Radiation Incident On An North-pointed Tilted Surface - Perez/Page Method

Surface Plot - November

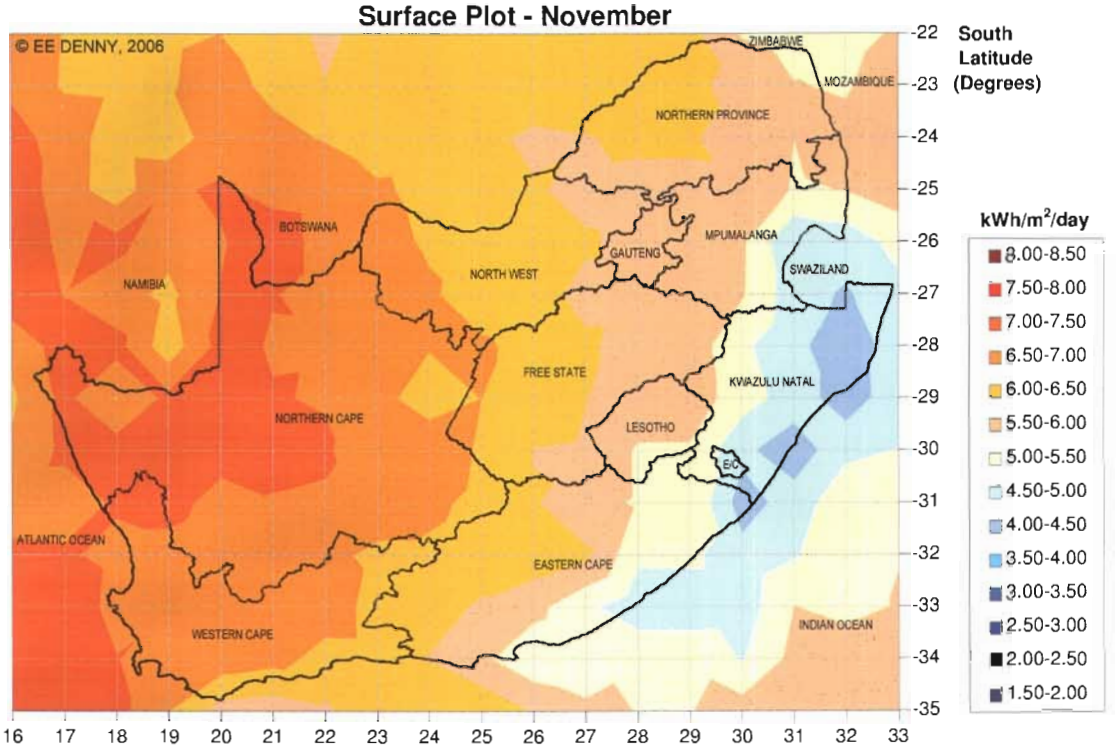

Monthly Averaged Equivalent Sun Hours Radiation Incident On An North-pointed Tilted Surface - Perez/Page Method

Surface Plot - December

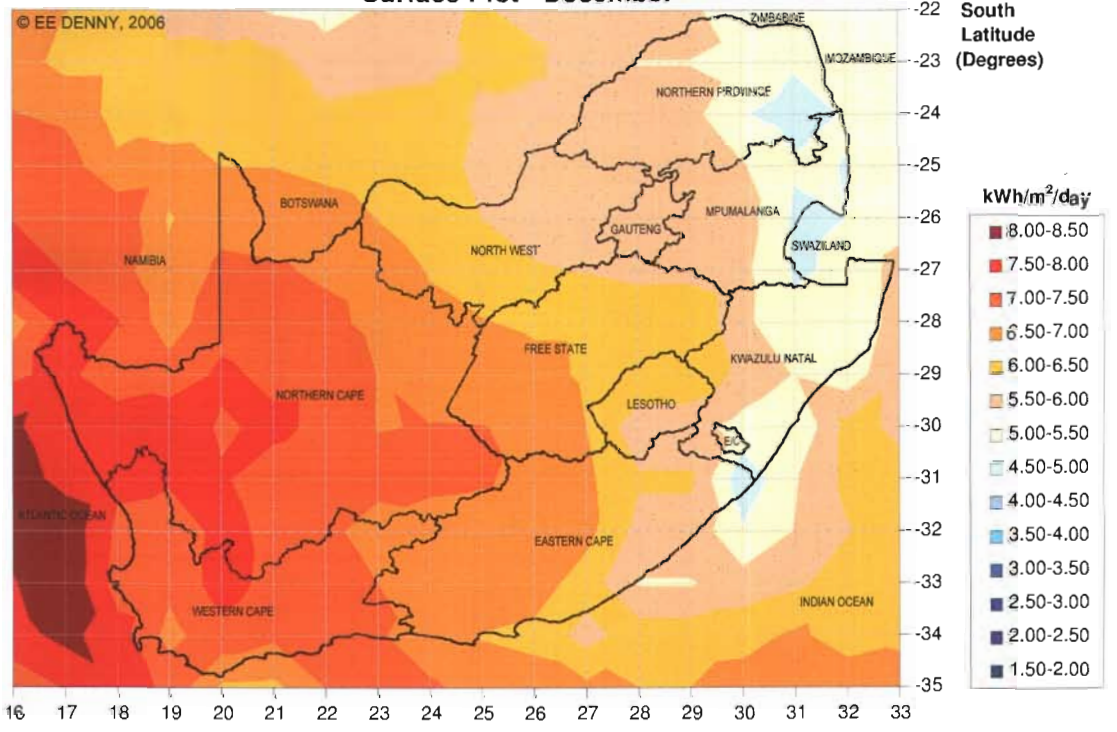

Monthly Averaged Equivalent Sun Hours Radiation Incident On An North-pointed Tilted Surface - Perez/Page Method

ANNEXURE 5

SAS-SWP Surface Meteorology and Solar Energy Database Listing

Location

This Annexure is provided in Portable Document Format (.PDF) and can be found on the enclosed companion CD under the following directory and file name:

../Annexure/Annexure_5_Solar_Database.pdf

SAS-SWP Surface Meteorology and Solar Energy Database Listing

Database listing for the application program in SAS-SWP .dat format

Data Source (Base)

NASA Atmospheric Sciences Data Centre; SSE Data Set, Release 5.1

Application Program

SAS-SWP version 1.0

Database File

RSAsolarData.dat

Creation Date

16 October 2006

Pages

129 pages, excluding this cover page

Annexure to:

DEVELOPMENT OF A COMPUTER PROGRAM FOR GENERAL USE IN THE DESIGN OF SOLAR POWERED WATER PUMPING SYSTEMS

ANNEXURE 6

SAS-SWP Pump Set Database Listing

Location

This Annexure is provided in Portable Document Format (.PDF) and can be found on the enclosed companion CD under the following directory and file name:

../Annexure/Annexure_6_PumpSet_Database.pdf

SAS-SWP Pump Set Database Listing

Database listing for the application program in SAS-SWP .dat format

Data Source (Base)

Relevant pump set (motor + pump combination) manufacturer data sheets

Application Program

SAS-SWP version 1.0

Database File

PVPumpDB.dat

Creation Date

10 October 2006

Pages

16 pages, excluding this cover page

Annexure to:

DEVELOPMENT OF A COMPUTER PROGRAM FOR GENERAL USE IN THE DESIGN OF SOLAR POWERED WATER PUMPING SYSTEMS

ANNEXURE 7

SAS-SWP PV Module Database Listing

Location

This Annexure is provided in Portable Document Format (.PDF) and can be found on the enclosed companion CD under the following directory and file name:

../Annexure/Annexure_7_PVmodule_Database.pdf

SAS-SWP Module Database Listing

Database listing for the application program in SAS-SWP .dat format

Data Source (Base)

Relevant PV (Solar) Module manufacturer data sheets

Application Program

SAS-SWP version 1.0

Database File

PVModuleDB.dat

Creation Date

03 October 2006

Pages

3 pages, excluding this cover page

Annexure to:

DEVELOPMENT OF A COMPUTER PROGRAM FOR GENERAL USE IN THE DESIGN OF SOLAR POWERED WATER PUMPING SYSTEMS

ANNEXURE 8

VUT Pumping Trial Data

Location

This Annexure is provided in Portable Document Format (.PDF) and can be found on the enclosed companion CD under the following directory and file name:

../Annexure/Annexure_8_VUT_Pumping_Trial.pdf

VUT Pumping Trial Data

Relevant data from the VUT pumping trial for comparison with SAS-SWP design results

Data Source

VUT Solar Laboratory

Data Set

30 March 2006

Pages

16 pages, excluding this cover page

Annexure to:

DEVELOPMENT OF A COMPUTER PROGRAM FOR GENERAL USE IN THE DESIGN OF SOLAR POWERED WATER PUMPING SYSTEMS